Chimeric Antigen Receptor for Treatment of T-cell Malignancies and HIV-1 Cure

Weiwei Ma

Imperial College London

Department of Infectious Disease

Centre for Immunology and Vaccinology

Thesis Submitted For The Degree of Doctor of Philosophy

December 2019

Declaration of Originality

I, Weiwei Ma, declare that all the work presented in this thesis is my own work, and that any information used here from other published, unpublished sources or collaboration is correctly referenced.

Abstract

Chimeric Antigen Receptors (CARs) T cell therapy has achieved great success in the treatment of B-cell malignancies by targeting B-cell specific antigen CD19. However, a similar approach targeting the CD4 molecule for T cell lymphoma has thus far been unrealised. CD4, a cell surface glycoprotein, is highly expressed in the majority of mature T-cell malignancies, and absent in hematopoietic stem cells. Anti-CD4 monoclonal antibodies have been widely assessed for T-cell leukaemia/lymphoma treatment, but yielded limited efficacy, suggesting more potent therapies targeting CD4 are required.

Here T cells were transduced with a third-generation CAR specifically targeting CD4 molecule (CART4) via a two-step retroviral system, incorporating with truncated epidermal growth factor receptor (tEGFR) as tracking marker and inducible caspase-9 (iC9) as safety switch. CART4 transduced T cells showed remarkable cytotoxicity against $CD4^+$ T cells *in vitro*. Those CART4 cells effectively eliminated $CD4^+$ T tumour cell line and primary tumour cells from patients with adult T-cell leukaemia/lymphoma (ATLL) and cutaneous T-cell lymphoma (CTCL). In a xenograft model bearing T cell leukaemia cell line, CART4 cells efficiently suppressed tumour progression and prolonged mouse survival, suggesting that CART4 T cells could be a promising strategy for T-cell malignancy.

Besides, as CD4 as serves the primary receptor for HIV-1 entry, it was hypothesised that the anti-CD4 CAR could be applied for HIV eradication. By *in vitro* co-culture assays, CART4 cells effectively eliminated target cells, including $CD4^+$ T cells, dendritic cells (DCs), and macrophages. *In vivo* test utilizing A humanized mouse model of HIV treatment demonstrated that CART4 cells were superior at expanding upon antigen stimulation, eliminating target cells, and controlling HIV rebound after antiretroviral therapy (ART) interruption.

Together, these results support the therapeutic potential of CART4 in patients with T-cell malignancies and HIV-1 infection, respectively.

Acknowledgements

First and foremost, I would like to thank my supervisor, Prof. Xiao-ning Xu, for providing me with the opportunity to undertake my PhD in the lab. Thank you for the continuous support, encouragement and scientific advice throughout my study. I really enjoyed the time with you in the Kings Arms and the Sporting Page.

Secondly, I would like to thank Dr Juthathip Mongkolsapaya and Dr Peter Kelleher for the helpful advice during my PhD assessments. I would like to thank Dominic Smith for all his help with lab orders and facility maintenance, and Sima Fulford for her help with lab management, and Prisa Amjadi for her expertise on flow cytometry. A special thanks to Dr Nesrina Imami for her helpful advice on PhD study. I would like to thank past the present members of the Centre for Immunology and Vaccinology (Dr Adriano Boasso, Dr Jia Guo, Dr Michael Liu, Dr Alex Cocker, Dr Scarlett Turner, Dr Katie McFaul, Dr Lizzie Atkins, Nadia Khan, Qiao Gao, Alessia Dalla Pria, Sai Liu, Dr Hantao Liu, Dr Steven Patterson, Di Tian). I appreciate your support and friendship. I'm also grateful to my co-supervisor Dr Marcus Donor, for your help and patience.

Thirdly, I would like to thank Prof. Lishan Su from the University of North Carolina at Chapel Hill, for allowing me to perform my project in animal models. I am very grateful to Dr Guangming Li for help with animal experiments and friendship too. I'd also like to thank the members in Prof. Lishan Su's lab, including Dr Yaxu Wu, Dr Qi Wang, Dr Liang Cheng, Dr Jianping Ma, Dr Zhuo Wang, Dr James Ahodantin, Dr Caroline Marnata. A special thanks to Rania Tsahouridis for taking care of the animals.

Fourthly, I would like to thank alumnus Richard Lee and the Lees Charitable Foundation for providing the funding for my PhD study in Imperial College London.

Fifthly, I would like to thank my incredible mother, for getting me where I am today, and for all of your love and believing on me. Without you, I would have never gotten this far. Thank all of my fantastic friends, who have always support me.

Table of Contents

List of Tables

List of Figures

List of Acronyms

3TC	Lamivudine
ACK	Ammonium-Chloride-Potassium
ADCC	Antibody-dependent cellular cytotoxicity
AE	Adverse event
AIDS	Acquired immunodeficiency syndrome
ALCL	Anaplastic large-cell lymphoma
ALL	Acute lymphoblastic leukaemia
APCs	Antigen-presenting cells
ATLL	Adult T cell leukaemia/lymphoma
AZT	Zidovudine
bNAb	Broadly neutralizing antibody
Ca^{2+}/CaM	Calcium-bound calmodulin
CARD	Caspase activation domain
CARs	Chimeric antigen receptors
cART	Combination antiretroviral therapy
CART20	A CD20-specific CAR
CART4	A CD4-specific CAR
CDC	Complement-dependent cytotoxicity
CID	Chemical inducer of dimerization
CLL	Chronic lymphocytic leukaemia
CR	Complete remissions
CRS	Cytokine release syndrome
CTCL	Cutaneous T-cell lymphoma
CTL	Cytotoxic T lymphocyte
D10	completed DMEM with 10% fetal bovine serum

DAG	Diglyceride
DC	Dendritic cell
DLBCL	Diffuse large B-cell lymphoma
DMEM	Dulbecco's Modified Eagle Medium
DMSO	Dimethyl sulfoxide
DN	Double negative
DP	Double positive
EDTA	Ethylenediaminetetraacetic acid
eGFP	Enhanced green fluorescent protein
EGFR	Epidermal growth factor receptor
Env	Envelope
FBS	Fetal bovine serum
FDA	Food and Drug Administration
ffluc	Firefly luciferase
FG12-EG	Lentiviral vector FG12 containing eGFP and Gluc genes
FKBP12	FK506-binding protein 12
FL	Follicular lymphoma
Foxn1	Forkhead box protein N1
FTC	Emtricitabine
G-Rex	Gas-permeable static cell culture system
GaLV	The Gibbon ape leukaemia virus
Gluc	Gaussia luciferase
GM-CSF	Granulocyte-macrophage colony-stimulating factor
gp	Glycoprotein
GPCR	G-protein-coupled receptor

GVHD	Graft-versus-host disease
HL	Hodgkin lymphomas
HIV	Human immunodeficiency virus
HSC	Hematopoietic stem cell
HTLV1	human T cell lymphotropic virus type 1
IACUC	Institutional Animal Care and Use Committee
iC9	Inducible caspase-9
IFN-γ	Interferon-γ
IgG	Immunoglobulin G
IL-2	Interleukin-2
Il2rg	IL-2 receptor common gamma chain
IP3	Inositol triphosphate
ITAM	Immunoreceptor tyrosine-based activation motif
ITK	Inducible T cell kinase
Lck	Lymphocyte protein tyrosine
LRAs	Latency-reversing agents
mAb	Monoclonal antibody
MF	Mycosis fungoides
MFI	Mean fluorescence intensity
MHC	Histocompatibility complex
MM	Multiple myeloma
MΦ	Macrophage
NHL	Non-Hodgkin lymphoma
NHP	Non-human primate
NK	Natural killer
NNRTI	Non-nucleoside reverse transcriptase inhibitor
NOD	Non-obese diabetic

NRG	NOD/RAG1/2$^{-/-}$IL2Rγ$^{-/-}$
NRTI	Nucleoside reverse transcriptase inhibitor
NSG	NOD.Cg-Prkdc^{scid}Il2rg^{tm1Wjl}
NTD	Non-transduced
ORF	Open reading frames
OS	Overall survival
PAMPs	Pathogen-associated molecular patterns
PBL	Peripheral Blood Leukocytes
PBMCs	Peripheral blood mononuclear cells
PCP	Pneumocystis carinii pneumonia
PDX	Patient-derived xenograft
PIP2	Phosphatidylinositol-4,5 diphosphate
PKG	Phosphoglycerate kinase 1 promoter
PLCγ1	Phospholipase C γ1
pMHC	Peptide-MHC complex
Pol	Polymerase
PTCL	Peripheral T-cell lymphoma
PTCL-NOS	Peripheral T-cell lymphoma, not otherwise specified
R10	Completed RPMI with 10% fetal bovine serum
Rag	Recombination-activating gene
RM	Rhesus macaque
RPMI 1640	Roswell Park Memorial Institute Medium 1640
RT-PCR	Reverse transcription-quantitative PCR
scFv	Single-chain antibody fragment
scid	Severe combined immunodeficient
SIV	Simian Immunodeficiency Virus

SP	Single-positive
SP	Phosphoglycerate kinase 1 promoter
SS	Sezary syndrome
T2A	*Thosea asigna* virus 2A
TCR	T cell receptor
TCR Vβ	β chain of the T cell receptor
TDF	Tenofovir
tEGFR	Truncated epidermal growth factor receptor
TFH	Follicular Helper T cells
TM	Transmembrane domain
TNF-α	Tumour Necrosis Factor- α
TRAC	T cell receptor α-chain constant
TRBC	T-cell receptor β-chain constant
Treg	Regulatory T cell
UCART7	Universal anti-CD7 CAR-T cells
VH	Antibody variable heavy chain
VL	Antibody variable light chain
VSV-G	G glycoprotein of the vesicular stomatitis virus
WHO	World Health Organizations
Zap-70	Zeta-chain-associated protein kinase 70
Δ32	32 base pair homozygous depletion

Chapter 1. Introduction

1.1. T lymphocytes

A basic feature of the immune system is to distinguish between the structural aspects of self-tissues and non-self-pathogens. While the innate immune cells target and eliminate pathogens by recognizing pathogen-associated molecular patterns (PAMPs), the adaptive immune cells, which mainly consists of B and T lymphocytes, are capable of generating an extensive repertoire (B and T cell receptors) of antigen-binding molecules to mediate humoral and cellular immune responses.

1.1.1. T cell development from thymus

The pluripotent stem cells differentiate into lymphoid precursor before migrating to the thymus, where they undertake a series of differentiation processes and eventually develop to matured T cells with a variety of antigen specificities. After migrating to the thymus, the development of T lymphocytes subdivided into two stages based on the expression of CD4 and CD8. The early committed $CD4^-$ $CD8^-$ T cells (double negative, DN) gain $CD4^+$ $CD8^+$ phenotype (double positive, DP). DP cells subsequently undergo positive selection and then negative selection to obtain an intermediate level of activating signalling. The DP thymocytes become single-positive (SP) of CD4 or CD8 and then migrate to the peripheral lymphoid organs[1].

1.1.2. T cell subsets

$\alpha\beta$ T cells are the major subtype of the T cells in the human body, named after the expression of $\alpha\beta$ TCR on their cell surface. $\alpha\beta$ T cells mainly consist of $CD8^+$ cytotoxic T cells and $CD4^+$ helper T cells, which are the population of interest in the context of this thesis. The co-receptor

CD4 and CD8 bind a conserved region of major histocompatibility complex (MHC) molecules, serving an essential role in TCR signalling[1].

$CD8^+$ T cells are cytotoxic T cells, capable of targeting virus-infected or neoplastic cells. They bind to a short peptide (8-11 amino acids) loaded onto the MHC class I molecule. Upon being stimulated, they rapidly produce multiple cytokines and lytic granules, such as IL-2, tumour necrosis factor-α (TNF-α), interferon-γ (IFN-γ), granzyme and perforin, to result in different anti-pathogenic effects[1].

On the other hand, $CD4^+$ helper T cells also play a critical role in immune protection. The CD4 molecule has an affinity to the peptide-MHC class II molecule complex, activating helper T cells. $CD4^+$ T cells are subdivided into several subtypes Th1, Th2, Th17, Th9, Tfh, by the expression of unique key transcription factors. Each of them plays different roles in the immune response[1].

1.1.3. T cell receptor signalling

95% of human T cells express T cell receptor (TCR) formed by α subunit and β subunit, while the rest express γσ TCR. The αβ TCR has a relatively low but significant affinity to peptide-MHC complex (pMHC), recognizing infected or neoplastic cells. In addition to the αβ TCR heterodimer, the TCR complex contains a CD3 complex as signalling modules, which is made up of CD3σ, CD3γ, CD3ε, and CD3ζ chains. The intracellular tail of TCR is very short; thus, the CD3 complex containing the intracellular signalling motifs is required to transduce the signal from TCR into the cell. The signalling motifs residing in immunoreceptor tyrosine-based activation motif (ITAM) are tyrosine residues, which can be phosphorylated by Src kinase family member lymphocyte protein tyrosine kinase (Lck) upon TCR activation[2]. The TCR complex contains 10 ITAMs in total. CD3δ, CD3γ, and CD3ε each contain a single ITAM, while CD3ζ contains three ITAMs[3].

The activation of the TCR induces multiple signalling transduction cascades and determines cell fate by regulating cytokine production, proliferation and differentiation (Figure 1-1). Firstly, the Lck phosphorylates the ITAMs on the cytoplasmic residue of TCR/CD3 complex. Zeta-chain-associated protein kinase 70 (ZAP-70) is recruited to the ITAMs at the TCR/CD3 complex followed by its phosphorylation and activation. The activation of ZAP-70 phosphorylates two main substrates, the linker for activation of T cells (LAT) and lymphocyte cytosolic protein 2 (SLP-76), thereby amplifying the signalling. The phosphorylated LAT recruits GRB2-related adaptor downstream of Shc (GADS), and an inducible T cell kinase (ITK), which subsequently results in the phosphorylation of phospholipase C γ1 (PLCγ1). The activated PLCγ1 hydrolyses phosphatidylinositol-4,5 diphosphate (PIP2), producing of second messenger diglyceride (DAG) and inositol triphosphate (IP3). DAG activates a number of downstream proteins, such as protein kinase Cθ (PKCθ) and MAPK/Erk pathways. IP3 binds the IP3 receptor on the surface of ER, triggering the release of Ca^{2+} from the endoplasmic reticulum (ER). The increase of Ca^{2+} triggers the Ca^{2+} release activated Ca^{2+} (CRAC) channels and results in the influx of extracellular Ca^{2+}, which activates the protein phosphatase calcineurin. The activated calcineurin then dephosphorylates nuclear factor of activation T cell (NFAT), which promotes the transcription of IL-2 gene[1].

1.1.4. T cell activation

The induction of T cell activation, proliferation, and differentiation requires a dual signal stimulation: the engagement of TCR and peptide-MHC complex provides the signal 1; signal 2 is provided by the binding of surface-stimulatory receptors on the ligands of antigen-presenting cells (APCs) and relevant receptors on T cells[1].

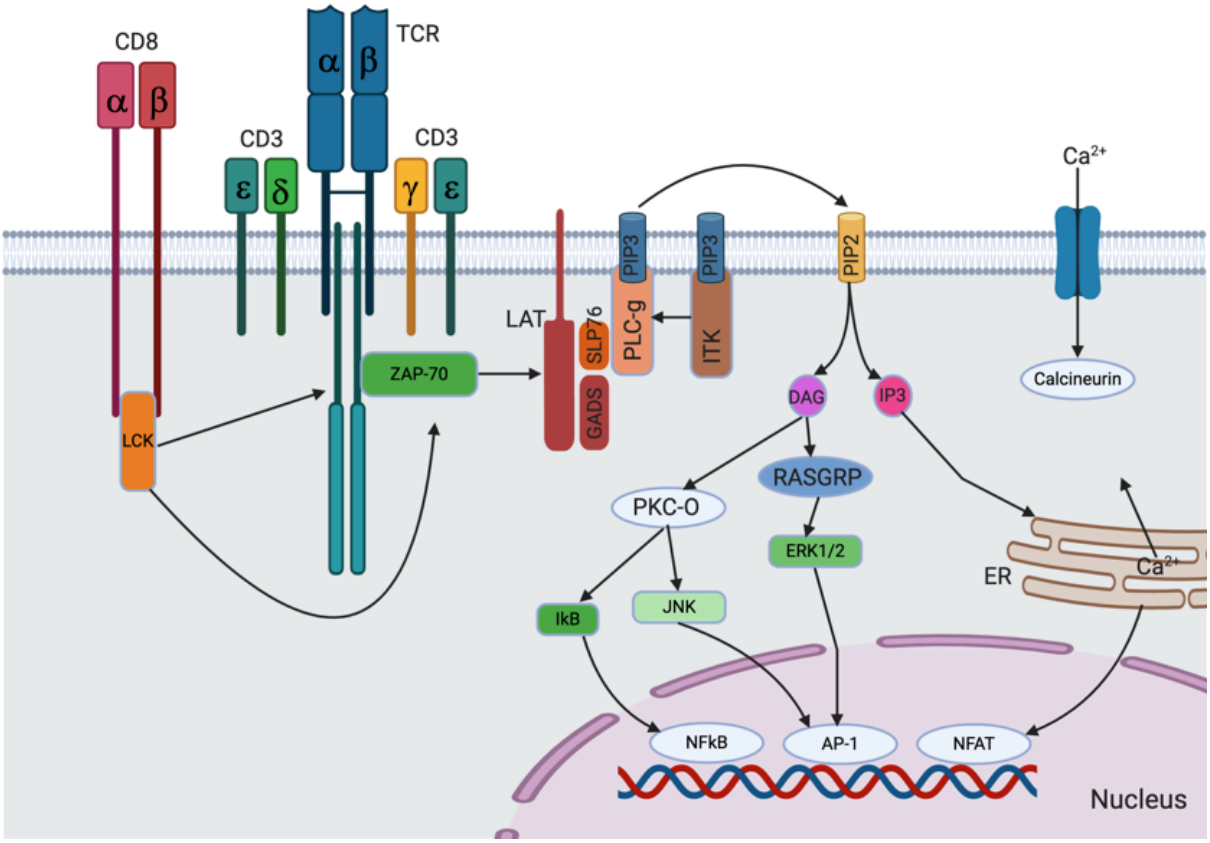

Figure 1-1 T cell receptor signalling.

The engagement of a TCR with a peptide-MHC complex trigger phosphorylation of ITAMs on intracellular regions of CD3ζ chains by Lck, leading to recruitment and phosphorylation of ZAP-70. ZAP-70 subsequently phosphorylates LAT and SLP76, to which PLC-γ binds and is activated by ITK. PIP2 is cleaved by PLC-γ to produce IP3 and DAG, which subsequently lead to the translocation of NFκB, AP-1 and NFAT transcription factors into the nucleus to regulate multiple gene transcriptions to mediate T cell proliferation and differentiation. Adapted from Janeway's Immunology[1].

Signal 1 alone is insufficient to activate T cells. A lack of a signal 2 during T cell activation will result in anergy, immune tolerance, and even cause programmed cell death, which may be due to sustained internalization of the TCR/CD3 complex[1]. Two main co-stimulatory receptor families have been identified: the CD28 family and the TNF superfamily. The CD28 family includes multiple surface receptors, of which CD28 and ICOS act as positive regulators of T cell activation. CD28 and ICOS bind to their ligands CD80/CD86 and B7-H2 on the surface of

APCs. The TNF superfamily, mainly including 4-1BB, CD27, and OX40, interact with 4-1BBL, CD27L, and OX40L. These co-stimulatory signals regulate T cell activation, survival, function, and memory formation[1].

1.2. Chimeric Antigen Receptors

Chimeric antigen receptors (CARs), which were initially named as 'T-bodies', were first developed by Eshhar *et al.*in 1990s[4,5]. In general, CARs were engineered host cells by viral or non-viral delivery systems, to redirect their target specificity (Figure 1-2). Mostly, $CD3^+$ T cells are used as host cells, though other cell subsets, such as natural killer (NK) cells, were also utilized.

The CAR-T cell therapy involves a multistep process, including T cell activation, CAR gene engineering, *ex vivo* expansion, and infusion (Figure 1-2).

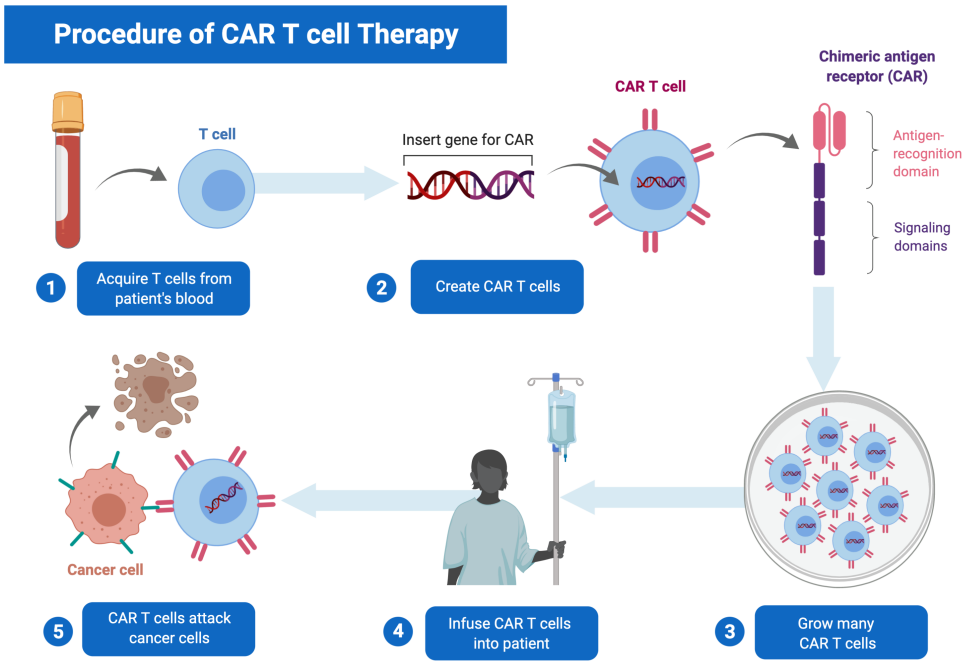

Figure 1-2 Overview of CAR-T cell therapy

The process of CAR-T manufacture begins by collecting blood from the patient. T cells are separated from the blood and inserted the gene for CAR to possess specificity against tumour cells. These engineered T cells are expanded *in vitro* and infused into the patient. Once in the body, the CAR-T cells recognize and attack tumour cells.

1.2.1. Structure of CARs

In general, CARs were composed of an extracellular domain for target recognition, a transmembrane domain for expression on the cell membrane, and an intracellular domain with signalling functions.

The structure of single-chain antibody fragments (scFv) was most commonly used as the extracellular domain for antigen recognition of CAR-T. Generally, an scFv consists of an antibody variable light chain (VL) and heavy chain (VH), which are connected by a peptide linker to enhance flexibility. By this design, scFv retains the specificity of the original monoclonal antibody. The scFv on the CAR-T cells enables the engineered host cells to possess specificity against different types of antigens, such as polypeptides, glycoproteins, glycans, or glycolipids. This means the antigen recognition of CAR-T cells is not limited by HLA, in contrast to ordinary $\alpha\beta$ TCRs. Thus CAR engineering can bypass the downregulation of HLA expression by transformed cells and the limitation of HLA haplotype. Additionally, the affinity between scFv and target proteins is relatively higher (K_D=80-1 nM) compared to natural TCR-pMHC affinity (K_D=1-50 μM)[6,7], which might increase the specificity and sensitivity of the CAR-T cells.

The transmembrane domain, which is usually derived from the lymphocyte molecules such as CD4, CD8, CD28, serves a structural role[8,9].

The intracellular signalling domain is designed for cell activation. Physiologically, T cell activation requires the co-localization of TCR and CD3, which is composed of four subunits ζ, δ, ε, γ. In CAR-T cells, CD3ζ alone was found to be sufficient to trigger signalling for host T cells activation and is commonly chosen as the signalling motif of CAR construct[10]. The first-

generation CARs only had the CD3ζ acting as signalling domain and successfully induced T cell activation and cytotoxicity against target tumour cells. However, clinical studies showed the first-generation CAR-T cells yielded limited therapeutic efficacy[11-13]. The lack of the signal 2 provided by co-stimulation was considered as the main reason for the limited expansion and persistence of the first-generation CAR *in vivo*, which is required for potent anti-tumour effects[14,15].

The second-generation CARs were developed by complementing one more co-stimulatory signalling domain to the CAR endodomain[16]. A series of signalling motifs from different co-stimulation molecules, such as 4-1BB[14,15], CD28[16,17], OX40[14,18], ICOS[14,19], CD27[20] were tested and compared. Both pre-clinical and clinical studies showed a combination of CD3ζ and a co-stimulatory motif was required for the improved capacity of expansion and persistence *in vivo*. Helene *et al*. incorporated the CD28 signalling domain with primary signalling domain in one single gene, and found that the signal 2 provided from CD28 signalling domain enhanced cytokine production[16]. Several subsequent studies also supported that the addition of the CD28 co-stimulatory domain improved anti-tumour efficacy of CAR-T cells by improving cell activation, proliferation, and cytokine release[17,21-24]. Later on, signalling from 4-1BB was found to improve the persistence of CD19-specific CAR-T cell in human acute lymphoblastic leukaemia (ALL) xenograft models[14,15], which was supported by other studies with a mesothelin-specific CAR in a xenograft model[25] and CD19-specific CAR in clinical trials[26,27].

Based on the success of the second-generation CARs, the third-generation CARs contained multiple co-stimulatory motifs in the intracellular domains. The stronger stimulation from signal 2 was considered to achieve a better anti-tumour response. Indeed, the animal experiments showed that the third-generation CARs outcompeted the second-generation CARs. Jinjuan *et al*. found that the incorporation of CD28 and 4-1BB co-stimulatory domains improved the efficacy of CAR-T therapy by enhancing activation, proliferation, and cytotoxicity of CAR-T cells[28]. Indeed, a pilot clinical trial with anti-CD20 CAR-T using both CD28 and 4-1BB domains demonstrated its safety and clinical efficacy for patients with relapsed indolent B-cell and mantle cell lymphoma[29].

More recently, the fourth generation CARs were described that incorporate a immune-stimulatory cytokine, such as IL-12[30-32], IL-15[33], and IL-18[34]. The cytokines co-expressed by CAR-T cells were suggested to improve CAR-T expansion and persistence in the tumour microenvironment, where T cells were usually significantly suppressed. Additionally, the expression of transgenic cytokines would enhance the anti-tumour immune response by triggering bystander immune cells to eliminate tumour cells at the target site. Nonetheless, limited data is published of the clinical output using these concepts. Additionally, the safety issue must be addressed when overexpressing stimulatory cytokines *in vivo*.

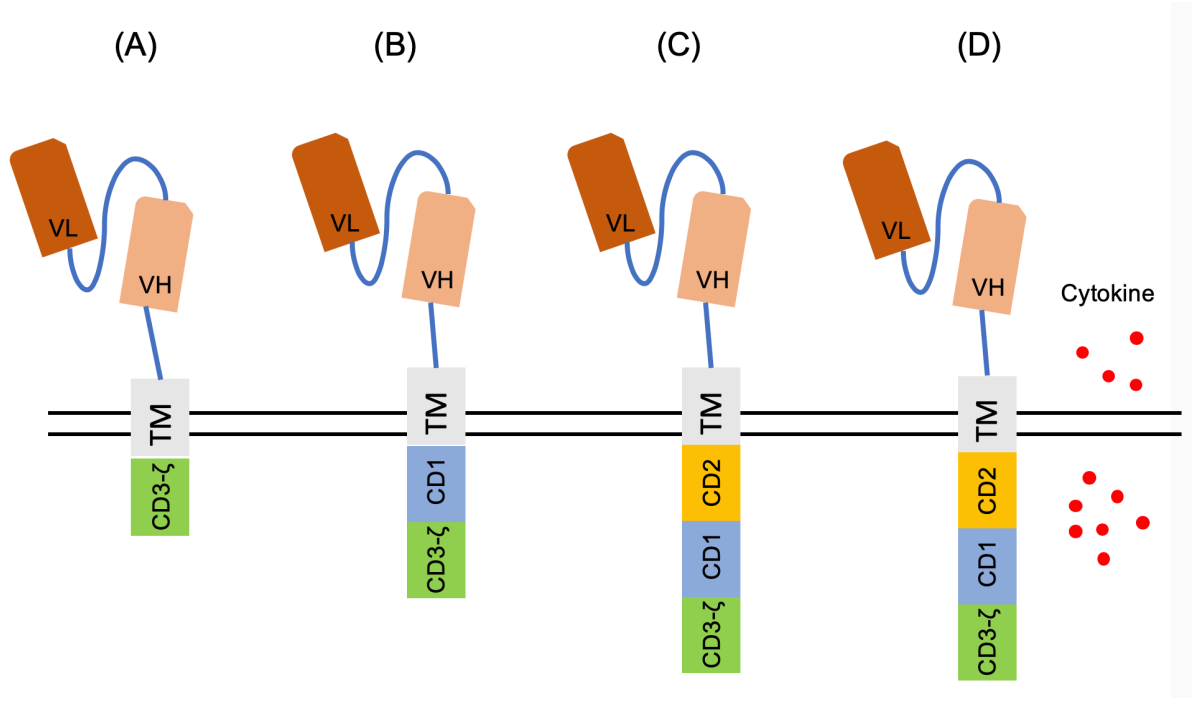

Figure 1-3 Evolution of Chimeric Antigen Receptors.

(**A**) First-generation CARs incorporate a CD3ζ activation domain. (**B**) Second-generation CARs add a costimulatory domain (CD1). (**C**) Third-generation CARs have two co-stimulatory domains CD1 and CD2. (**D**) Fourth-generation CARs co-express immune-stimulatory cytokines. VL: variable light chain; VH: variable heavy chain; TM: transmembrane domain; CD: co-stimulatory domain. Adapted from Wang et al[28].

1.2.2. Application of CAR-T therapy

To date, CD19-specific CAR-T cells have been demonstrated to be radically useful for relapsed/refractory B-cell malignancies, such as B-cell acute lymphoblastic leukaemia (ALL), non-Hodgkin lymphoma (NHL) and chronic lymphocytic leukaemia (CLL). Even though most of the treated patients failed in multiple treatment therapies, CD19 CAR-T therapy achieved a percentage of complete remissions (CR) from 70% to 94% in different trials[35]. The revolutionary success of anti-CD19 CAR accelerated the approval of two CAR-T therapies by the Food and Drug Administration (FDA) and the European Medicines Agency (EMA). Nowadays, two CAR-T therapy products, Kymriah from Novartis and Yescarta from Kite Pharm, have been widely applied for the clinical treatment of ALL, diffuse large B-cell lymphoma (DLBCL), CLL and multiple myeloma (MM). Both therapies use a retrovirus-based gene method to produce CAR-T cells[35].

Currently, more clinical trials are evaluating the efficacy of CAR-T in other B-cell malignancies, such as follicular lymphoma (FL)[36], MM[37]. Besides, more targets are being under assessment in clinical studies, such as CD20[38], B-cell maturation antigen (BCMA)[39], epidermal growth factor receptor (EGFR)[40].

1.2.3. Toxicity of CAR-T therapy

While CAR-T therapy has exhibited potent unprecedented efficacy in clinical treatment for hematologic malignancies, an obstacle for the application of CAR-T therapy is toxicity, including cytokine release syndrome (CRS), neurological toxicity, and 'off-target' toxicity.

Cytokine release syndrome

CRS, a life-threatening toxicity, was first observed after the administration of monoclonal antibodies[41,42], and immune-stimulatory cytokine IL-2[43]. It is also the major adverse event during CAR-T therapy[35]. The first syndrome of CRS is fever, which can occur from hours to

20 days after the administration of CAR-T cells[44,45]. For some patients, the initial fever can develop into a higher fever, hypoxia, depressed cardiac function, and other organ dysfunction[46-50]. The accumulation of inflammatory cytokines released from CAR-T cells and other immune cells, including IL-6, IL-10, IFN-γ, and TNF-α, was considered to induce CRS[44,45,49-51].

Neurologic toxicity

Besides the CRS, neurologic toxicity is another problem during CAR-T therapy, which is another serious side-effect that has frequently been observed in patients undergoing CAR-T treatment. The clinical phenomenon of neurologic toxicity can be delirium[50], hallucinations[44], cognitive defects[52], tremors[53], nerve palsies[46], and many other neurological symptoms. Although neurologic toxicity of CAR-T therapy does not correlate to the appearance of CRS, it is partially correlated to elevated cytokine levels[54,55].

'Off-tumour' toxicity

While most tumour targets of CAR-T therapies are also expressed on healthy tissues, the other toxicity induced by CAR-T therapy is an "off-tumour' effect. The 'off-tumour' toxicity can cause severe organ damage or even be life-threatening[56]. One typical example of an 'off-tumour' effect is B-cell aplasia in anti-CD19 CAR-T therapy, which is induced by the eradication of normal B cells by the persistence of CAR-T cells[55,57,58]. Moreover, one case was reported that a patient treated with HER2-specific CAR-T therapy died of respiratory failure. This was considered to be induced by the recognition of HER2 expression in pulmonary parenchyma[56].

Though two CAR-T cell therapies have been approved for clinical use by the Food and Drug Administration (FDA), the toxicity of CAR-T therapy is still problematic. The clinical management of CRS and neurologic toxicity is becoming more streamlined with the standard grading system[49] and recommendation of clinical management[59]. In parallel, new and safer

CAR-T targets are need to be identified. Ongoing development of CAR-T techniques will provide new generation CAR-T therapies that will increase anti-tumour efficiency while decreasing clinical toxicity.

1.2.4. Improving the safety of CAR-T: suicide genes

Several strategies have been described utilizing suicide genes incorporated with CAR-T to control the CAR-T toxicity. Suicide strategies use transgenes, which will induce host cell death after exposure to specific molecules. An ideal safety switch should have several desirable characteristics. Firstly, the switch expressed from the suicide gene should be non-immunogenic, and the compound is non-toxic to endogenous cells. Also, the switch/activation system should function with a very low threshold, as it would allow accurate control of adverse side-effects without complete depletion of the therapeutic benefits.

Truncated human EGFR

One approach to deplete CAR-T cells *in vivo* is to co-express on the host T cells a transmembrane protein, which is recognisable by clinically approved mAb. The introduction of mAb would eliminate the CAR-T cells by antibody-dependent cellular cytotoxicity (ADCC) and complement-dependent cytotoxicity (CDC). Initially, CD20 mAb rituximab was used to induce cell depletion by targeting human CD20. The administration of rituximab induced up to 90% of CAR-T cell death[60-62]. However, this approach would also deplete normal B cells. An alternative approach used truncated human epidermal growth factor receptor (EGFR), a kinase receptor of the ErbB family of growth factor receptors, without expression on the hematopoietic or lymphopoietic cells[63]. The truncated version of EGFR (tEGFR) does not have the extracellular binding domains and intracellular signalling domains (Figure 1-4), eliminating

its natural function. The tEGFR co-expressed on CAR-T cells enables cell purification, tracking, and elimination *in vivo* after administration of cetuximab, a widely used anti-EGFR mAb[64,65].

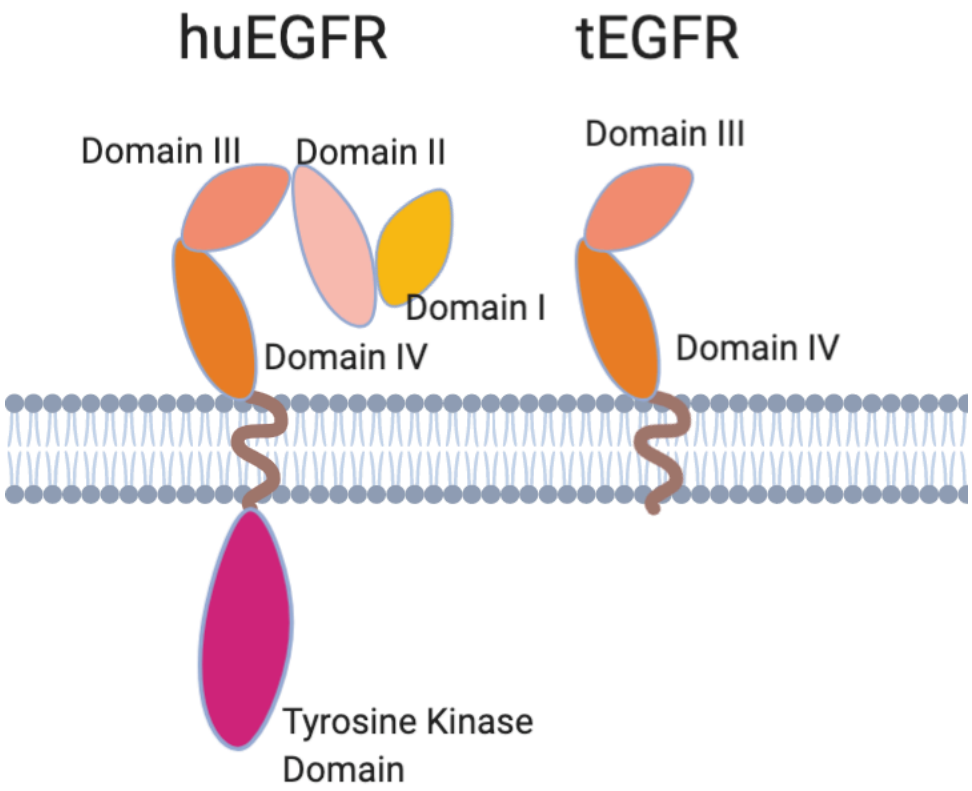

Figure 1-4 Structure of truncated EGFR

Schematic representation of wildtype human EGFR, including one intracellular domain and four extracellular domains. The truncated EGFR (tEGFR) lacks the extracellular domain I and II and most of the cytoplasmic tyrosine kinase domain. Adapted from Zhang *et al*.[35]

Inducible Caspase-9

Another potent suicide gene was developed based on an adapted caspase-9 molecule and a reformed FK506-binding protein 12 (FKBP12). In physiological conditions, caspase-9 is activated by the cytochrome C released from damaged mitochondria, which will then activate downstream signalling and trigger cell apoptosis[66]. The bulky phenylalanine of FKBP12, which initially function as an inhibitor of calcineurin, was substituted by a smaller valine residue

(FKBP12-F36V). The alteration has a high affinity for FKBP12-F36V and minimizes the interaction with endogenous FKBP[67]. While the modified caspase-9, which was derived from the natural caspase-9 molecule by deleting its caspase activation domain (CARD), and it cannot dimerize properly[68]. The modified caspase-9 and redesigned FKBP12-F36V are linked by a flexible GGGGS linker, forming the inducible caspase-9 molecule (iC9). In 2001, a chemical inducer of dimerization (CID) AP1903, was validated in a clinical trial on healthy volunteers and did not elicit significant side effects[69]. The iC9 has been clinically assessed in hematopoietic stem cell transplantation patients to prevent graft-versus-host-disease (GVHD)[70]. A single dose of AP1903 induced apoptosis in up to 99% of CAR-T cells with high expression of iC9 *in vitro* and animal model[68,71]. Additionally, a comparison study of different suicide gene strategies demonstrated that iC9 exhibited a more rapid and effective ablation of CAR-T cells than any other method, such as Herpes simplex virus thymidine kinase (HSV-TK) and mutant human thymidylate kinase (mTMPK)[72].

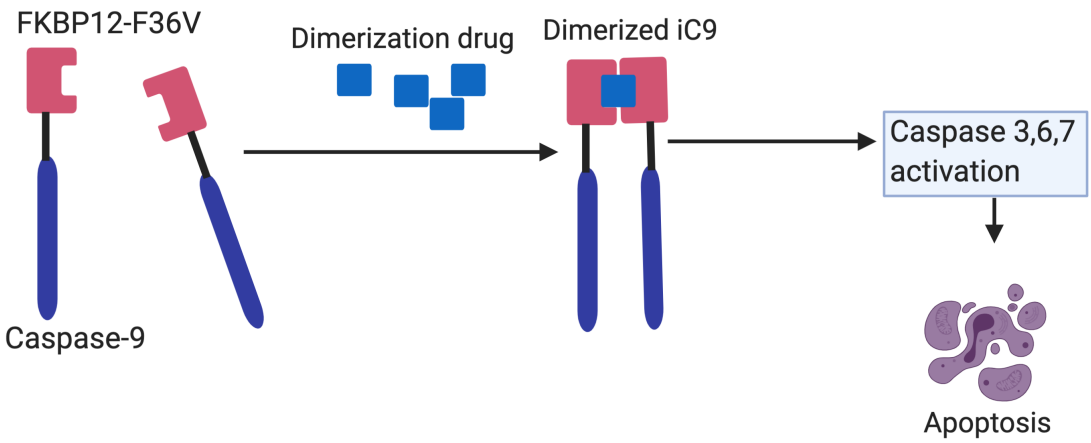

Figure 1-5 Armed CAR T cell suicide gene —iC9 to kill itself by apoptosis.

iC9 is co-expressed in CAR T cells. Once AP20187, the chemical inducer of dimerization (CID), is added, it dimerizes iC9 and triggers apoptosis of CAR-T cells. iC9, inducible caspase-9. Adapted from Marin *et al*.[72]

1.3. T-cell malignancy

T-cell malignancies are a heterogeneous group of hematologic cancers that account for 7-15% of NHL[73]. T-cell malignancies are defined as a broad group of disorders, characterized by clonal expansion and disorders of T cells. Until recently, there is no standard therapy for these diseases. Compared with B-cell malignancies, the outcomes of patients with T-cell malignancies remains unsatisfactory.

1.3.1. Classification of T-cell malignancy

Mature T-cell neoplasms are classified into 27 subsets (Table 1.1). The most common subtype is peripheral T-cell lymphoma, not otherwise specified (PTCL-NOS), accounting for 26%. Angioimmunoblastic lymphoma accounts for 18%, followed by anaplastic large-cell lymphoma (ALCL) (12%). Adult T-cell leukemia/lymphoma represent 10%[74]. PTCLs are mainly derived from $CD4^+$ T cells, while only a small proportion originates from $CD8^+$ T cells. Cutaneous T-cell lymphomas (CTCLs) are a heterogeneous group of non-Hodgkin T-cell original lymphomas that distribute in the skin. Mycosis fungoides (MF) and Sezary syndrome (SS) are the most common subtypes of CTCLs, compromising for about 60%-70% of all CTCLs[75]. Adult T cell leukaemia/lymphoma (ATLL) is a subtype of rare, but extremely aggressive T-cell malignancies, induced by infection of human T cell lymphotropic virus type 1 (HTLV1)[76]. HTLV1 is relatively common in Japan, the Caribbean, and South and Central America and Africa. Only 5% of individuals with HTLV1 infection will develop $CD4^+$ ATLL, while the mechanisms involved are not fully understood[77]. Although significant progress has been made in therapy for ATLL, the prognosis of ATLL is still quite poor. Acute ATLL patients have a median survival of about one year.

Table 1.1 List of T-cell neoplasms adapted from 2016 WHO classification

T-cell prolymphocytic leukaemia

T-cell large granular lymphocytic leukaemia

Systemic EBV^+ T-cell lymphoma of childhood

Hydroa vacciniforme–like lymphoproliferative disorder

Adult T-cell leukaemia/lymphoma

Extranodal T-cell lymphoma, nasal type

Enteropathy-associated T-cell lymphoma

Monomorphic epitheliotropic intestinal T-cell lymphoma

Indolent T-cell lymphoproliferative disorder of the GI tract

Hepatosplenic T-cell lymphoma

Subcutaneous panniculitis-like T-cell lymphoma

Mycosis fungoides

Sézary syndrome

Primary cutaneous $CD30^+$ T-cell lymphoproliferative disorders

Lymphomatoid papulosis

Primary cutaneous anaplastic large cell lymphoma

Primary cutaneous γδ T-cell lymphoma

Primary cutaneous $CD8^+$ aggressive epidermotropic cytotoxic T-cell lymphoma

Primary cutaneous acral $CD8^+$ T-cell lymphoma

Primary cutaneous $CD4^+$ small/medium T-cell lymphoproliferative disorder

Peripheral T-cell lymphoma, NOS
Angioimmunoblastic T-cell lymphoma
Follicular T-cell lymphoma
Nodal peripheral T-cell lymphoma with TFH phenotype
Anaplastic large-cell lymphoma, ALK^+
Anaplastic large-cell lymphoma, ALK^-
Breast implant–associated anaplastic large-cell lymphoma

1.3.2. Current clinical management of T-cell malignancy

The standard treatment for patients with T-cell malignancies is the similar anthracycline-based chemotherapy CHOP or CHOP-like regimens used for B-cell lymphomas, including cyclophosphamide, doxorubicin, vincristine, and prednisone. However, the outcome for PTCL patients is significantly lower than patients with B-cell lymphomas, with a five-year overall survival (OS) of 41% vs 53%. While chemotherapy has improved for the response rate in adult and childhood T-cell lymphoma up to 90%[78,79], two-thirds of these patients relapse[76]. For these patients with relapsed T-cell malignancies, there are limited effective therapies. Other T-cell malignancies, such as cutaneous and peripheral T-cell lymphoma (CTCLs and PTCLs), have even poorer outcomes[76]. One-third of PTCL progress during primary therapy, the OS after relapse is 5.5 months[76].

The side effects of chemotherapeutic agents are also concerns. Because of the lack of specificity, most chemotherapies have negative effects on healthy cells, causing severe adverse events (AEs) in both haematological and non-haematological systems[80]. The most common AEs include leukocytopenia, neutropenia, anaemia, fatigue, alopecia, nausea[81].

Allogeneic stem cell transplantation (HSC) has been used to treat T-cell lymphoma and leukaemia in eligible patients, achieving long-term remission rates. Though it is considered as

the only curative strategy for a subset of T-cell lymphoma, the transplant-related mortality and graft versus host complication remain problematic[82-84]. Additionally, relapses after SCT are common, the majority of which occurred within 12 months[82].

While significant progress of immunotherapies, particularly immune cellular therapy, has been made in the treatment of B-cell malignancies, the outcome of patients with T-cell malignancies remains poor.

1.3.3. CAR-T cells for T-cell malignancy

Recently, immunotherapy has achieved an unprecedented efficacy in patients with either relapsed or refractory malignancies. CAR-T therapy is one of the most promising immunotherapies for cancers, achieving outstanding efficiency in B-cell malignancies. Several groups have developed CAR-T cells targeting different T cell antigens like CD3, CCR4, CD30, for the treatment of T-cell malignancies (Table 1.2).

Table 1.2 CAR-T cells for the treatment of T-cell malignancies

Target antigen	Modifications	Clinical trials	References
CD3	CD3 CRISPR/Cas9 KO		85
CD4		NCT03829540	86
CD5		NCT03081910	87
CD7	CD7 CRISPR/Cas9 KO	NCT03690011	88
CD30		NCT03049449, NCT01316146,	89

	NCT02690545, NCT02917083	
CCR4		90
TRBC1	NCT0359054	91
TRBC2		92

CD3 CAR-T

CD3 is expressed in the majority of T cells and a small number of T-cell acute lymphoblastic leukaemia (T-ALL). The restriction of CD3 expression in T cell subset and thymocytes[93] makes it a potential target of T-cell malignancies. Indeed, CD3-specific monoclonal antibody (mAb) has been assessed in patients with T-cell lymphoma and its safety was demonstrated[94]. Since the expression of anti-CD3 CAR on T cells leads to self-killing, so-called fratricide, removal of surface CD3 is required. CD3 CAR-T cells that avoid fratricide by gene disruption of T cell receptor α constant (*TRAC*) locus, showed robust cytotoxicity against $CD3^+$ childhood T-ALL *in vitro* and *in vivo*[85].

However, it also requires extra caution, because targeting CD3 on the tumour cell surface by CAR-T cells may cause T cancer cell activation and rejection of the infused CAR-T cells. More studies are required to the further clinical research for CD3 CAR-T cells.

CD5 CAR-T

CD5 is widely expressed in healthy T cells and ~80% of T-ALL and T-cell lymphoma, as well as a small population of B-cell lymphomas, but not in other hematopoietic cells[95,96]. CD5 was validated as a potential tumour target in clinical trials using CD5 mAbs, demonstrating the tolerability of this target[97-99]. CD5 molecule can be internalized upon ligation by the engagement with an antibody, which was used for preventing fratricide[87]. CD5 CAR-T cells

showed potent cytotoxicity against CD5-expressing T cell lines and primary tumour cells *in vitro*. CD5 CAR-T cells also significantly inhibit tumour progression in a xenograft mouse model of T-ALL[87]. Currently, a clinical trial is under recruitment to evaluate CD5 CAR-T therapy in a clinical setting.

CD7 CAR-T

CD7 is expressed on most normal T cells and NK cells, and on more than 95% of T lymphoblastic leukaemia and lymphomas[96,100]. CD7 was initially assessed as a tumour target in clinical trials using specific mAbs. Those trials showed that CD7-directed toxicities did not cause severe side-effect, but only achieved modest anti-tumour efficacy[101]. Lack of CD7 did not alter development, homeostasis, and function of murine T cells, which makes it a promising target for CAR-T therapy[96].

Several groups have independently demonstrated the feasibility and function of CD7-directed CAR-T against T-cell malignancies[88,102,103]. All of those studies showed that CD7 expression on CAR-T cells lead to fratricide that limited the *in vitro* generation of CAR-T cells. To avoid fratricide, CD7 must be removed from the cell surface, either by gene editing of CD7 gene locus[88,103], or by blocking intracellular trafficking of CD7 protein to cell surface[102]. CD7 CAR-T cells had robust cytotoxicity against $CD7^+$ T cell lines and primary T-ALL and T-cell lymphoma *in vitro* and *in vivo*. A Phase I clinical trial is being conducted to evaluate CD7 CAR-T cells.

CD30 CAR-T

CD30 is widely expressed on activated T and B cells, and also can be found on all Hodgkin lymphomas (HL) and subsets of TCL and T-ALL[104]. CD30 CAR-T therapy has been validated in two Phase I clinical trials for patients with HL[89,105]. In one clinical trial, one patient with relapsed HL achieved a complete remission (CR), which lasted three years[89]. In the other clinical trial by Wang *et al*. with eighteen patients recruited, seven patients had a partial response (PR), and six achieved stable disease (SD)[105]. Moderate adverse events were

observed in those clinical trials, but no severe toxicities were reported. Though only a limited proportion of T-cell malignancies express CD30, these encouraging results were the first CAR-T therapy which could target T-cell malignancies without impairing systemic T cell immunity.

CCR4 CAR-T

CCR4 is widely expressed in all adult ATLL, most CTCL and PTCL[106]. CCR4 is considered as a promising target in the treatment of T-cell malignancies, as its regular expression is limited in regulatory T cells (Tregs), Th2, and Th17 cell subsets[106-108]. Mogamulizumab, an FDA-approved CCR4-specific mAb, had modest anti-tumour efficacy in clinical trials for patients with ATLL and CTCL[109]. In a preclinical study, CCR4 CAR-T cells could effectively target $CCR4^+$ tumour cell lines *in vitro* and *in vivo*[90]. However, caution should be taken to evaluate CCR4 CAR-T therapy as targeting CCR4-expressing Tregs may lead to severe toxicities.

TRBC CAR-T

Two genes are encoding the T-cell receptor β-chain constant region (TRBC): *TRBC1* and *TRBC2*, each of which account about 35% and 65% of the T cells, respectively[110]. After demonstrating the TRBC monoclonality in T-cell malignancies, Maciocia *et al*. engineered T cells with a CAR specific to TRBC1 or TRBC2. The TRBC1/2-targeting CAR effectively eliminated tumour cells and maintained a considerable antiviral repertoire[91 92]. Currently, the safety and efficacy of TRBC1-targeting CAR-T cell therapy are being evaluated in a Phase I/II clinical trial.

CD4 CAR-T

CD4 is expressed in most mature TCLs and a subset of T-ALLs. The restriction of regular expression in T cells and some myeloid cells makes it another potential therapeutic candidate for T-cell malignancies[111]. Indeed, mAb therapy targeting CD4 have been assessed in the treatment of autoimmune disorders, CTCL and PTCL for over 25 years[112-114]. These studies

demonstrate that short-term CD4 cell reduction is well-tolerated and reversible. Pinz *et al*. developed an CAR against CD4 molecule in T cells and found the eradication of endogenous $CD4^+$ T cells during CAR-T manufacture. CD4 CAR-T cells showed potent cytotoxicity against $CD4^+$ tumour cells *in vitro* and xenograft models[86]. However, as complete depletion of $CD4^+$ cells will induce HIV/AIDS-like immunodeficient symptoms, it will be critical to eliminate CD4 CAR-T cells after eradication of tumour cells, allowing the recovery of $CD4^+$ cells from hematopoietic stem cells.

1.4. HIV-1 infection

1.4.1. The HIV Epidemic

The acquired immunodeficiency syndrome (AIDS) was first reported in 1981 in the United States[115]. Soon the human immunodeficiency virus (HIV), the cause of AIDS, was identified in 1984 by National Cancer Institute[116]. After discovery over 30 years, HIV/ AIDS has been a significant burden on society and is now the 6th leading reason of death worldwide (WHO, 2019).

At the end of 2018, 37.9 million people worldwide were living with HIV, with 2 million new infections in that year (UNAIDS, 2019). The socioeconomic disparity results in some regions being more severely affected than others. Particularly in Sub-Saharan Africa, nearly 5% of adults are living with HIV, but constitute 71% of those affected globally[117].

1.4.2. HIV Virus

Classification of HIV

HIV is a type of single-stranded, positive-sense, enveloped RNA virus. Upon entry into the target cell, HIV uses reverse transcriptase to convert RNA genome to double-stranded DNA. The viral DNA is then integrated into the host genome by an integrase enzyme and host co-factors[118]. Once incorporated, the virus may be transcribed along with the host cell's genes, producing new viral genes and viral proteins to assemble new copies of virus. In some cases, the virus may stay latent for decades.

There are two types of HIV identified: HIV-1 and HIV-2. HIV-1 is more transmissible and is the cause of AIDS, whilst the HIV-2 virus is thought to be less infective than HIV-1 and mainly confined to West Africa[119].

Origin of HIV

HIV is generally believed to originate as a result of the hybridization of two strains of simian immunodeficiency virus (SIV). The hybridized SIV was then believed to have infected chimpanzee in Central African, which was then passed to human through blood-to blood exposure and/or the consumption of bushmeat. A study in 2004 suggested that the common ancestor of HIV-1 group M, which results in almost 75 million infections to date, was highly likely to have emerged in Kinshasa around 1920. HIV probably arose from different SIV lineages since each is more closely related to a particular SIV than to each other. SIVcpz, a strain of SIV that infects wild chimpanzees in southern Cameroon, is almost identical to HIV-1 in humans[120]. However, the closest relative of HIV-2 is SIVsmm, a virus of the wild sooty mangabey of the Tai forest, an Old World monkey living in western Ivory Coast[121].

Structure and Genome of HIV

HIV is around 120 nm in diameter. The innermost of the HIV virion contains a nucleic acid core, including two copies of single strain RNA genome, enzyme integrase, reverse transcriptase and other viral proteins, as shown in Figure 1-6. The protein around the capsid is a matrix. The envelope outside of the matrix is formed when the capsid buds from the host cells. The envelope includes two types of glycoproteins (gp120 and gp41), by which HIV binds and invades the target cells[118].

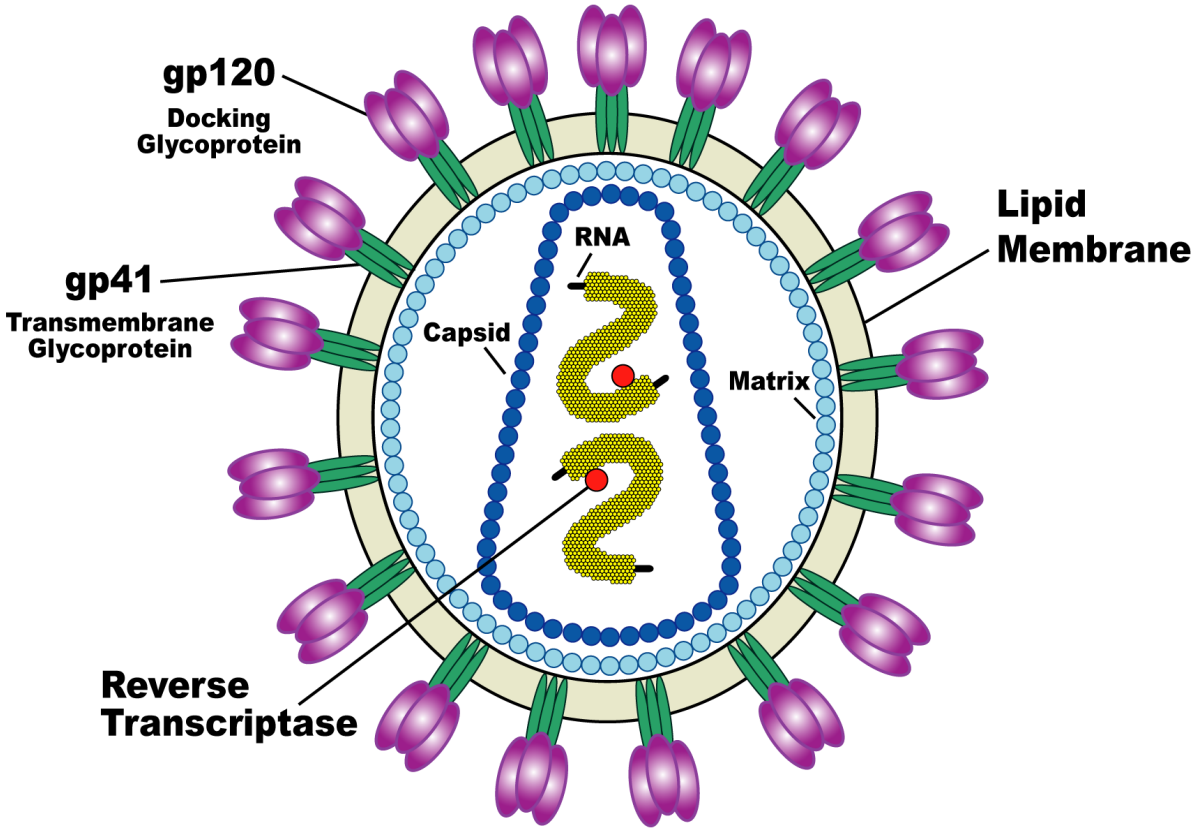

Figure 1-6 Diagram of HIV

Each virion expresses 72 glycoprotein projections composed of gp120 (purple) and gp41 (green). Gp120 serves as the viral receptor for CD4 on target cells. Gp41 is a transmembrane glycoprotein that crosses the envelope. The innermost of the virion is the viral core, which includes matrix (light blue) and capsid (dark blue). The HIV genome consists of two copies of single-stranded RNA (yellow), which are associated with reverse of transcriptase (red). Picture derived from Daniel *et al.*[118]

The proviral DNA of HIV-1 is produced by reverse transcription of the viral RNA. The DNA genome bears long terminal repeat (LTR) sequences at both ends (Figure 1-7). The *gag* gene encodes the major structural proteins of the virus, including the outer core membrane (p17), the capsid protein (p24) and the nucleocapsid (p7). The *gag* ORF (open reading frame) is followed by *pol* ORF, which encodes the enzyme protease (p12), reverse transcriptase (p51), RNase H (p15) and transcriptase (p51). The *env* ORF, adjacent to the *pol* gene, encodes two envelop glycoproteins gp120 (surface protein) and gp41 (transmembrane protein). In addition, the HIV genome encodes several regulatory proteins, including transactivator protein (Tat), RNA splicing-regulator (Rev), negative regulating factor (Nef), viral infectivity factor (Vif), virus protein r (Vpr) and virus protein unique (Vpu)[118].

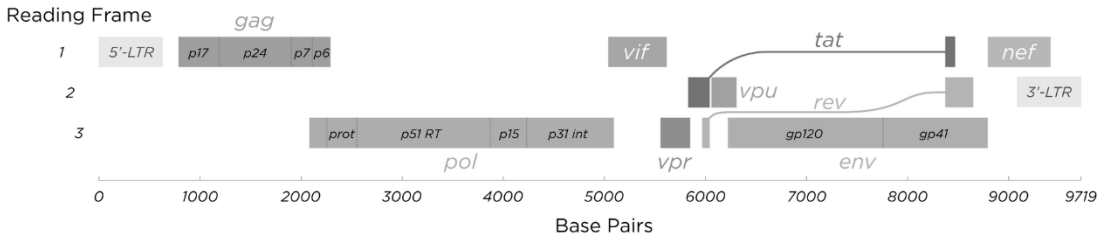

Figure 1-7 Structure of the RNA genome of HIV-1

Structure and organization of the HIV-1 provirus. The genome of HIV-1 contains about 9,200-9,600 nucleotides. The genome contains nine genes that encode fifteen viral proteins. Picture derived from Daniel *et al*.[18]

CD4: HIV-1 primary receptor

The entry of HIV to cells initiates through the interaction of trimeric envelope complex (gp160 spike) on the virus and primary receptor CD4 and co-receptor CCR5 or CXCR4[122,123]. Gp120 binds to the CD3 binding domains, initiating the structural change of envelope complex and exposing the binding site of CCR5 or CXCR4 to gp120. The N-terminal fusion peptide gp41 is allowed to penetrate the cell membrane. After the virus has bound to the cell membrane, the viral RNA and various enzymes are injected into the cells[123].

Based on its critical role in HIV infection, many studies have been conducted to develop anti-HIV strategies based on CD4. Inhibition of virus infection by TNX-355, a humanized monoclonal antibody that targets the CD4 molecule, was assessed in clinical trials[124,125]. TNX-355 binds to the second domain of the extracellular part of CD4, and blocks CD4-dependent HIV entry. Weekly administration of TNX-355 to HIV-1 infected volunteers showed no drug-related severe adverse effects[124]. Administration of TNX-355 reduced plasma viremia and increased $CD4^+$ T cells in peripheral blood[125]. Another preclinical study with SIV infected rhesus macaques (RMs) assessed CD4 depletion by administrating the rhesus macaque CD4R1, a recombinant anti-CD4 antibody[126]. They found a shift in the tropism of infected cells from $CD4^+$ T cells to other CD4-low cells, such as macrophages, microglia. Though the anti-HIV efficacy is modest, these immunotherapies demonstrated CD4 as a potential target for HIV eradication studies.

CCR5, an HIV-1 co-receptor

Besides the primary receptor CD4, HIV-1 requires the presence of a co-receptor to bind and enter the host cells. Two co-receptors have been identified: CCR5 and CXCR4, which stand for R5 tropic and X4 tropic strains, respectively.

Both CCR5 and CXCR4 belong to G-protein-coupled receptors (GPCRs) family. For R5 tropic virus, following the engagement of the HIV envelope glycoprotein gp120 and CD4, CCR5 then forms a complex with CD4 and HIV, allowing viral entry into the cell. CXCR4 is very similar to CCR5 in structure[127].

There is a small population with a natural 32 base pair homozygous depletion (Δ32) in CCR5 genome locus. Individuals with Δ32 mutation show resistance to R5 tropic HIV-1 infection[128]. Thus, CCR5 is a potentially desirable target for HIV treatment by mimicking the natural CCR5 mutation. Indeed, the only two cases of HIV remission in history were achieved by stem cell transplantation donation with Δ32 homozygous mutation[129].

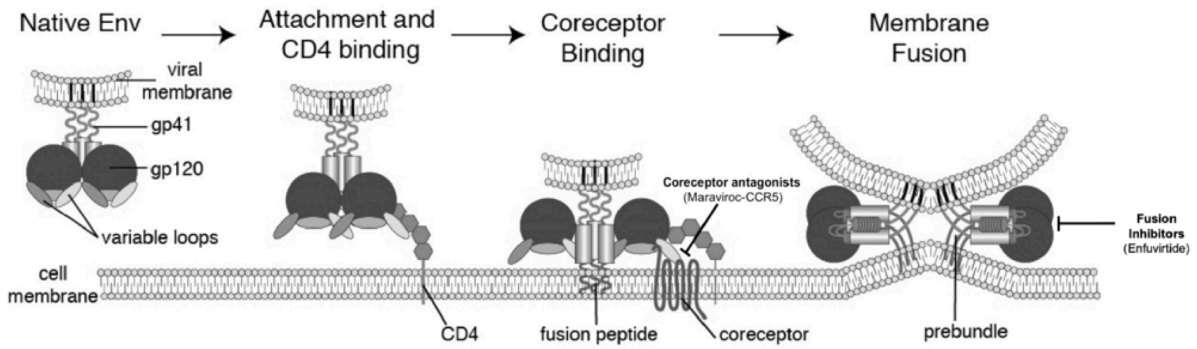

Figure 1-8 Overview of HIV entry.

The first event of HIV entry is that HIV env portion binds CD4 on the surface of host cell, which induces conformational changes of env. The co-receptor CCR5 subsequently binds CD4 and virus, which triggers the penetration of the fusion peptide of gp41 into the cell membrane, allowing the virus entry into the cell. Picture derived from Pierson *et al*.[123].

1.4.3. Pathogenesis and treatment for HIV infection

The clinical course of HIV-1 infection

After transmission, the infection of HIV-1 induces a high peak of plasma viral load within several weeks without treatment[130], which will later decrease with the development of immune response against HIV-1 virus[131]. The HIV-1 virus disseminates to the immune organs, and establishes a viral reservoir and latency subsequently[132-134]. Gradual elimination of the $CD4^+$ T lymphocyte population is the immunological hallmark of AIDS.

Combination antiretroviral therapy

In 1987, the first effective therapy for HIV, nucleoside reverse transcriptase inhibitor (NRTI) zidovudine (AZT) was approved by FDA. To date, the most popular treatment is combination antiretroviral therapy (cART), which consists of several medications belonging to two to four types of antiretroviral agents[135]. Generally, cART consists of a non-nucleoside reverse transcriptase inhibitor (NNRTI) plus two NRTIs. Usually, NRTIs include zidovudine (AZT) or

tenofovir (TDF) and lamivudine (3TC) or emtricitabine (FTC)[136]. cART is effective in about 95% of HIV-1 patients during the first year[137].

However, the long-term cART taken will induce some adverse effects. Some relatively common adverse events include diarrhoea, nausea, rash, higher levels of cholesterol and triglycerides. Other common symptoms include hypersensitivity or allergic reactions, bone loss, high blood sugar and diabetes[138].

1.4.4. HIV reservoir: the obstacle for HIV cure

cART has achieved robust success in HIV control, transforming HIV infection into a chronic disease. However, even long-term treatment of cART is not able to eliminate HIV-infected cells from the body, which means lifelong therapy is the only option for HIV-infected patients. Once cART is interrupted, these latencies will immediately fuel viral rebound and cause significantly high-level viremia within two weeks.

Memory $CD4^+$ T cells have been widely considered as the most important reservoir for HIV in patients on cART[139,140]. After being infected by HIV, some $CD4^+$ effector cells can differentiate to a long-lived memory state[141]. Among different types of memory $CD4^+$ T cells, central memory $CD4^+$ T cells are considered as the primary reservoir of HIV[139,140]. One group recently identified CD32 as a marker of latent HIV-infected $CD4^+$ T cells[142]. However, the conclusion was not repeated by several other studies and needs to be validated further[143-146].

Other cell subtypes have also been implicated as a source of the latent reservoir. Macrophages are a target of HIV infection because of their expression of CD4 and co-receptors[140], but their role in the establishment of HIV reservoir is still debated[140,147]. The diversity of macrophages increases the difficulty of the studies on HIV latency in these cells. Macrophages are intrinsically resistant to the cytopathic effect, which would potentially facilitate them to latent reservoir[148]. Besides, dendritic cells (DCs) are also susceptible to HIV

infection *in vitro*. Although DCs appear less susceptible to HIV infection than $CD4^+$ T cells *in vivo*, they are considered as a potential source of the HIV reservoir[149].

1.4.5. T Cell-based Gene Therapy for HIV

Despite the significant success of cART for the treatment of HIV infection, the virus is not eradicated from the infected individual. Some infected cells persist for decades, leading to viral rebound following cART interruption. Recently, T-cell based immunotherapy for cancer has been widely studied. Whether the use of T cells can be applied for treating HIV infection remains to be investigated. However, a few studies have been performed to ask the question[150].

Endogenous HIV-specific T Cell

The response of HIV-specific cytotoxic T lymphocyte (CTL) is essential to control HIV infection and strongly correlates with decreases in viral load in patients. CTLs are thought to identify and lyse infected cells with HIV antigen presentation[151]. A strong immune response of $CD8^+$ T cell against HIV is frequently found in HIV elite controllers, patients who can keep the virus in check[131]. $CD8^+$ T cells isolated from elite controllers can effectively recognize and kill HIV-infected $CD4^+$ T cells *ex vivo*[152].

However, for the majority of patients, it is impossible to prevent AIDS without an antiretroviral therapy regimen. There are probably multiple reasons for this. For example, Tregs in patients have shown the ability to inhibit anti-HIV immune responses of CTLs[153]. Moreover, due to the high mutation rate of HIV, a decrease in plasma viral loads is usually unstable[154]. CTLs from HIV^+ patients show exhaustion markers, such as PD-1, due to prolonged antigenic stimulation. Additionally, several lines of evidence indicate that the benefit of $CD8^+$ T cell responses may be restricted to certain HLA alleles. Most of elite controllers are HLA-B*5701. CTLs from these

individuals show robust specificity for the Gag epitope TW10 (240-249), which is a relatively conserved region because mutant variants are disadvantaged in their replicative capacity[155].

Redirecting CD8$^+$ T Cells to HIV

Though HIV-specific CTLs initially exist in most patients, their inability to control virus suggests the quality but not the quantity of T cells is more important for therapeutic development. Consequently, one idea is to improve the recognition and cytotoxicity of CTLs to HIV-infected cells. Currently, the T-cell based cellular therapy research field is split into two main approaches, artificial TCR-T and CAR-T cell. Each has its own advantages and disadvantages.

TCR-T cells are more like natural T cells, but its obstacle is to find the ideal TCR receptors with ideal specificity and affinity to a certain antigen. CD8$^+$ T cells artificially expressing SL9 TCR, which recognized HLA-A02/HIV-1-gag p17 epitope SLYNTVATL, showed specificity and cytotoxicity against infected cells *in vitro*, and SCID humanized mice[156]. However, the death of two participants in a different trial with artificial TCRs technology indicates the concerns about off-target toxicity. Moreover, because T cell specificity is restricted by HLA allele, which means patients' eligibility has been highly limited. Additionally, the artificial TCR could probably mispair with endogenous TCR α and β chains, generating off-target specificities. Also the artificial TCR can also compete for endogenous CD3 with endogenous TCRs, which is also a concern in this field.

Compared with artificial TCRs, CAR technology has one advantage that the antigen recognition of CAR- T cells is not limited by MHC-I expression and presentation, while Nef of HIV will downregulate MHCI expression[157,158]. The efficacy of CARs technology has been validated for patients with CD19$^+$ B cell malignancies[26,27].

Though CAR-T therapy has made an enormous impact on cancer treatment, the first study to utilize the concept of "chimeric antigen receptor" was for HIV disease. In 1991, Romeo *et al*.

engineered $CD8^+$ cytolytic cells with chimeric proteins, composed of the extracellular domain of CD4 and the intracellular domain of CD3ζ[159]. By utilizing the antigen recognition of CD4 and intracellular signalling domain of CD3ζ (considered as first-generation CAR construct), this construct efficiently eliminated envelope-expressing cells *in vitro*. In a pioneering clinical trial, both $CD4^+$ and $CD8^+$ T cells equipped with CD4ζ CAR persisted for longer than ten years, despite the low frequency (0.01%-0.1% circulating CD4ζ CAR-T cells), without evidence of toxicities. Unfortunately, the impact on HIV viral load was low[160,161], likely because of limited persistence of the CAR-T cells, suboptimal CAR constructs, and the potential risk for HIV entry upon transgenic CD4 expression on the CAR-T cell surface.

First-generation CAR-T therapies had limited efficacy for cancer treatment. However, the addition of co-stimulatory domain to CAR construct achieved a significant improvement in clinical efficacy[27,50,162,163]. The signal 2 provided by co-stimulatory molecules is important for the activation and persistence of engineered T cells. After the success of second-generation CAR-T therapy for hematopoietic malignancies, several new generation anti-HIV CAR-T therapies were developed and evaluated[164-169]. Almost all of these constructs were functional. Some studies continued to optimize the CD4ζ CAR with second or third-generation CAR constructs. The optimized CD4ζ CAR was validated *in vitro* and *in vivo* in humanized mice and non-human primate (NHP) models[170,171]. However, it is still a concern if the expression of CD4 extracellular binding domain will render increased infectivity of engineered T cells.

Meanwhile, some studies validated the feasibility and efficacy to utilize broadly neutralizing antibodies (bNAbs) as the antigen-binding domain of CARs[160,161]. The new generations of bNAbs isolated from infected individuals have specific and broad binding affinity to the HIV-1 virus. Indeed, bNAb-based CAR-T cells showed potent cytotoxicity against HIV-infected cells *in vitro*. However, very few of these constructs have been assessed *in vivo* models of latent infection.

1.5. Aims and objectives

The overarching aim of this project is to systematically investigate the feasibility of CD4-directed CAR-T cell therapy for T-cell malignancies and HIV-1 infection *in vitro* and *in vivo*.

To specify the objectives:

- To generate a third-generation CAR construct with CD4-specificity, tracking marker, and safety switch.
- To phenotypically characterize T cells transduced with the CART4 construct.
- To characterize the anti-tumour efficacy of CART4 cells *in vitro* and xenograft model of T-cell leukaemia.
- To characterize the anti-HIV function of CART4 *in vitro* and humanized mice model with HIV infection.

Chapter 2. Materials and Methods

2.1. Tissue culture

2.1.1. Maintenance of cell lines

All the cell lines used in this thesis were listed in ***Table 2.1***. For the adherent cell lines, the medium was composed of 90% High glucose Dulbecco's Modified Eagle Medium (DMEM), 10% fetal bovine serum (FBS), 100 IU/mL penicillin, 100μg/mL streptomycin, and 2mM L-glutamine (all from Gibco) (D10). Every two to three days, all the adherent cells were dissociated from flasks or plates by trypsinization with trypsin-ethylenediaminetetraacetic acid (0.25% Trypsin-EDTA, Gibco) for 2 minutes. After neutralization with D10 medium, the cell suspension was centrifuged and resuspended in fresh D10. For Plat-GP and 293T cell line, passage them one to five; for PG-13 cell line, passage it on to ten, as PG-13 grows much faster.

The suspension cell lines were cultured in the R10 medium, which was composed of 90% Roswell Park Memorial Institute Medium 1640 (RPMI 1640), 10% FBS, 100 IU/mL penicillin, 100μg/mL streptomycin, and 2mM L-glutamine (all from Gibco). They were split every three days by discarding four-fifths of total cell suspension and supplying fresh R10.

Table 2.1 Cell lines used in this thesis

Cell Line	Description	Source
Plat-GP	Transient retroviral packing cell line	Cell Biolabs
PG-13	Stable retroviral packing cell line	ATCC
BCL	B cell lymphoblastoid cell line	CIV lab

293T	Lentiviral packing cell line	Prof. Lishan Su's lab, UNC
Jurkat	Immortalized T lymphocyte cell line	ATCC
CEM-ss	T lymphoblast cell line	NIH AIDS Reagent Program

2.1.2. Isolation of human PBMCs and T cells

The whole blood was collected from healthy donors using a 21-gauge butterfly needle. Blood was collected into EDTA collection tubes and transferred into a 50 ml Falcon tube immediately. The peripheral blood mononuclear cells (PBMCs) were isolated from blood using density gradient centrifugation over Histopaque (Sigma). The blood was added by the same volume of PBS and mixed by pipette. Transfer 15 ml of Histopaque to a clean 50 ml Falcon tube. Tilt the tube as close to horizontal as possible. Draw up the PBS-diluted blood into a 25 ml pipette and layer on the top of the Histopaque gently, without disrupting the interface between the blood and Histopaque. Centrifuge the tubes at 500 g for 25 minutes, with the brakes set to the zero. Transfer the PBMCs layer, which presented at the interface between the Histopaque and the plasma, to a clean 50 ml Falcon tubes with a sterile Pasteur pipette. Centrifuge the cells at 500 g for 10 minutes after diluting with PBS to a final volume of 50 ml. Aspirate the supernatant and resuspend the cells in 50 ml PBS. Repeat centrifuge and aspirate the supernatant. The isolated PBMCs are then ready for further applications or cryopreservation.

In some experiments, PBMCs or manufactured $CD3^+$ T cells were separated for $CD8^+$ T cells by using untouched microbeads human CD8 T cell kit (Miltenyi). Before adding Biotin-Antibody Cocktail, determine cell number and resuspend cell pellet in 40 µL of MACS buffer (PBS added 1% FCS and 2 mM EDTA) per 10^7 total cells. Add 10 µL of Biotin-Antibody Cocktail per 10^7 total cells. Mix well and incubate at 4°C for 10 minutes. Then add 20 µL of $CD8^+$ T Cell MicroBead Cocktail and 30 µL of MACS buffer per 10^7 total cells. Mix well and incubate at 4°C

for 10 minutes. Plate LS or MS column to a suitable MACS separator. Rinse the column by adding 3 ml MACS buffer. Then apply the cell suspension to the column and wash the column with 3 ml MACS buffer. Collect the flow-through containing unlabelled cells, representing enriched $CD8^+$ T cells. The cells were subsequently counted by automatic Vi-cell XR cell counter (Beckman), and assessed CD8 purity by flow cytometry analysis (BD).

2.1.3. Activation and expansion of human T cells

Human PBMCs can be prepared from fresh blood or recovered from frozen aliquots. To activate T cells, Dynabeads Human T-Activator CD3/28 (Life Technologies) was washed by PBS and mixed with PBMCs in R10 to obtain a bead-to-cell ratio of 1:1. The cells were plated at a density of 2 $x10^6$ /ml in a six-well plate (4 ml per well). 10 ng/ml Human IL-7 and 14 ng/ml IL-15 (Miltenyi) were added 24 hours after stimulation and replenished every two to three days.

After two to three-day activation, the cells are ready for CAR transduction or expansion. For the conventional expansion method, the T cells would be replenished with fresh R10 and cytokines IL-7 and IL-15 every two to three days, to maintain cell concentration at 0.5-1$x10^6$ cells/ ml. Usually, cells were harvested on the 14^{th} day.

To expand cells in the G-Rex culture plate, 10-20 $x10^6$ activated T cells were transferred to G-Rex six-well plate with 130 ml of R10 supplied with IL-7 and IL-15, to achieve cell confluency at 1-2 $x10^6$ cells/ cm^2. The cytokine combination of IL-7 and IL-15 was added every two to three days. Harvest the cells on 15^{th} day.

2.1.4. Cryopreservation and revival of cells

The cells for cryopreservation were collected and centrifuged at 300 g for 5 minutes. After discarding the supernatant, resuspend the cell pellets at the desired concentration with freezing medium, which was composed of 90% FCS and 10% dimethyl sulfoxide (DMSO).

The cell suspension was immediately aliquoted into sterile 1.8 ml CryoTubes (Corning). Place the CryoTubes in an isopropanol-filled freezing container and frozen at -80℃, to reduce the temperature of the vials by 1°C/minute. On the next day, the vials were transferred in liquid nitrogen for long-term storage.

2.2. Molecular biology techniques

2.2.1. Cloning CD4- or CD20-targeting CAR into MSCV retroviral vector

The diagrams of CD4- and CD20-specific CAR used throughout this thesis are shown in *Figure 2-1*. The DNA sequences of the mouse IgG antibodies Hu5A8 and Leu16 were found from public patents (CN103282385, US6410319B1). The DNA fragments encoding the scFv of Hu5A8 and Leu16 and human Igκ leading sequence were synthesised by Genewiz. *NcoI* and *NotI* were used to cleave these fragments as well as MSCV CAR expression retroviral vector. MSCV CAR expression vector was modified from MSCV-IRES-GFP vector (Addgene) by replacing IRES-GFP area with human CD8 transmembrane domain and third-generation CAR intracellular signalling domain (costimulatory domains of CD28 and 4-1BB, CD3ζ signalling domain). Following restricted enzymes digestion, the DNA fragments were run on a 1% agarose gel. The bands with correct size were collected, and DNA extracted using the QIAquick Gel Extraction Kit (Qiagen). The ligation reaction was performed with each insert and vector backbone using T4 ligase (New England Biolabs). The *E.coli* DH5a bacteria were transformed with the ligated solutions and spread on ampicillin LB plate. Single clone was picked and inoculated to 5 ml LB medium. Plasmid DNA was extracted using QIAprep Spin Miniprep Kit (Qiagen) according to the manufacturer's instructions. The extracted DNA was confirmed by double-digestion and DNA sequencing. The bacteria clones with correct DNA

sequence were expanded in 100 ml LB medium. The QIAprep Spin Midiprep Kit (Qiagen) was used to obtain large quantities of vector purification.

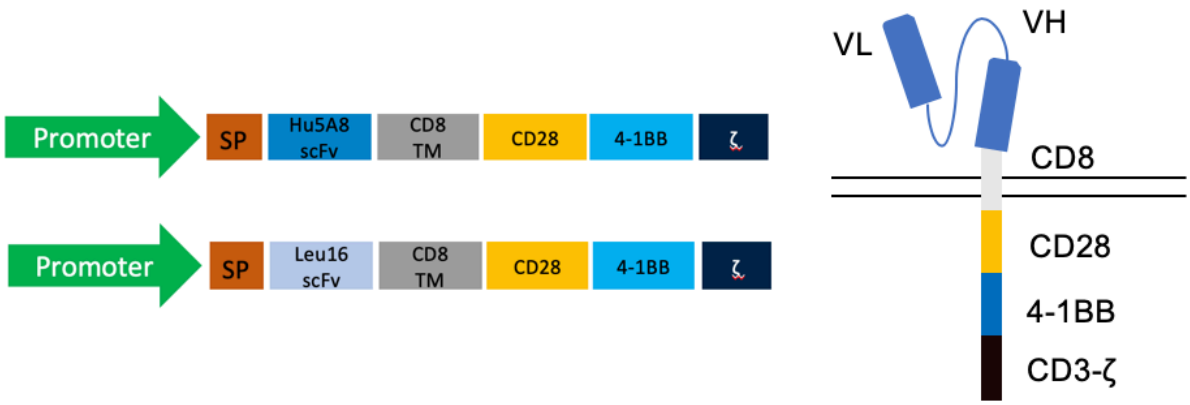

Figure 2-1 Schematic representation of the third generation CD4- and CD20-targeting CAR construct used in this thesis

Sequence portions of the CD4- and CD20-specific, CD28/4-1BB costimulatory CAR, are indicated, along with the phosphoglycerate kinase 1 (PGK) promoter sequences, Igκ chain leader sequence (SP). ScFv: single-chain variable fragment; TM: transmembrane motif; ζ: CD3 ζ chain.

2.2.2. Cloning truncated human EGFR into CAR vector

The tEGFR was used to track CAR-expressing cells in this thesis, as shown in Figure 2-2. The sequence of tEGFR was obtained from the public patent (US 8802347B2), deleting Domain I and II of extracellular part and intracellular domains of human EGFR protein[63]. The tEGFR was synthesised by Genewiz with the self-cleaving T2A sequence and the human granulocyte-macrophage colony-stimulating factor (GM-CSF) receptor's leader peptide. The DNA fragment was inserted into the MSCV CAR construct by a T4 ligation reaction. The final construct was confirmed by double-digestion and sequence analysis.

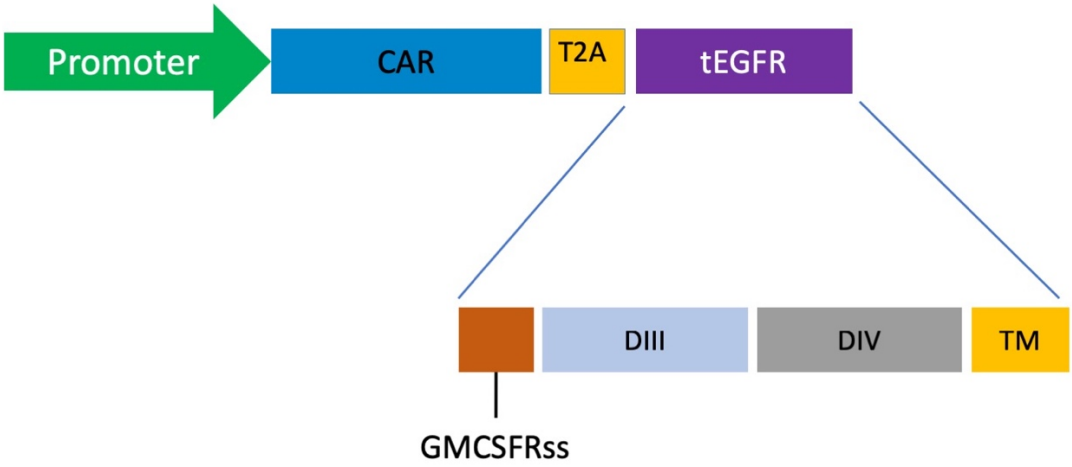

Figure 2-2 Schematic of the tEGFR amino acid sequence and CAR-T2A-tEGFR contained in the MSCV retroviral vector

Amino acid ranges that were used from the GM-CSF receptor-α chain signal sequence (GMCSFRss, which directs surface expression) and the truncated EGFR sequence (domains III, IV and the transmembrane domain) are indicated.

2.2.3. Cloning inducible Caspase-9 safety switch into CAR vector

The DNA sequence of iC9 was kindly provided by Prof. Lishan Su from the University of North Carolina at Chapel Hill. The DNA fragment of iC9 consists of truncated caspase 9, including its large and small subunit of caspase molecule linked to one 12-kDa human FK506 binding proteins (FKBP12) via a short Gly-Gly-Gly-Ser (GGGS) flexible linker[68], as shown in Figure 2-3. The DNA was synthesised by Genewiz with the self-cleaving P2A sequence and inserted into MSCV-CAR-tEGFR retroviral vector by T4 ligation reaction. The final construct was confirmed by double-digestion and sequence analysis.

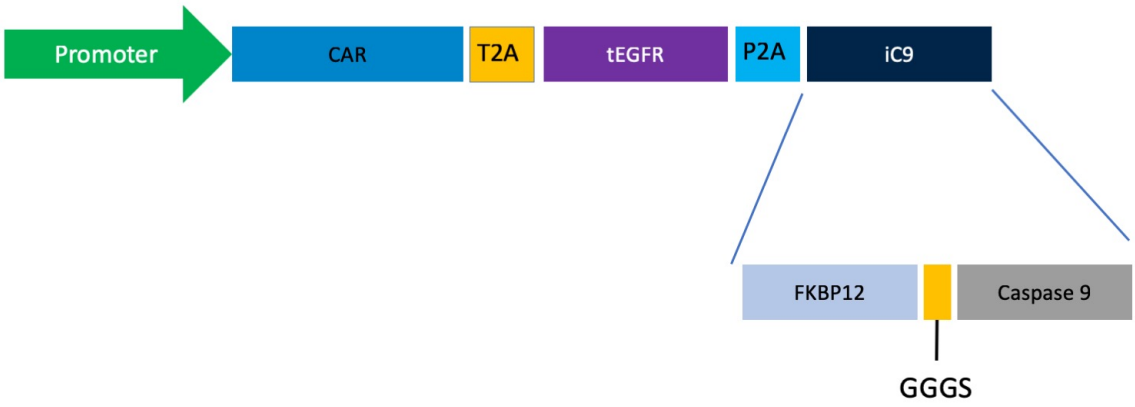

Figure 2-3 Schematic of the iC9 amino acid sequence and CAR-T2A-tEGF-P2A-iC9 contained in the MSCV retroviral vector

The schema diagram indicates sequence portions of iC9, which consists of FKBP12 with an F36V mutation combined with truncated caspase 9 protein via GGGS linker to enhance flexibility.

2.2.4. DNA sequencing

DNA was sent and sequenced by Genscript using primers custom-made. The sequencing result was analysed by Snapgene software.

2.3. Transduction Protocols

2.3.1. Transfection of Plat-GP cell line with retroviral vectors

The Plat-GP retroviral packaging cell line (Cell Biolabs) was derived from 293T cell line with the insertion of gag and pol genes, achieving high retroviral yield. By co-transfection with VSV-G envelope vector and transfer vector containing the interested gene, the cell line produce pseudotyped pantropic retrovirus, which can easily infect nearly any cell types. Here the Plat-

GP cell line was utilized to produce retroviral particles and infect another cell line for a stable virus-producing cell line.

The Plat-GP cells were maintained in D10 and passaged one to five every three days. On the day before transfection, $1.5x10^6$ cells were plated to one well of a six-well plate with 2 ml D10. The cells would reach 80-90% confluency the next days. To prepare transfection mixture, 0.5 μg pCMV-VSV-G vector and 2 μg CAR vector were added to 200 μl Opti-MEM serum-free medium (Gibco). After 5 minutes of incubation at room temperature, 7 μl of X- tremeGENE HP Transfection Reagent (Roche) was added and mixed by pipette. The solution was incubated for another 15 minutes, before being added to the target well in a dropwise manner.

After 24 hours, replace the medium with fresh D10. The supernatant containing retroviral particles was harvested after 48 hours and 72 hours post-transfection. The supernatant was centrifuged at 300 g for 5 minutes to remove host cells, before being aliquoted and stored at -80℃.

2.3.2. Establishment of stable retrovirus producing PG-13 cell line

The retrovirus produced by Plat-GP cell line was less amenable for transfection for human T cells. Thus, a subsequent stable virus-producing cell line with PG-13 was performed. PG-13 cell line was derived from TK-NIH/3T3 cell and based on the Gibbon ape leukaemia virus (GaLV). PG-13 cell line was widely used to establish stable virus-producing cell bank for large-scale virus production.

On the day for transduction, $0.3x10^6$ PG-13 cells were propagated in a well of the six-well plate containing 2 ml of D10 medium at 37℃ and 5% CO_2. The cells would reach 30% confluency the next days in order to achieve productive infection by Plat-GP derived viral particles. Replace the medium with 2 ml of Plat-GP derived viral particles containing 8 μg/ml polybrene (Sigma). The plate was wrapped with cling-film and centrifuged at 1000 g at 32℃

for 2 hours. The plate was returned to the incubator for 24 hours. 2 ml of fresh D10 was added to maintain the necessary nutrition for cell growth.

The transduction efficiency could be assessed by flow cytometry analysis in two days post-transduction. In brief, the cells were trypsinised and stained with Biotin-labelled anti-EGFR antibody (R&D Systems). Incubate on ice for 20 minutes followed by one wash using PBS. A second antibody PE streptavidin was added to cells for another 20 minutes. Analyse stained cells by flow cytometry after two washed using PBS. Ensure that PG-13 cell line generated as described above is close to 100% positive for CAR expression.

The transduced cells were maintained in a T75 flask. To produce high titre viral particle, passage the confluent cells one in two by trypsinisation. Collect the supernatant after 24 hours. Aliquot the medium and store at -80℃ after centrifuging at 300 g for 5 minutes.

2.3.3. Retroviral transduction of primary human T cells

Human PBMCs can be prepared from fresh blood or recovered from frozen aliquots. To activate T cells, Dynabeads Human T-Activator CD3/28 (Life Technologies) was washed by PBS and mixed with PBMCs in R10 to obtain a bead-to-cell ratio of 1:1. The cells were plated at a density of 2 x10^6 /ml in a six-well plate (4 ml per well). Human IL-2 (Roche) was added 24 hours before performing gene transfer. Retroviral transduction was performed 48 hours after T-cell activation.

One day before retroviral transduction, prepare RetroNectin (Takara Bio) coated plates following the manufacturer's instruction. In brief, add 1 ml PBS containing 15 μg RetroNectin to a well of the non-tissue culture treated twenty four-well plates. Wrap the plate by fling-film and keep in 4℃ fridge over-night. On the day of gene transfer, remove unbound RetroNectin from the plate and wash twice with PBS. Transfer 1 ml of PG-13 viral conditioned medium to each well of the RetroNectin-coated plate. Centrifuge the plate at 1000 g at 32℃ for 2 hours.

During the centrifuge, collect the activated PBMCs, which are activated $CD3^+$ T cells mainly. Centrifuge the cells and resuspend the pellet by R10 containing 100 U/ml IL-2 to 1 $x10^6$ /ml. Discard the supernatant from the plate after the centrifuge. Add 1 ml of cell suspension and centrifuge at 500 g for 10 minutes. Return the plate to the incubator. Repeat the transduction step to achieve higher transduction efficiency, if necessary.

Two days after gene transfer, analyse transgene expression by flow cytometry. Typically, a transduction efficiency above 40% is expected.

2.3.4. Lentivirus production and transduction of CEM-ss cell line

A third-generation lentivirus production with 293T was performed. Seed 1.2 $x10^6$ 293T cells (ATCC) to one well of a six-well plate with 2 ml D10. The cells would reach 80-90% confluency the next days. Replace the medium by 2 ml fresh D10 2 hour before transfection. To prepare transfection mixture, 0.25 μg pMD2.G envelope plasmid, 0.75 μg psPAX2 packaging plasmid and 1 μg pF12-eGFP-Gussia Luciferase plasmid were added to 20 μl Opti-MEM serum-free medium. In another polypropylene tube, add 74 μl OPTI-MEM and 6 μl Lipofectamine 2000 transfection reagent (Invitrogen). Mix by swirling or gently flicking the tube. After 5 minutes of incubation at room temperature, Add 80 μl of Lipofectamine 2000 master mix each containing vector mixture for a total volume of 100μl. Pipette master mixes directly into the liquid and not onto the walls of the tube. Mix by swirling or gently flicking the tube. Incubate for 20 – 30 minutes at room temperature. Retrieve HEK293FT cells from incubator. Without touching the sides of the dish, gently ass DNA: Lipofectamine 2000 mix dropwise to cells. Swirl to disperse mixture evenly. Do not pipette or swirl too vigorously, avoiding to dislodge the cells from the plate.

After 24 hours, replace the medium with 1 ml fresh D10. The supernatant containing lentiviral particles was harvested after 48 hours and 72 hours post-transfection. The supernatant was

centrifuged at 300 g for 5 minutes to remove host cells, before being aliquoted and stored at -80℃.

The protocol for CEM-ss cell transduction was similar to the retroviral transduction of primary T cells described above. By one round transduction, almost 100% of CEM-ss cells were GFP-positive by flow cytometry analysis.

2.4. Phenotypic and functional assay for CAR-T cells

2.4.1. Flow cytometry of transduced T cells and target cells

The antibodies used to label CAR-transduced T cells, and target cells were listed in Table 2.2. The cells were collected and washed using PBS by centrifuge at 500 g for 5 minutes. After being resuspended in 100 μl PBS containing a specific concentration of antibodies, the cells were incubated in the dark at 4℃ for 30 minutes. They were washed with five to ten-volume of PBS for another centrifuge at 500 g for 5 minutes and resuspended with 300 μl PBS before flow cytometry analysis. T cells with successful CAR transduction were identified by positive staining of EGFR marker, which was included in the CAR construct and co-expressed in the host cells (Figure 2-2).

Flow cytometry analysis was also performed to quantify CD4 expression on relevant target cells. The staining protocol was similar to the one described above.

Table 2.2 List of Antibodies used for staining transduced T cells and target cells for CD4 expression.

Target	Clone	Conjugation	Manufacture	Dilution
Human CD3	OKT3	APC-Cy7	Biolegend	1:100
Human CD4	RPA-T4	PE-Cy7	Biolegend	1:100
Human CD8	RPA-T8	FITC	Biolegend	1:100
Human CD20	2H7	Pacific Blue	Biolegend	1:100
Human EGFR	Cetuximab	Biotin	R&D Systems	1:100
Biotin	Streptavidin	PE	Biolegend	1:200
Mouse IgG F(ab)'$_2$	Polyclonal	Biotin	Jackson ImmunoResearch	1:50
Human CD45RO	UCHL1	APC	Biolegend	1:100
Human CD62L	DREG-56	PE-Cy7	Biolegend	1:100

2.4.2. Co-culture cytotoxicity assay

This non-radioactive killing assay was performed as previously reported[172]. In brief, target cells were stained with 1 μM CFSE (Biolegend) for 15 minutes at 37℃. After being washed with PBS for three times, 100,000 target cells were mixed with CAR-T cells in ratio at 1:1, 1:3, 1:5. The 200 μl co-culture was incubated for 4 hours in the incubator at 37℃. 1 μl DAPI and 5μl Countbright beads (BD Biosciences) were added to the samples. The samples were acquired by flow cytometry at constant speed. The gating strategy was shown in Figure 2-4.The number of surviving target cells was calculated as follows:

Cells in tube = (cells collected/ beads collected) x total beads added to the tube.

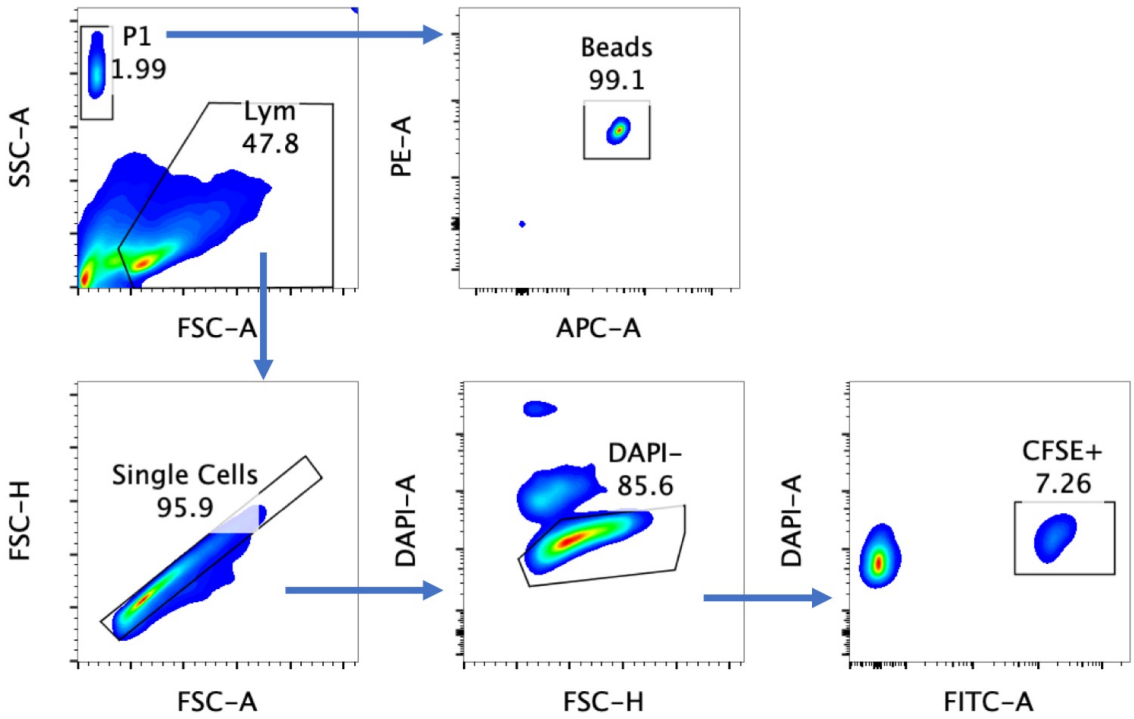

Figure 2-4 Gating strategy for flow cytometry analysis of cytotoxicity result

The CountBright beads were first gated by SSC and FSC, as they were smaller than cells. The second gating with PE and APC channels was to further exclude non-CountBright-beads noise. Surviving target cells were gated on lymphocyte and single cells, before gating on $DAPI^-$ and $CFSE^+$.

2.4.3. Intracellular cytokine staining

CART4 or CART20 T cells were co-cultured with specified target cells in 96-well u bottom plates. All the cells were seeded at $2x10^5$ cells/well in 200 μL/well R10 medium. T cells cultured alone as negative control, and T cells cultured with the combined stimuli of 10 ug/ml PMA and 10 ug/ml Ionomycin (Biolegend) were included as positive control. 10 μg/mL brefeldin A (Biolegend) was added to all the wells after one-hour incubation. The co-culture system was incubated for another five hours before being harvested. The cells were stained for surface markers using the antibodies specified in Table 2.3 for 30 minutes in the dark. The cells were fixed by using 4% paraformaldehyde solution (Biolegend) for 15 minutes at room temperature after being washed with PBS. After another wash with fix buffer, cells were

resuspended by a mixture containing intracellular staining antibodies. Incubate the cells at 4℃ for 30 minutes before washing with fix buffer. They were analysed by flow cytometry with fluorescence minus one (FMO) controls, to determine the expression level of IFN-γ and TNF-α.

Table 2.3 List of Antibodies used for intracellular cytokine detection

Target	Clone	Conjugation	Manufacture	Dilution
Human CD3	OKT3	APC-Cy7	Biolegend	1:100
Human CD8	RPA-T8	FITC	Biolegend	1:100
Human EGFR	Cetuximab	Biotin	R&D Systems	1:100
Biotin	Streptavidin	PE	Biolegend	1:200
Human IFNγ	4S.B3	Pacific Blue	Biolegend	1:50
Human TNFα	Mab11	PE-Cy7	Biolegend	1:50

2.4.4. *In vitro* suicide assay

CART4 with or without iC9 cells were generated with retroviral transduction with CART4 or CART4 w/o iC9 construct. CAR-T cells were kept expanded for five to seven days after transduction. A caspase inducible drug (CID), the B/B homodimerizer AP20187 (Clontech Laboratories), was added at a various concentration to T cell culture. The induction of apoptosis induced by CID was evaluated 24 hr later using Annexin-v/7-AAD (BD Biosciences) staining and flow cytometry analysis. Survival cells were quantified by counting beads (BD Biosciences). Survival index was calculated as follows: number of living $tEGFR^+$ cells/number of living $tEGFR^+$ cells in untreated control samples.

2.5. *In vivo* models

2.5.1. Ethics statement

The animal studies were performed within the UNC Lineberger Animal Studies Core Facility at the University of North Carolina at Chapel Hill. All the animal experiments using human tissues were conducted according to guidelines for the housing and care of laboratory animals (60) and following protocols approved by the Institutional Animal Care and Use Committee (IACUC) (approval 14-100.0) at the University of North Carolina at Chapel Hill. The human fetal liver was obtained from elective or medical indicated termination of pregnancy through a non-profit intermediary working with outpatient clinics (Advanced Bioscience Resources, Alameda, CA). The project was reviewed by the University's Office of Human Research Ethics, which has determined that this submission does not constitute human subjects research as defined under federal regulations [45 CFR 46.102 (d or f) and 21 CFR 56.102(c)(e)(l)]. The University of North Carolina at Chapel Hill IACUC has reviewed and approved this research. All animal experiments were conducted following NIH guidelines for housing and care of laboratory animals and in accordance with The University of North Carolina at Chapel Hill in accordance with protocols approved by the institution's IACUC (ID: 11-103.0).

2.5.2. Tumour xenograft study

Construct of xenograft model

6- to 8-week old NRG mice (Jackson Laboratory) were used for *in vivo* experiments with T leukaemia cell line. 0.5 x10^6 CEM-ss cells co-expressing Gaussia luciferase and EGFP were injected into mice via retro-orbit. Mice have weekly monitored luciferase activity from peripheral blood following the protocol in step 2.5.2.3. Mice were randomised subsequently before T cell injection.

Retro-orbit injection of T cells

PBMCs from healthy donors were activated and transduced to generate CART4 T cells or non-transduced T cells. On the day of transfusion, CART4 $CD8^+$ T cells and non-transduced $CD8^+$ T cells were negatively isolated from CART4 T cells or non-transduced T cells by using an untouched microbeads human CD8 T cell kit (Miltenyi) according to the manufacturer's instructions. $4x10^6$ isolated cells were washed by PBS twice, resuspended in 100 μl and infused to xenografted mice via retro-orbital injection.

Mouse monitoring and tail bleeding

Mice were closely monitored throughout all the studies described. 30-50 μl peripheral blood was bled weekly via vain tail. The blood was collected in microcentrifuge tubes containing 50ul 20 mM EDTA solution. The tubes were centrifuged at 500 g for 5 minutes to separate the plasma.

The plasma was used to detect the luciferase activity following the manufacturer's instrument (Thermo Fisher Scientific). Add 20 μl plasma to a well of a white opaque 96-well plate. Transfer 50 μl of Working Solution to each well. Wait for 10 minutes for signal stabilisation and detect the light output by a luminometer at 485 nm (ATTO, Phelios).

500 μl Ammonium-Chloride-Potassium (ACK) lysis buffer (Gibco) was added to the tubes with cell pellets to lyse red blood cells. The tubes were centrifuged again after 5-minute incubation. The supernatant was discarded. The cell pellets were resuspended in 500 μl PBS, followed by another centrifuge for 5 minutes at 500 g. After discarding the supernatant, the cell pellets were resuspended with 100 μl antibodies master mix for surface marker staining, which contained human CD45, mouse CD45, human CD3, human CD8, human EGFR, and live/dead dye. The cell subset composition was analysed by using flow cytometry (BD AriaIII). The gating strategy was shown in Figure 2-5.

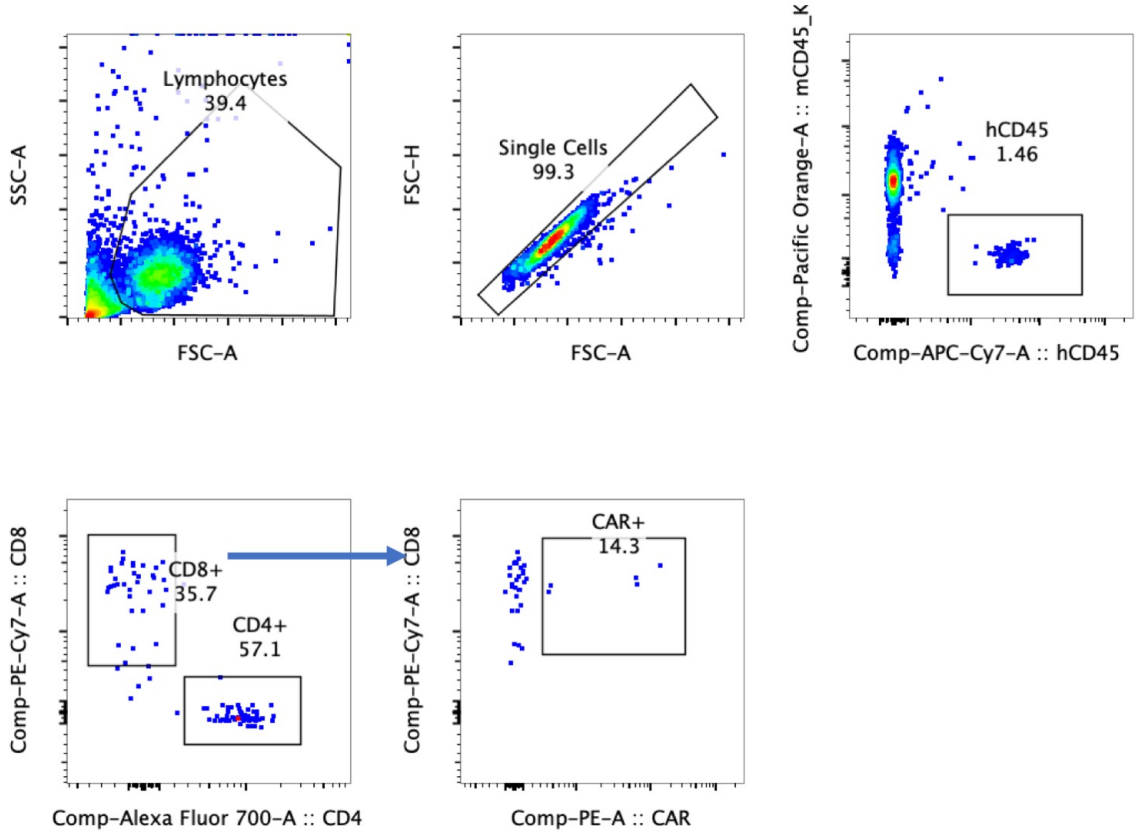

Figure 2-5 Gating strategy for flow cytometry analysis of CAR-T engraftment

CAR-T cells were gated on lymphocyte and single cells, before gating on hCD45$^+$, mCD45$^-$, CD4$^-$, CD8$^+$ and EGFR$^+$. The CD4$^+$ population was considered as CEM-ss tumour cells transplanted.

Ending the experiments

If significant health issues or toxicity were observed during the experiment, the mice with healthy problems were killed. At the end-point, splenocytes and bone marrow cells were isolated after euthanasia. Cell suspensions were obtained by grinding the tissues and passed through a 70 μm cell strainer (BD Falcon). Surface markers, including human CD45, mouse CD45, human CD3, human CD4, human CD8, human EGFR, and live/dead dye, were analysed by flow cytometry. Red blood cells were lysed by being incubated with ACK lysis buffer (Gibco) for 5 minutes at room temperature. Cells were stained with fluorescence-labelled antibodies for surface markers, including human CD45, mouse CD45, human CD3, human CD4, human CD8, human EGFR, and live/dead dye, followed by flow cytometry

analysis. The absolute amount of cells were counted by a Guava easyCyte flow cytometry (Millipore).

2.5.3. HIV-infection study on humanized mice

Construct of PBL humanized model

In each experiment, NRG mice (Jackson Laboratory) at 4-6 weeks were irradiated at 600 rad. $10x10^6$ fresh isolated PBMCs in 100ul PBS were injected into each mouse via retro-orbit. The engraftment was measured at day seven post-transfusion by quantifying human $CD45^+$ cells in peripheral blood using flow cytometry. 50 μl Blood was bled through the tail vein. Red blood cells were lysed by being incubated with ACK lysis buffer (Gibco) for 5 minutes at room temperature. Cells were stained with fluorescence-labelled antibodies for surface markers, including human CD45, mouse CD45, human CD3, human CD4, human CD8, and live/dead dye, followed by flow cytometry analysis. The absolute amount of cells were counted by a Guava easyCyte flow cytometry (Millipore). All the recipients were detected with more than 20% human leukocytes in the peripheral blood at second week. The gating strategy was shown in Figure 2-6.

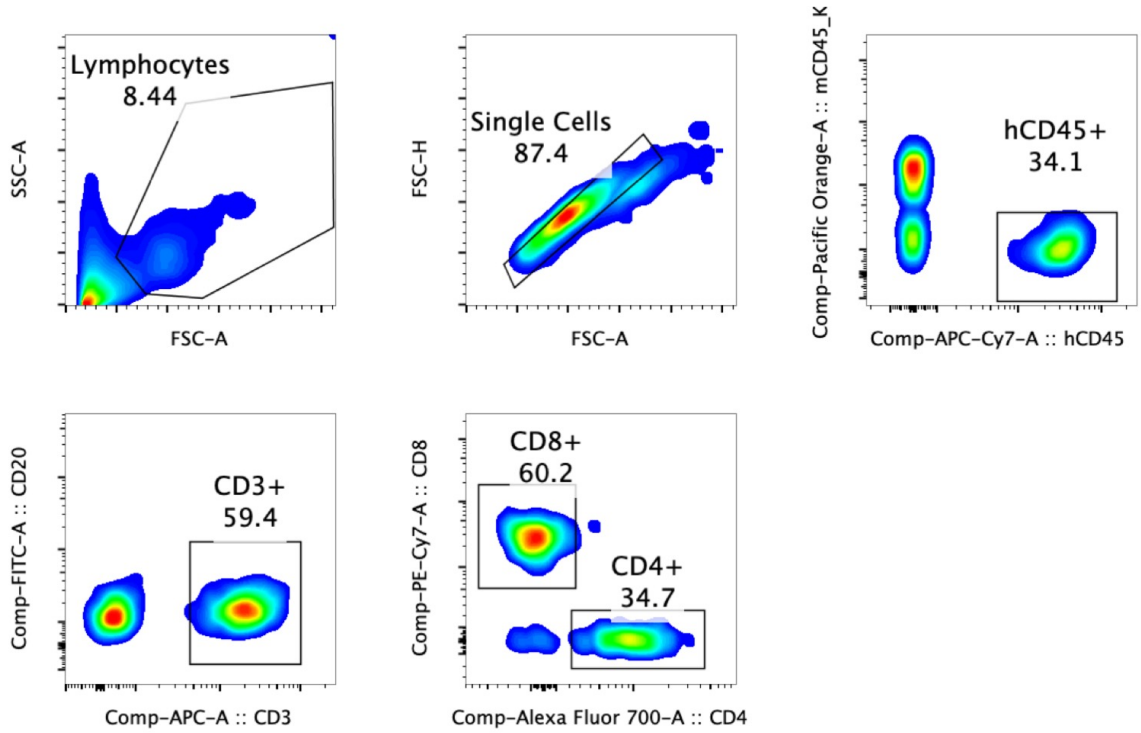

Figure 2-6 Gating strategy for flow cytometry analysis of human leukocyte engraftment in peripheral blood

Human leukocyte cells were gated on lymphocyte and single cells, before gating on hCD45$^+$, mCD45$^-$. The majority of human leukocytes were CD3$^+$ T cells, which mainly consisted of CD8$^+$ and CD4$^+$ T cells. Percentage population of each gate is shown.

CD34$^+$ transplanted humanized model

Human CD34$^+$ cells were isolated from 16- to 20-week-old fetal liver tissues. The tissues were digested with Liver Digest Medium (Invitrogen) for 30 minutes. The suspension was filtered through a 70 μm cell strainer (BD Falcon) followed by centrifuging at 150 g for 5 minutes to isolate mononuclear cells by Ficoll. CD34$^+$ HSC cells were isolated from cell suspension by using human CD34 cell sorting kit (Miltenyi) according to the manufacturer's protocol. 0.5x10^6 CD34$^+$ HSC cells were injected into the liver of 2- to 6-day-old NRG mice, which has been irradiated at 300 rad previously. More than 90% of the humanized mice were successfully

reconstructed with more than 10% human leukocytes in the peripheral blood at eighth weeks. The gating strategy was shown in Figure 2-7.

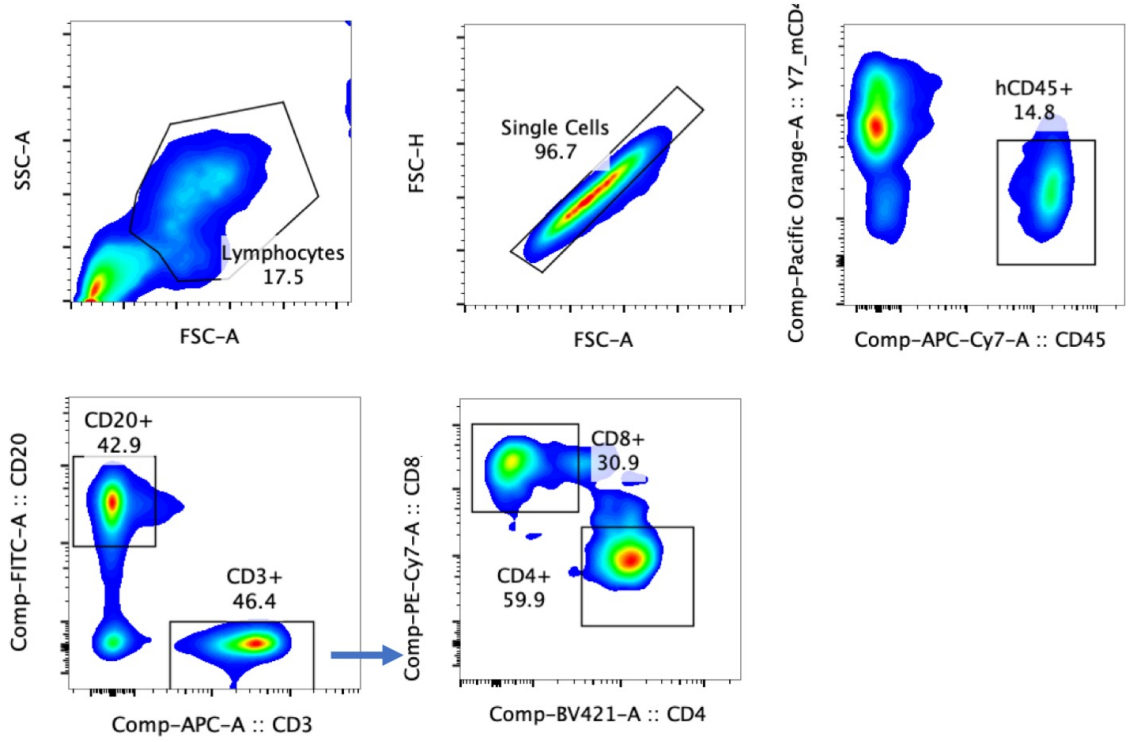

Figure 2-7 Gating strategy for flow cytometry analysis of humanization efficiency in peripheral blood

Human leukocyte cells were gated on lymphocyte and single cells, before gating on $hCD45^+$, $mCD45^-$. The majority of human leukocytes were $CD3^+$ T cells and $CD20^+$ B cells.

HIV virus stock and infection of humanized mice

An R5 tropic strain of HIV-1, JR-CSF was generated by transfection of 293T cells with a plasmid containing full-length JR-CSF genome. The viral particle was titrated by using p24 ELISA (Takarabio). Humanized mice with stable human leukocyte engraftment were anaesthetised and infected with JR-CSF (10 ng p24) via retro-orbital injection. Humanized mice injected with PBS were used as mock control groups.

Combination antiretroviral therapy

The cART drugs were administrated by feeding. Manufacture of food with antiretroviral drugs was prepared as reported[173]. Emtricitabine and tenofovir disoproxil fumarate (Truvada; Gilead Sciences) and raltegravir (Isentress; Merck) were crushed into powder and manufactured with TestDiet 5B1Q feed (Modified LabDiet 5058 with 0.12% amoxicillin) into irradiated pellets. Final doses of drugs in the food were 4,800 mg/kg raltegravir, 1,560 mg/kg tenofovir disoproxil, and 1,040 mg/kg emtricitabine. The estimated daily drug doses were 768 mg/kg raltegravir, 250 mg/kg tenofovir disoproxil, and 166 mg/ kg emtricitabine.

Plasma HIV-1 RNA detection

The plasma was obtained by centrifuging peripheral blood from HIV infected humanized mice at 500 g for 5 minutes. The viral RNA was extracted by the viral RNA mini kit (QIAGEN). The viral RNA and standard RNA extracted from standard plasma (NIH AIDS Reagent Program) were analysed by reverse transcription-quantitative PCR (RT-PCR) (TaqMan One-Step RT-PCR master mix, ABI). The sequences of primers and probe used for RT-PCR were followed:

forward primer 5'-CAATGGCAGCAATTTCACCA-3',

reverse primer 5'-ATGCCAAATTCCTGCTTGA-3',

probe FAM (6-carboxyfluorescein)-CCCACCAACAGGCRGCCTTAACYG-QSY7 (TAMRA [6-car boxymethyltetrarhodamine]).

The components of the RT-PCR was listed in Table 2.4. The RT-PCR reactions were set up following the manufacturer's guidelines and were run on the QuantStudio 6 Flex PCR system (Applied Biosystems) following the conditions listed in Table 2.5. The fluorogenic signal was collected at the end of each annealing-extension step. A threshold was automatically set, and the threshold cycle value (Ct) was consequently determined. Three or four replicates of each sample were performed.

Table 2.4 The components of the RT-PCR for plasma viremia quantification

Mastermix	**µl per Reaction**
2X TaqMan RT-PCR master mix	3.75
20 µM F primer	0.05
20 µM R primer	0.05
5 µM Probe	0.19
Nuclease-free water	0.96
RNA template	10

Table 2.5 The conditions for one-step RT-PCR

Temperature	
Heated Lid 105°C	
50°C for 30 min	
95°C for 10 min	
95°C for 10 s	40 cycles
60°C for 45 s	
4 °C store	

2.6. Statistical analysis

Statistical analysis was performed by using GraphPad Prism software version 6.0 (GraphPad software). A two-tailed unpaired Student's t-test was used to compare data between two groups. *$P < 0.05$, **$P < 0.01$, ***$P < 0.001$. All the data with error bars are presented as mean values ± standard error of the mean (SEM). A P value of less than 0.05 was considered significant. Data was analysed using GraphPad Prism software (version 8).

Chapter 3. Design, expression and characterisation of CD4-targeting CAR *in vitro*

3.1. Cloning of CD4-targeting CAR constructs

A CAR specific for CD4 was designed for the genetic redirection of T-cell specificity. The CAR construct incorporates with a tEGFR as a tracking marker/selection gene, an iC9 as a safety switch.

The DNA sequence of the mouse IgG antibodies Hu5A8 with the specificity towards human CD4 was found from the public patent (CN103282385), as shown in Figure 3-1 A and B. Hu5A8, as known as TNX-355 or ibalizumab, was widely assessed in Phase I and Phase II clinical trials for inhibiting HIV entry by blocking the HIV-binding site of CD4 molecule[124,125]. As a control, the VH chain and VL chain of an anti-CD20 monoclonal antibody Leu16 was also synthesized, which had been evaluated for its efficacy in pre-clinical and clinical CAR-T studies[65,174] (Figure 3-1 C and D). The VH chain and VL chain of the Hu5A8 or Leu16 were fused in a scFv through a $(GGGS)_4$ linker. The length of the $(GGGS)_4$ linker was added to confer the proper flexibility to the scFv, which was then cloned into the backbone of a third-generation CAR plasmid in frame with a CD8 transmembrane domain, a CD28 endodomain, a 4-1BB endodomain and the CD3 ζ chain. A third-generation CAR was used in this thesis in consideration of the recent studies demonstrating its superiority over first- and second-generation CAR[175 176].

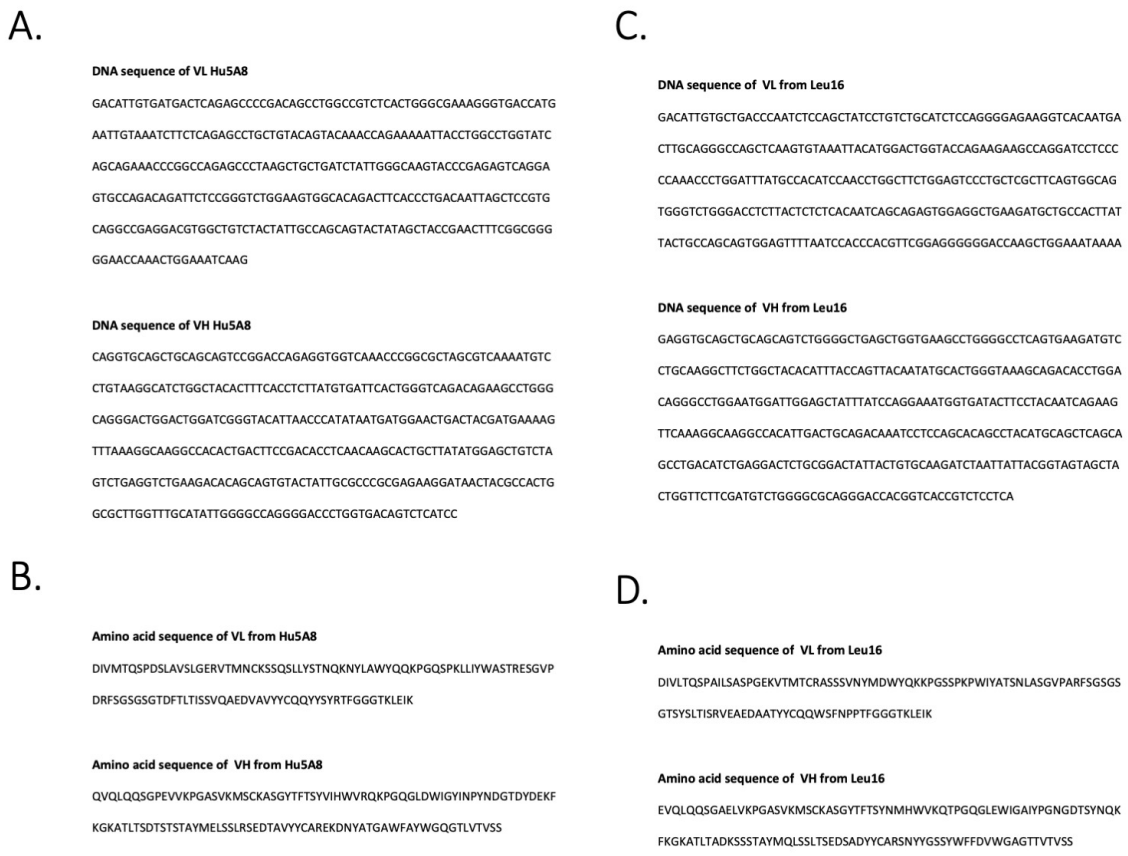

Figure 3-1 Nucleic acid sequences and amino acid sequences of CD4- and CD20-targeting monoclonal antibodies.

The nucleic acid sequences of VL and VH of Hu5A8 and Leu16 are listed in **A** and **C**, respectively. The VL of Hu5A8 contains 112 aa, and VH contains 122 aa (**B**). The VL and VH of Leu16 have 106 aa and 122 aa, respectively (**D**).

Previously, a truncated form of human EGFR was developed as a target for cetuximab, which is a clinically available mAb. The tEGFR molecule was truncated in the extracellular domain to avoid binding of endogenous ligands such as EGF or TCF-α, and in the intracellular domain to eliminate downstream signalling. The utility of tEGFR was examined as a selection, *in vivo* tracking marker, and ablation of engineered CAR-T cells[63,64]. Thus, this residual tEGFR sequence was linked with CAR sequence by the *Thosea asigna* virus 2A (T2A)-ribosomal skip sequence[177,178].

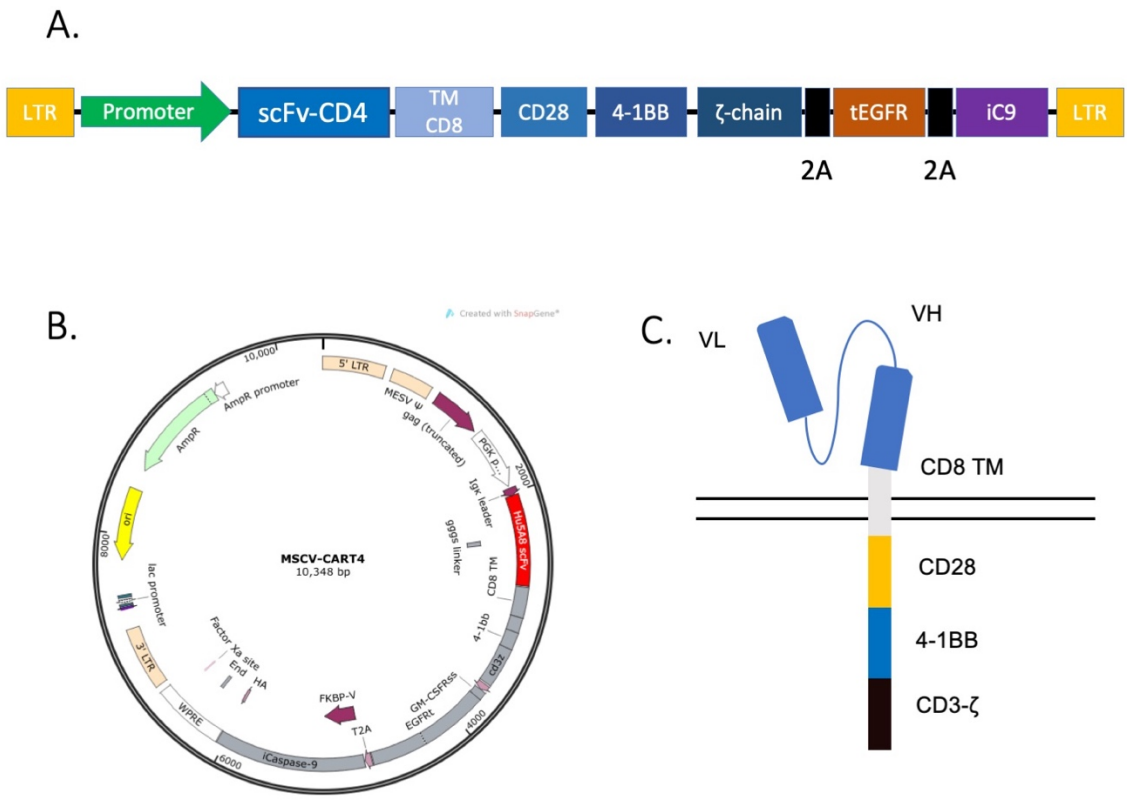

Figure 3-2 Schematic representation of the CD4-targeting CAR construct.

A. The diagram represents the functional elements included in the CAR construct. The scFv derived from monoclonal antibody Hu5A8 was fused with a CD8 transmembrane domain (TM), a CD28 endodomain, a 4-1BB endodomain and the CD3 ζ chain. The gene sequences of tEGFR and iC9 were tagged behind CAR via self-cleaving 2A linkers. **B**. The map of MSCV-derived retroviral vector CART4. **C.** Schematic diagram of the chimeric protein CART4.

CAR-T cells can remain in the patients as long as dozens of years as in the case of the anti-CD19[50] and anti-HIV CAR trials[161]. Unlike B-cell aplasia, long-term $CD4^+$ T-cell aplasia is life-threatening. Therefore, it would be necessary to establish the safety methods to remove CART4 cells from patients after tumour or virus depletion, or in emergency cases due to severe side effects during CAR-T therapy[49,179 180]. The depletion of CAR-T cells from patients must occur as quickly and efficiently as possible. Dimerization drug-induced Caspase-9 suicide switch is based on the fusion of human caspase-9 to a mutated human FKBP, which

allows conditional dimerization in the presence of a small chemical molecule drug[67,68]. iC9 has been proven the safety and utility in a clinical trial of haploidentical HSC transplantation[72].

Therefore, the gene fragment containing CD4 CAR, tEGFR and iC9 was then synthesized. In order to generate a retroviral vector, the DNA fragment was inserted into the MSCV backbone between the restrict enzymes sites *NcoI* and *BsiWI* (Figure 3-2). The cassettes cloned into the vector were verified by sequencing.

3.2. Establishing stable CAR-expressing retroviral packaging cell lines

Recently, retroviral and lentiviral vectors are most widely used tools for the gene delivery to T-cell therapy. They have been widely applied to clinic usage[72]. Comparatively, two-step retroviral vectors provide a more convenient and consistent system for pre-clinical and clinical study. The stable virus-packaging cell banks based on the PG13 cell line have been widely used to achieve high and stable gene delivery efficiency[181-184].

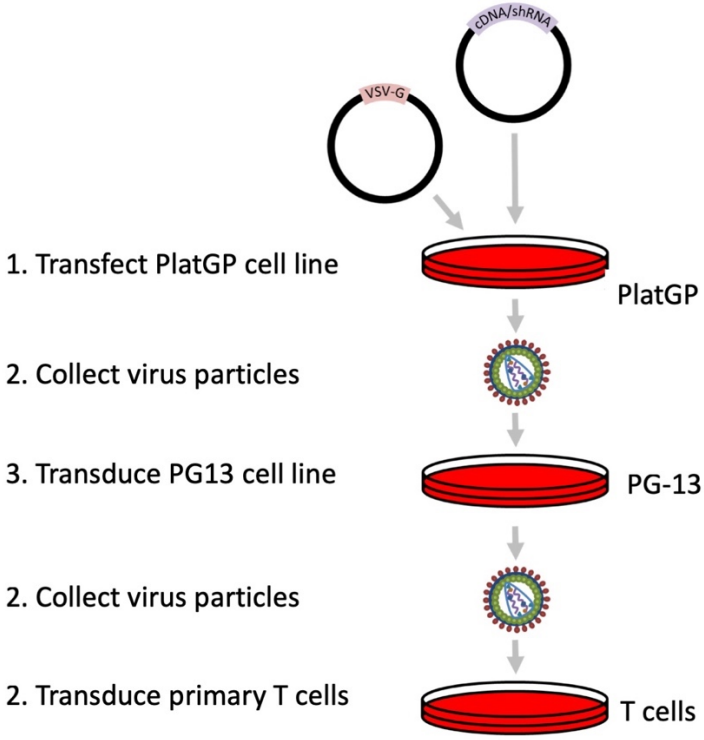

Figure 3-3 Flow chart representation of two-step retroviral transduction method

The retroviral production by the two-step method consists of the production of transient and stable virus-packaging cell lines. Comparatively, the stable virus packaging cells produce higher titres of viral particles, which are more effective for gene transfer for primary T lymphocytes.

Here to achieve high transduction efficiency to primary human T cells, a two-step retroviral system involving the sequential use of PlatGP and PG13 cell line was developed (Figure 3-3). Firstly, Plat-GP cells were transfected with G glycoprotein of the vesicular stomatitis virus (VSV-G) envelope vector, which is the most widely used envelope[185]. The supernatant containing viral particle was collected from Plat-GP with transduction higher than 95% (Figure 3-4 A) and transduce PG13 cell line to produce a stable virus packaging cell line. Both of PG13 cell line transduced by CART4 and CART20 were nearly 100% positive for the EGFR 48 hours post-transduction (Figure 3-4 B). This means that efficient gene delivery may be repeatedly achieved without single PG13 cell cloning for experimental pre-clinical testing. The titration of retroviral supernatant from PG13 ranged from $1.5x10^7$ to $2.5x10^7$ TU/ml (Figure 3-4C).

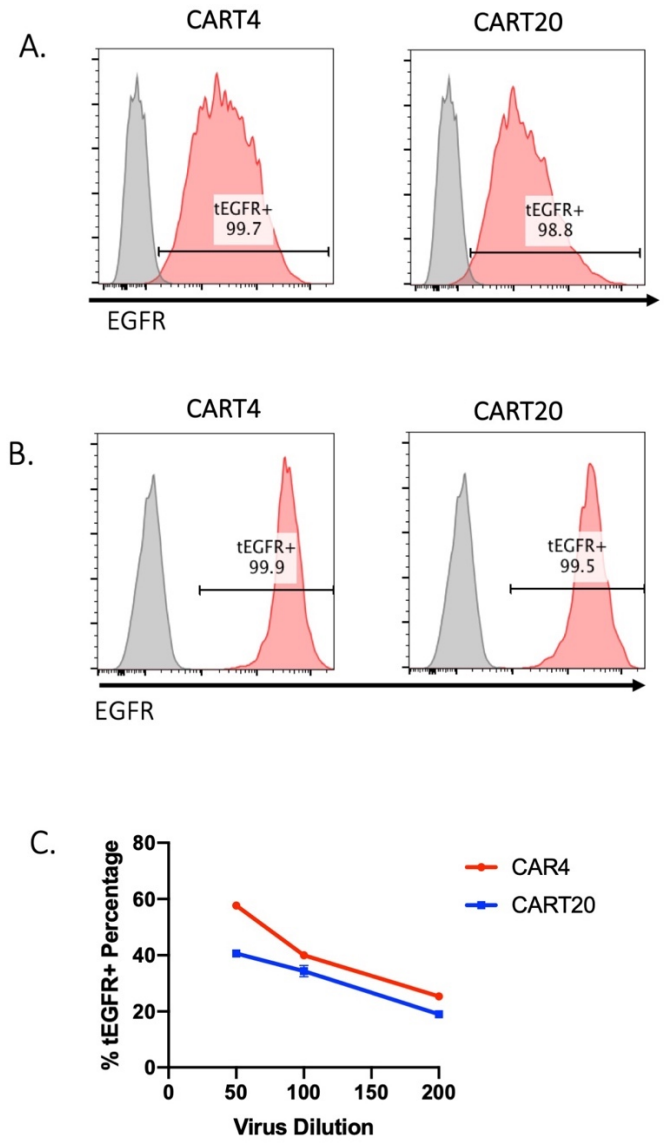

Figure 3-4 Flow cytometric assessment of gene transfer efficiency.

Virus packaging cell lines were transduced with CART4 or CART20 vectors. Transduced cells were dissociated from the plate and stained by EGFR-specific antibody before analysis by flow cytometry. Plat-GP (**A**) achieved close to 100% positive efficiency, while PG-13 cells (**B**) shown a uniform CAR-positive pattern. The grey histograms were non-transduced controls. **C**. The retroviral particles produced from transduced PG-13 cells were diluted and titrated with 293T cells. Dilution 2.5 μl virus into 500 μl medium reached about 20-30% transduction efficiency in $2x10^5$ cells, determining a titration ranging from $1.5x10^7$ to $2.5x10^7$ TU/ml. Three replicates of each sample were performed. Data with error bars are represented as mean ± SEM.

Thus, a robust methodology was established to make a stable virus packaging cell bank and produce high titration for pre-clinical testing within ten days (Figure 3-5).

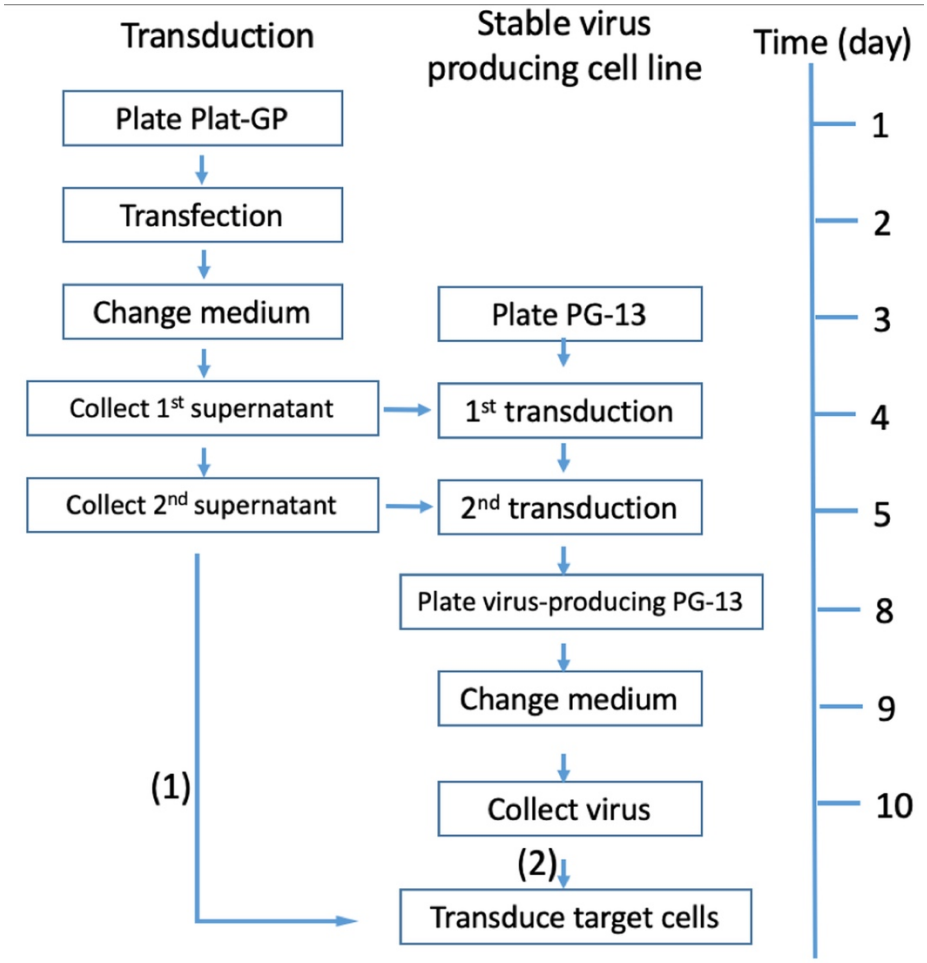

Figure 3-5 Flow chart of two-step retroviral production method

Retroviral vectors are packaged in a two-step procedure. First, PlatGP retroviral packaging cells are transfected with the VSV-G envelope vector and the vector of interest, which is packaged transiently in pseudotyped particles. These particles are used to deliver the vector to PG-13 cells to achieve stable packaging of GALV-pseudotyped particles for infection of primary human T cells.

3.3. Expression of CD4-targeting CARs on primary human T cells

In order to demonstrate co-expression of CAR and tEGFR, human PBMCs were activated with Dynabeads Human T-Activator and genetically engineered by retroviral transduction to express the CAR/tEGFR/iC9 gene construct (Figure 3-6 A). Indeed, expression levels of CAR and the tEGFR were found to be tightly correlated, as shown by the detection of double-positive cell populations upon surface staining with a mouse scFv-specific anti-mouse IgG $F(ab')_2$ antibody in combination with an EGFR-specific antibody (Figure 3-6 C).

After two-round transduction, activated T cells were expanded with recombinant human IL-7 and IL-15, which favour differentiation towards central memory phenotype[186]. CAR-T cells were expanded with a 70-fold increase in cell count (section 3.6). Along with T cell expansion, $tEGFR^+$ cell population maintained its proportion counting ~50% of total cells. (Figure 3-7 and Figure 3-8).

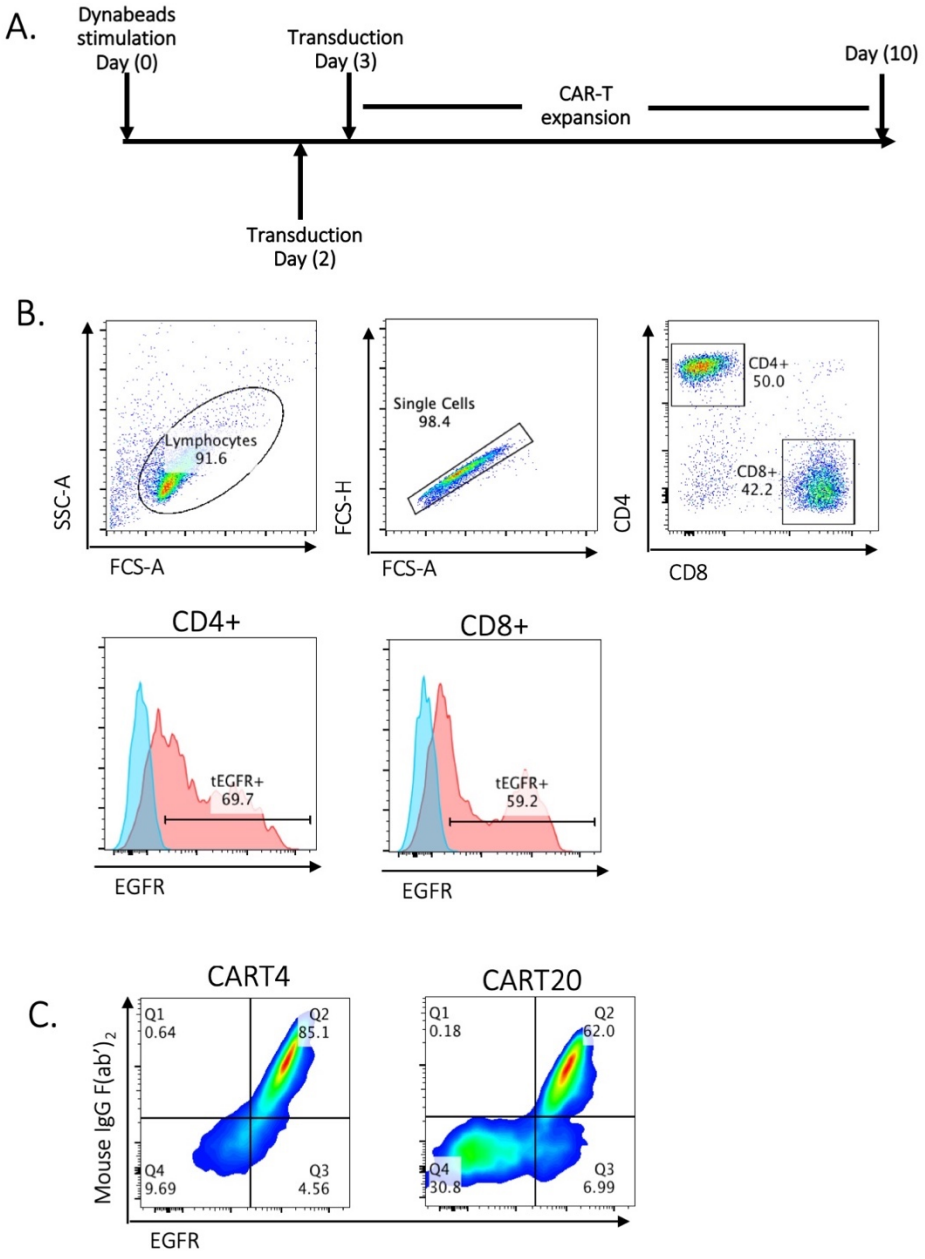

Figure 3-6 Production of CART4 cells

A. Experimental design. Human PBMCs were stimulated by CD3/CD28 Dynabeads for two days, before retroviral transduction of CAR. Three days after transduction, cells were collected and analysed for the transduction efficiency by flow cytometry. **B.** Gating strategy for flow cytometry analysis of CAR expression. The blue histogram was non-transduced control. **C.** Transduced T cells were stained by anti-mouse IgG F(ab)'$_2$ antibody and anti-EGFR antibody. Cells were propagated on CD3$^+$ single lymphocytes, and numbers indicate the percentage of CAR$^+$/ tEGFR$^+$ cells.

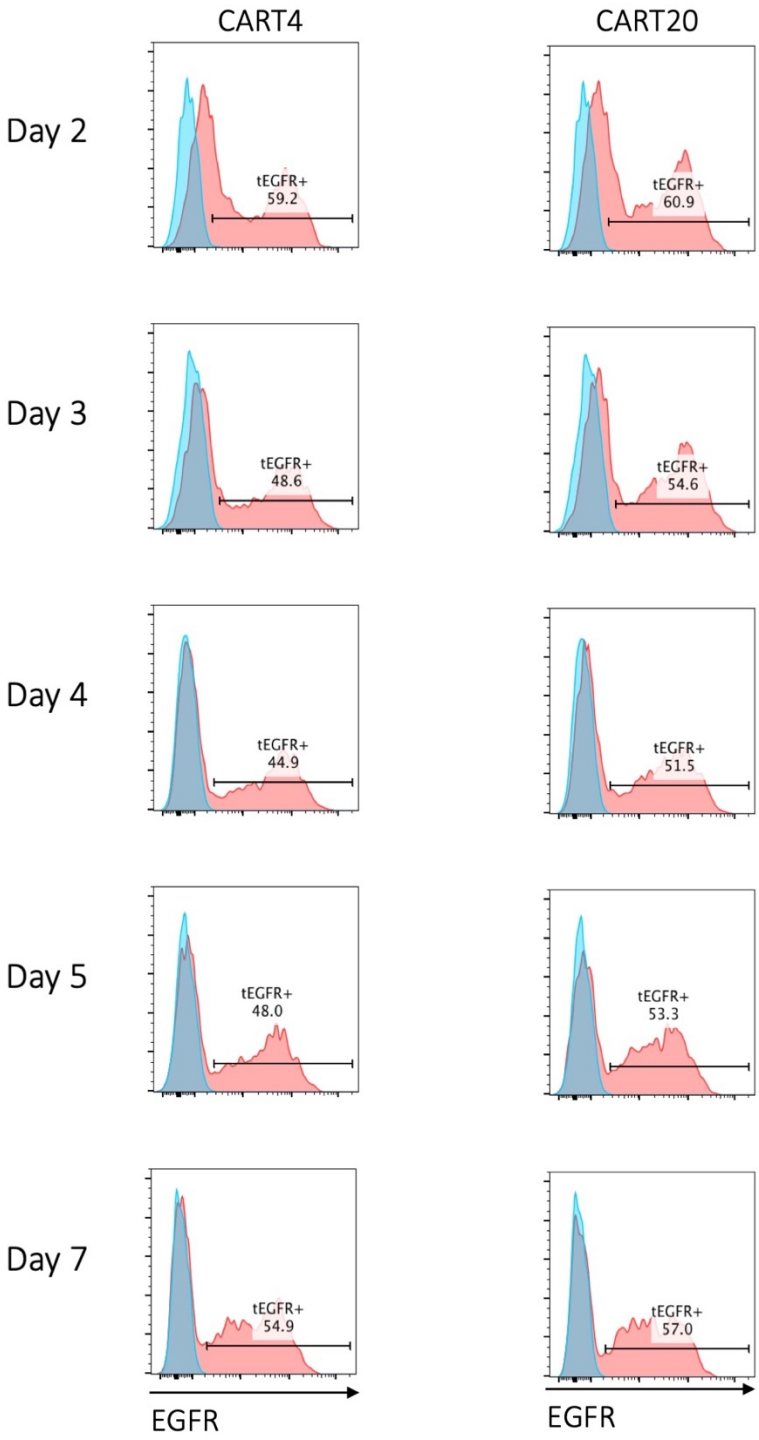

Figure 3-7 Representative cytometry plots of transduced T cells.

After retroviral transduction of CAR, primary T cells were sampled every day and stained for surface markers, including CD3 and tEGFR. The blue histogram was the result of non-transduced cells. The percentages of cells positive for CAR and marker are shown in the plots.

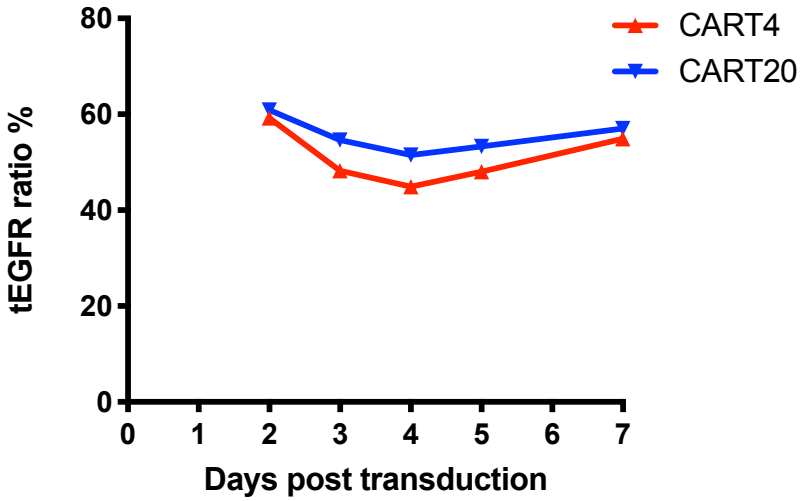

Figure 3-8 Dynamics of CAR expression on primary T cells

A summary of data from Figure 3-7. The transduced T cells maintained transduction ratio during the expansion period from two days to seven days pro retroviral transduction.

3.4. Targeting endogenous CD4$^+$ T cells using CART4 T cells

Next, the subset composition was analysed during CAR-T cell expansion following CART4 and CART20 transduction. The CD4$^+$ T cells were almost completed depleted within three days after CART4 transduction as compared with non-transduced (NTD) and CART20 control, in which about 45% of cells remained CD4-positive (Figure 3-9). These data indicated the potent activity against CD4 of CART4 cells during T cell expansion.

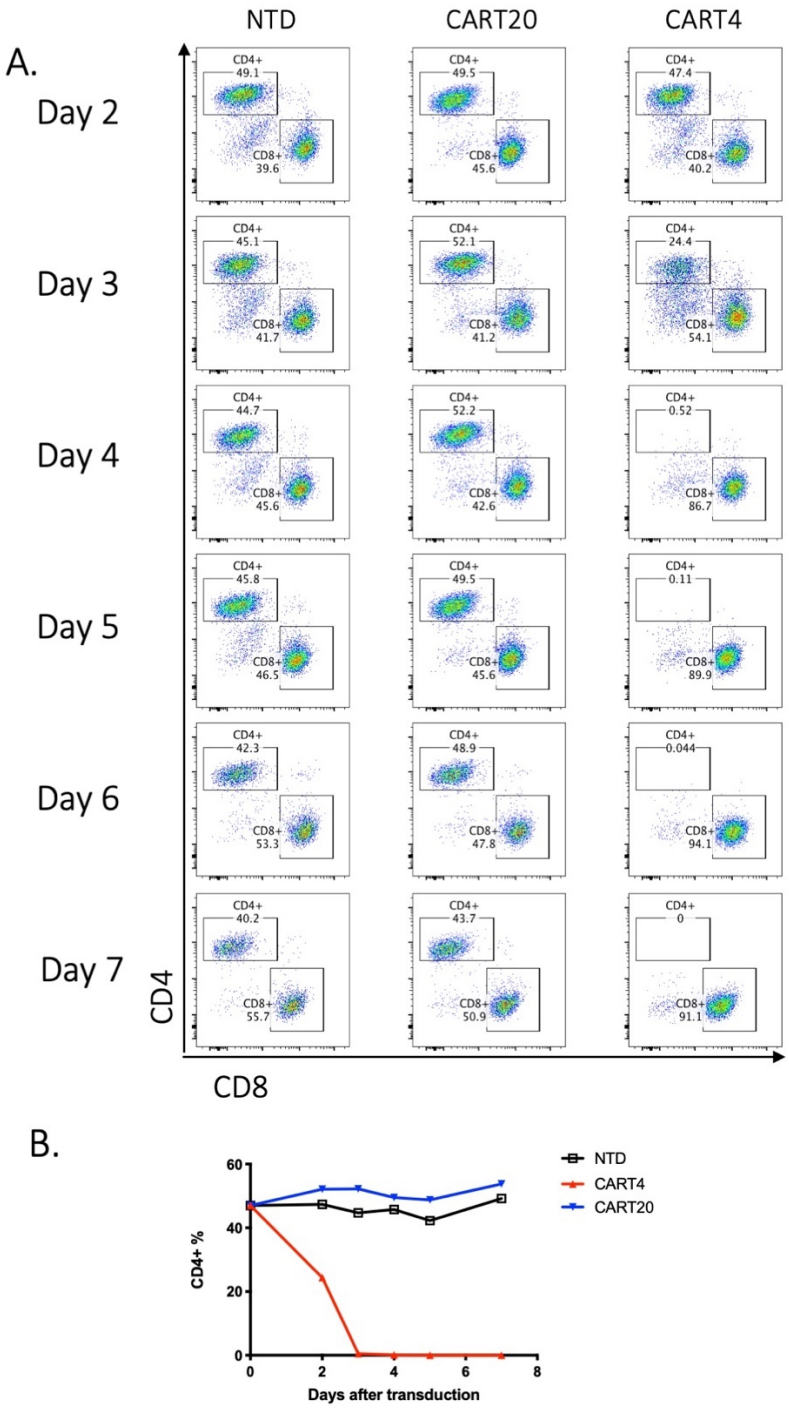

Figure 3-9 CART4 cells depleted the CD4⁺ population during T-cell expansion.

A. PBMCs were activated by Dynabeads Human T-Activator and IL7/IL15. The activated PBMCs contained two subsets of T cells, $CD4^+$ and $CD8^+$ (left). Cells were either transduced by CART20 (middle) or CART4 (right) retroviral particles. From the third day after transduction, cells were stained by anti-CD4 and anti-CD8 antibodies and analysed by flow cytometry. The statistics of $CD4^+$ ratio were summarized in **B**. Data reflects typical results from five healthy individuals.

3.5. Validation of suicide gene iC9 *in vitro*

As $CD4^+$ cell depletion will induce HIV/AIDS like immunodeficient syndrome, it will be necessary to eliminate CART4 cells after target cell depletion. Additionally, infusion of CAR-T cells may induce severe side effects, such as CRS. It will be critical to add a safety switch to control the activity of CAR-T cells *in vivo*. In order to evaluate the efficiency of iC9 safety switch *in vitro*, a CART4 variation without iC9 gene (CART4 w/o iC9) was cloned as control (Figure 3-10 A). T cells transduced with CART4 or CART4 w/o iC9 construct were exposed to increasing concentrations of CID AP20187 (0.1nM to 100nM) for 24 hours. Cell death was accessed by flow cytometry analysis. Representative flow cytometry plots of live gated cells by 7AAD and Annexin-V was shown in Figure 3-10 B. As the plots show, the tEGFR-positive percentage in the survived population dropped along with the increasing concentration of CID. 34.1% of $tEGFR^+$ CART4 T cells were eliminated after a single 100 nM dose of CID (Figure 3-10 C and Figure 3-11 A). Our data showed that iC9 was more efficient within $tEGFR^{high}$ population. 69.1% of $tEGFR^{high}$ cells were eliminated after a single 100 nM dose of CID (Figure 3-10 D and Figure 3-11 B). Consistent with the observations from other studies[67,68,71], the cells that escape killing were those expressing low levels of the transgene with a 50% reduction in mean fluorescence intensity (MFI) of tEGFR after CID (Figure 3-11 C). Therefore, the nonresponding T cells expressed insufficient iC9 for functional activation of CID. For clinical applications, CAR-T cells may have to be sorted for sufficient transgene expression before administration.

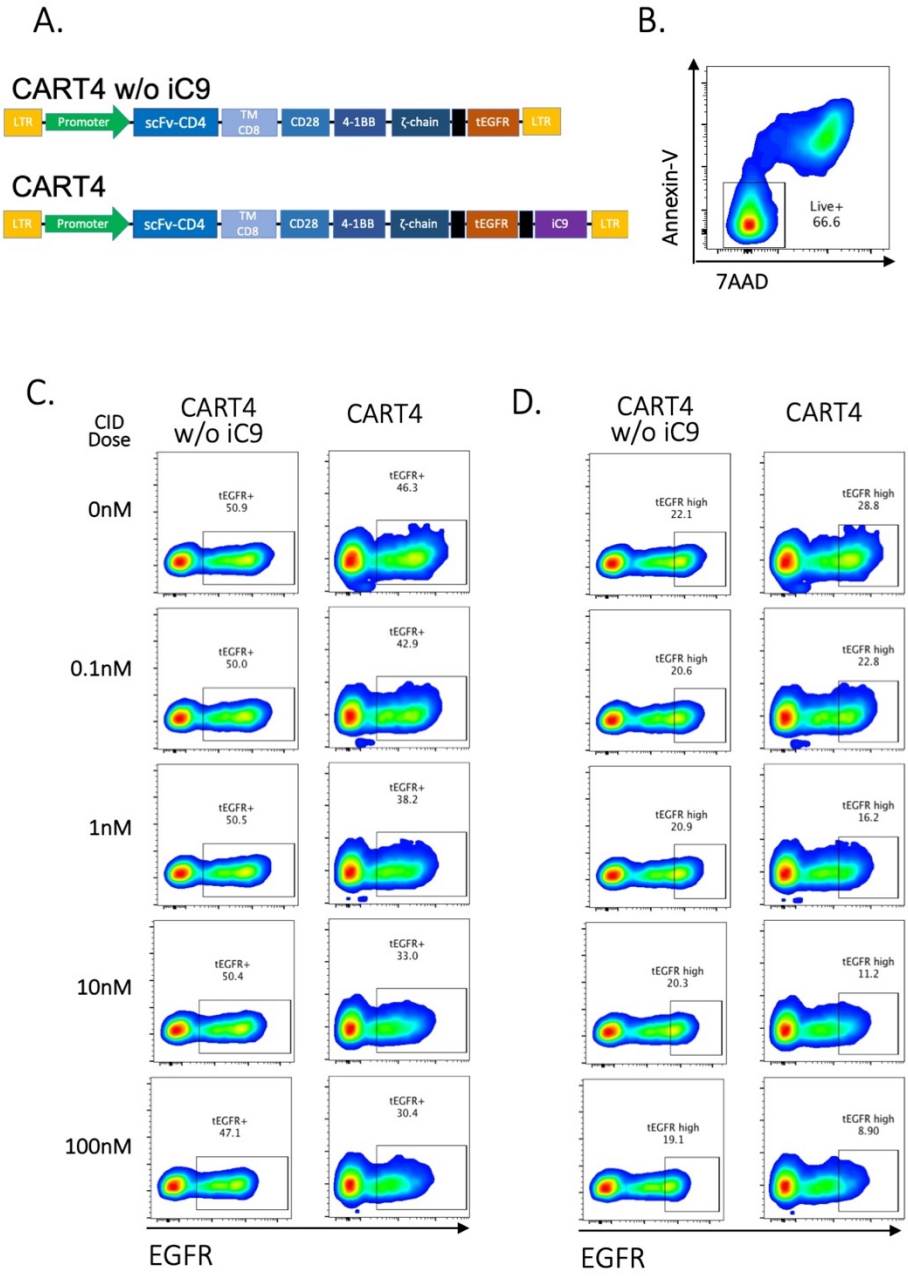

Figure 3-10 CID-induced dimerization triggered apoptosis of CAR-T cells

A. Schematic structure of CART4 and CART4 without iC9 element (CART w/o iC9). **B**. CAR-T cells were treated with CID AP20187 on day 5 after transduction. 24 hours after inoculation of CID AP20187, CAR-T cells were harvested and stained by flow cytometry antibodies targeting CD3, EGFR and apoptosis biomarkers Annexin V and 7AAD. 7AAD- and Annexin-V-double negative population was defined as live cells. Representative flow cytometry plots for population percentage of tEGFR-positive (**C**) and EGFR-high (**D**) cells in live cells after the treatment with CID AP20187 at different doses. Data reflects typical results from three replicates from separate donors.

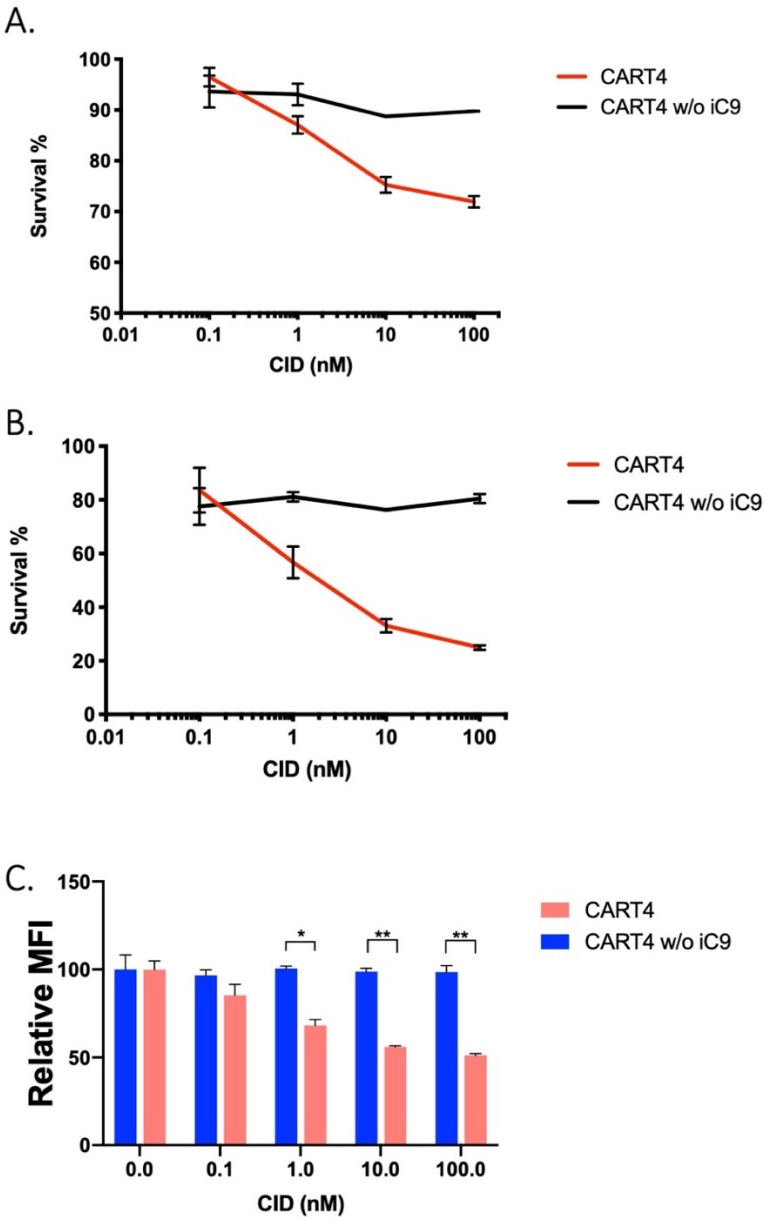

Figure 3-11 CART4 cells were sensitive to CID-induced apoptosis

Statistic summarized from the flow cytometry results shown in Figure 3-10C and D. Survival ratio was defined as the ratio of the EGFR-positive (**A**) or EGFR-high (**B**) percentage from untreated condition and CID-treated conditions 24 hours after the exposure to the indicated doses of CID. **C** shows the mean fluorescent intensity of EGFR expression in survived cells. Data reflects typical results from three replicates from separate donors. Three replicates of each sample were performed. Data are represented as mean ± SEM. Statistically significant difference was found between groups as determined by a two-tailed unpaired Student's t-test. ** = $p<0.01$; * = $p<0.05$.

3.6. Development of clinical-scale CAR-T cell manufacturing method

To assess scalability and simplify CAR-T cell manufacturing, an optimized standard operating procedure was established using a gas-permeable static cell culture system (G-Rex) for CAR-T manufacture (Figure 3-12A). G-Rex system contains a silicone membrane at the bottom of the plate. Gas exchange, including O_2 and CO_2 across the membrane, allows an increased depth of the culture medium, providing more nutrients and diluting waste[187]. PBMCs were activated and transduced, and $10x10^6$ cells were transferred and cultured further in G-Rex six-well plate (Figure 3-12B). The cells were replenished with the cytokines IL-7 and IL-15 every two to three days. Cells expanded to more than $3x10^8$ from initial number of $2x10^6$ cells, with an increase of 150-fold over 15 days (Figure 3-12C). Next, the transduction efficiency of the final product following T cell expansion in the G-Rex system was ascertained. The final transduction efficiency of CART4 was 57.6% ±7.1%, similar to the cells produced from the conventional flask (53.7%±5.3%), as shown in Figure 3-13A. As expected, endogenous $CD4^+$ population was depleted entirely in the final product, indicating the anti-CD4 activity of the CAR-T cells (Figure 3-13B).

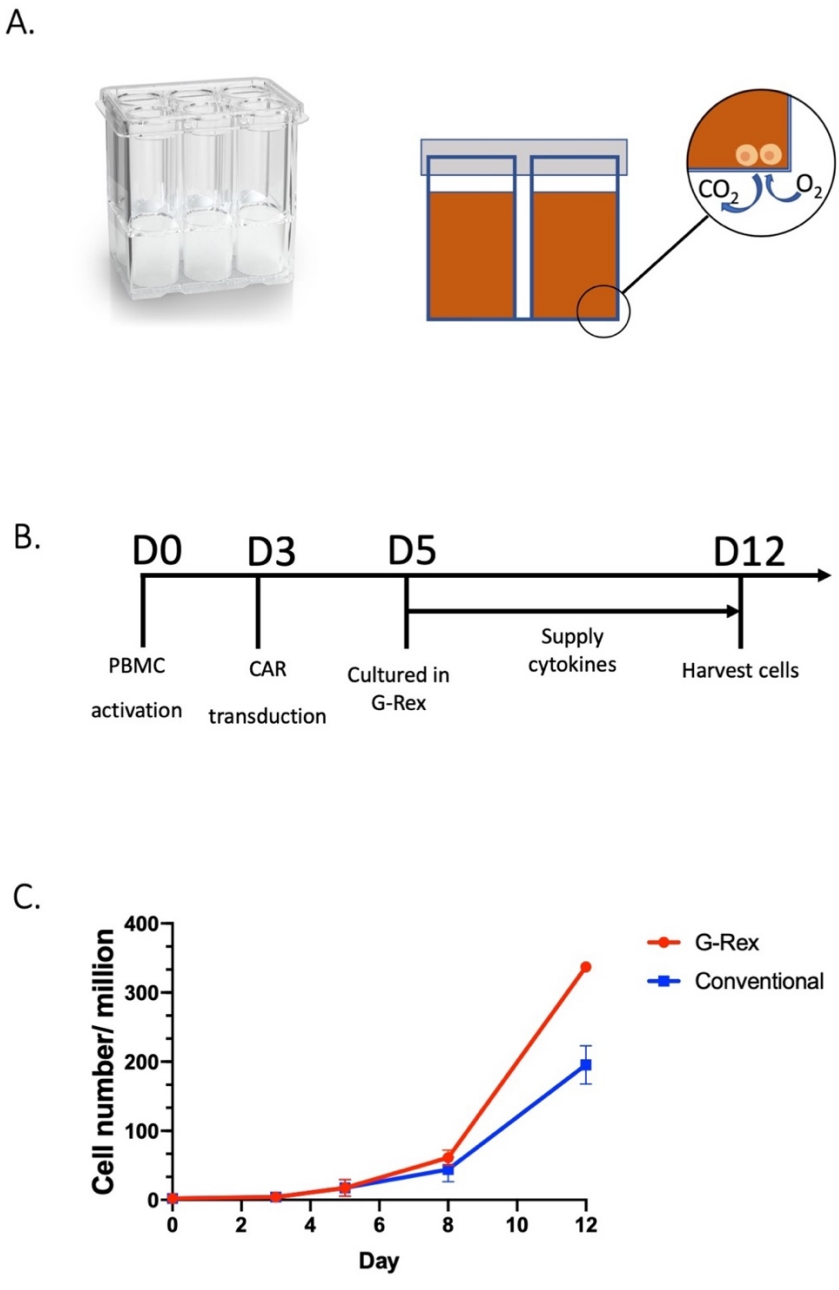

Figure 3-12 G-Rex accelerates T cell expansion.

A. Representative photograph of G-Rex plate. The diagram shows that gas exchange occurred at the bottom of the G-Rex device accelerates cell expansion. **B**. Time course for CAR-T cell manufacture. Human PBMCs are activated by CD3/CD28 Dynabeads and IL7/IL15 in the flasks before retroviral transduction of CAR. Transduced cells are transferred to G-Rex plate ($1x10^6$ per square metre) two days after transduction. Cytokines are replenished every two to three days until day 12. **C**. Cell expansion during the manufacturing procedure. Three replicates of each sample were performed. Data are represented as mean ± SEM. Data reflects typical results from four healthy individuals.

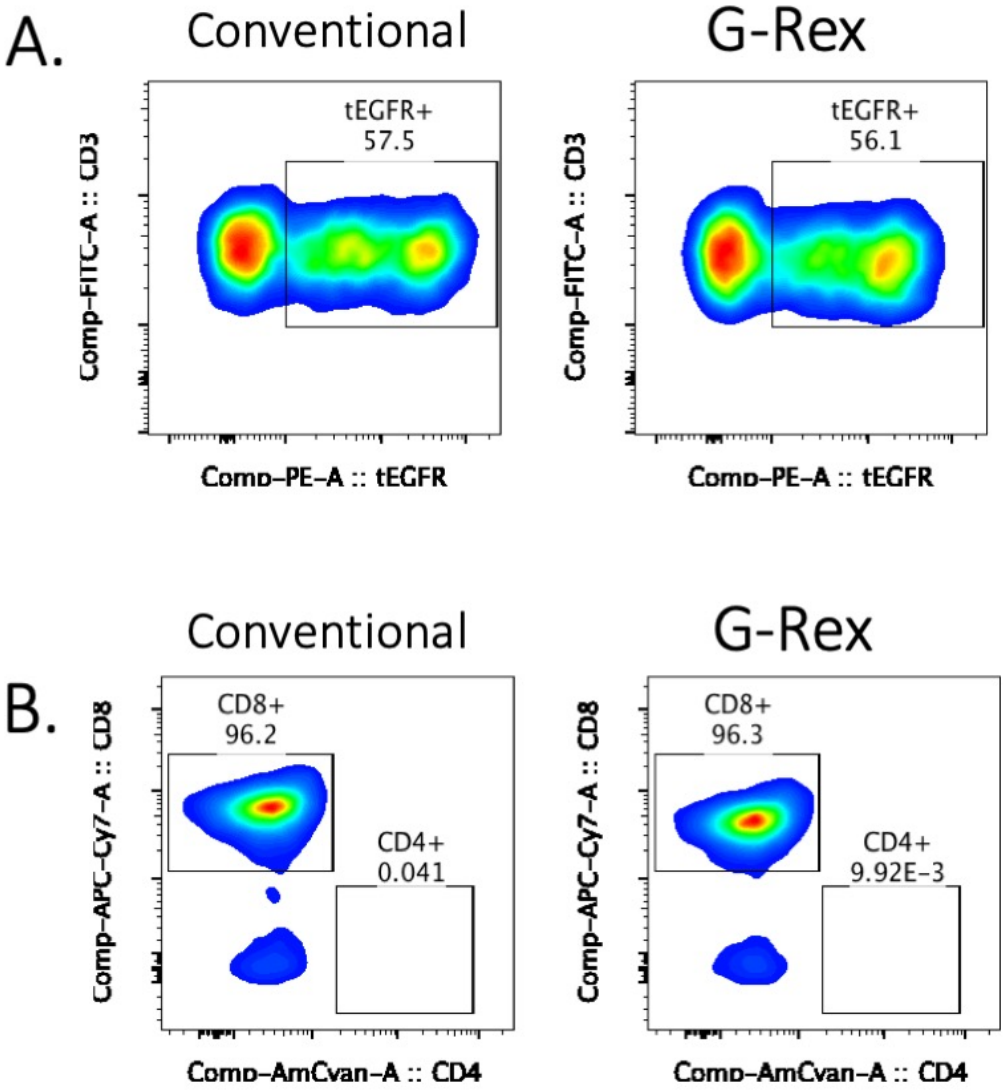

Figure 3-13 Cell manufactured from G-Rex maintained transduction efficiency and cytotoxicity function.

Activated PBMCs were transduced by CART4 retroviral particles and transferred to G-Rex device two days post-transduction. The cells were replenished with cytokines every two to three days, followed by measurement of the transduction ratio and $CD4^+$ population analysed using flow cytometry. Data reflects typical results from four healthy individuals.

The immunophenotype of CAR-T cells at the end of culture was also evaluated. Interestingly, CAR-T cells produced in the G-Rex exhibited differentiation preference towards central

memory phenotype. Evaluation of the memory markers CD45RO and CD62L, showed higher CD45RO CD62L double-positive population percentage (77%±7.1% vs 41%±5.5%), compared with cells cultured in conventional culture flask (Figure 3-14). CD45RO CD62L double-positive cells were central memory T cells, which are considered to be required for long-term persistence *in vivo*[188,189]. Thus this bioprocess optimization method increased the cell output and the proportion with a central memory phenotype while decreasing the number of technician interventions and cost of CAR-T manufacture.

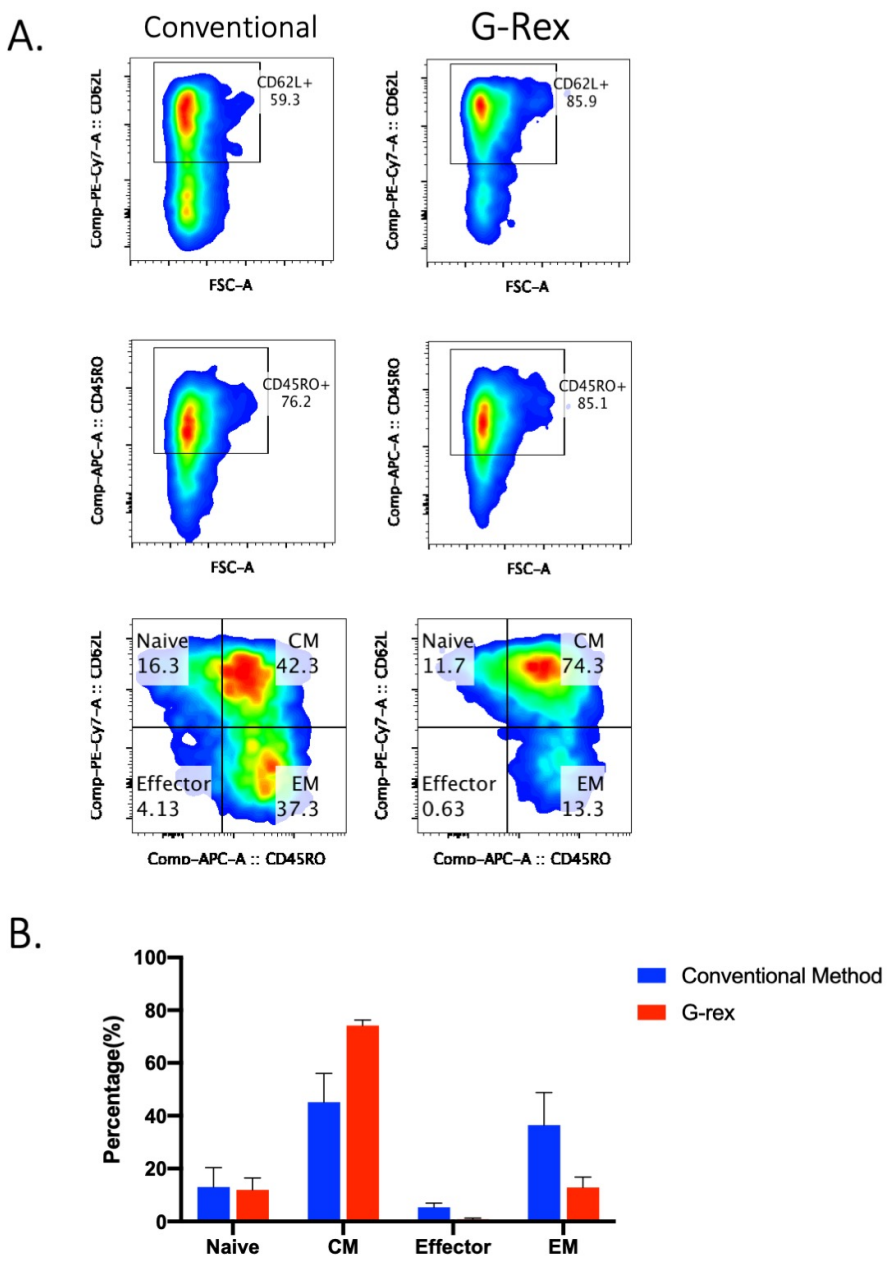

Figure 3-14 CAR-T cells produced from G-Rex preferentially differentiate to the central memory subset.

Cells harvested from the flask and G-Rex device were washed by PBS and stained by anti-CD45RO and anti-CD62L. Meanwhile, a control tube stained with isotype antibodies was prepared for determining the background of each channel. **A**. Representative flow plots of CD62L and CD45RO expression pattern. **B**. Statistic of T cell differentiation. CM, central memory; EM, effector memory. Three replicates of each sample were performed. Data are represented as mean ± SEM. Data reflects typical results from four healthy individuals.

3.7. Discussion

CD4 is an ideal target for immunotherapy for its broad expression on T-cell malignancy and absence on hematopoietic stem cells. Also, the application of anti-CD4 monoclonal antibody therapies in autoimmune diseases suggested that it would not induce serious side-effect to target CD4 transiently[112-114]. The third-generation CAR-T constructs with two co-stimulatory domains have been used in preclinical and clinical studies. Wang *et al*. tested multiple versions of CAR *in vitro* and found the CAR construct combining CD28 and 4-1BB signalling domains had the most capacity of proliferation and cytokine release[28]. Thus, to boost the activation signalling, a combination of co-stimulatory molecules CD28 and 4-1BB was designed.

The success of T-cell engineering for cancers is partially dependent on the development of gene delivery approaches. To date, multiple means have been applied to deliver CAR into primary human T lymphocytes, including non-viral delivery systems, such as Sleeping Beauty[190-194], mRNA electroporation[195,196], and viral delivery systems, such as retroviral and lentiviral vectors[197]. Retroviral vectors were the first system used for genetic engineering of T cells. They remain the most widely used vectors in clinical studies of CAR-T cell therapies. Compared with the lentiviral-based system, it is much simpler to establish a stable retroviral packaging cell line bank, which can significantly increase manufacturing consistency and decrease costs. Additionally, as most of the lentivirus-based gene delivery systems require concentration by ultracentrifugation, the retroviral particles harvested from PG-13 cell line can be directly applied for T cell transduction. Indeed, One round transduction consistently achieved 40%~60% of transduction efficiency, which increased to 85% after the second round of transduction.

The tracking marker tEGFR was successfully co-expressed on T cells, correlating with CAR expression (Figure 3-6). As anti-mouse IgG $F(ab)_2$ antibody will cross-react with other mouse antibodies, tEGFR was used to track CAR expression. It is difficult to directly detect iC9 expression, as it exists intracellularly. The success in the validation of suicide gene activation

has demonstrated the expression and function of iC9. Although tEGFR can also be used for ablation of engineered T cells, several side effects of EGFR-specific antibody Cetuximab do exist, such as grade 1 and 2 skin rash[198]. iC9 is considered to serve as a more specific and robust safety switch[72]. It has been assessed in clinical trials applied for adoptive T cell therapy[72] and stem cell transplantation[199]. Therefore, here for CART4, iC9 was considered as the primary safety switch. Of course, tEGFR can also be utilized if the urgent elimination of CAR-T cells is required in addition to iC9 as indicated below.

However, a small portion of $tEGFR^{+}$ cells were not sensitive to CID (Figure 3-10 and Figure 3-11). About 30% $tEGFR^{high}$ T cells remained after the 24-hour treatment with high dose CID. It was probably due to the insufficient expression and incomplete cleavage of the iC9[178]. To eliminate engineered T cells, it will be recommended to keep iC9 in the first gene position to achieve a higher expression level. For the rest of the thesis, the original version of CART4 was used, as iC9 was not further validated.

Although the conventional culture method is compliant with the manufacturing standard for clinical application, it is still a significant consideration to scale up the manufacture of CAR-T cells in an effective and efficient method. The G-Rex system, compared to the conventional platform, averts frequent manual intervention and yield a higher output of cell production. Indeed, CAR-T cells cultured in G-Rex expanded more than 150 fold (vs 100 fold from conventional method). More interestingly, the CAR-T cells produced in the G-Rex system exhibited differentiation preference towards central memory phenotype ($CD45RO^{+}$ $CD62L^{+}$). The central memory T cells are considered to be essential for the *in vivo* expansion and persistence of CAR-T[189]. Although the G-Rex is not a fully closed and automatic system, it provides a cost-effective platform for academic to scale up the manufacturing process of CAR-T cells for clinical trials.

The elimination of endogenous $CD4^{+}$ cell population suggested the potent cytotoxicity of CART4 cells against CD4-expressing cells. However, it is required to identify if the eradication

was mainly due to fratricide effect of CART4-transduced $CD4^+$ T cells, or the cytotoxic effect of CART4-transduced $CD8^+$ T cells. Therefore, the co-culture assay was performed to evaluate the CART4 systematically (see Chapter 4).

Chapter 4. Determining the anti-tumour potential of CART4 T cells

4.1. Targeting $CD4^+$ T cell lines using CART4 T cells

After generation of CART4 cells highly enriched for $CD8^+$ T cells, the cells were then tested *in vitro* for anti-tumour efficacy using the Jurkat cell line and CEM-ss cell line. Jurkat and CEM-ss cell lines were T-cell lines initially established from the peripheral blood of patients with T-cell leukaemia[200] or human T4-lymphoblastic leukaemia[201]. Both of the cell lines express CD4, while CEM-ss cell line expresses a higher level of CD4 (Figure 4-1A). Here, CAR-T cells were incubated with CFSE-labelled target cells at the ratio of 1:1, 3:1 and 5:1 ($2x10^4$, $6x10^4$ and $10x10^4$ cells to $2x10^4$ target cells respectively) for 4 hours. Later the cells were stained with DAPI to identify live/dead cells. The survived target cells were quantified by Countbright beads (Figure 4-1B). Indeed, CART4 cells targeted T tumour cell lines based on CD4 expression level. After short-term incubation, CART4 cells successfully eliminated CEM-ss cells at the E: T (effector: target) ratio of 5:1. As a control, CART4 cells were also tested for their activity to $CD4^-$ lymphoma cells, a human B-cell line (BCL) that does not express CD4 (Figure 4-1A). Flow cytometry analysis demonstrated that CART4 cells were unable to target BCL (Figure 4-1C). Moreover, CART4 cells cultured with $CD4^+$ tumour cells exhibited significant IFN-γ and TNF-α responses by intracellular cytokine staining (Figure 4-2).

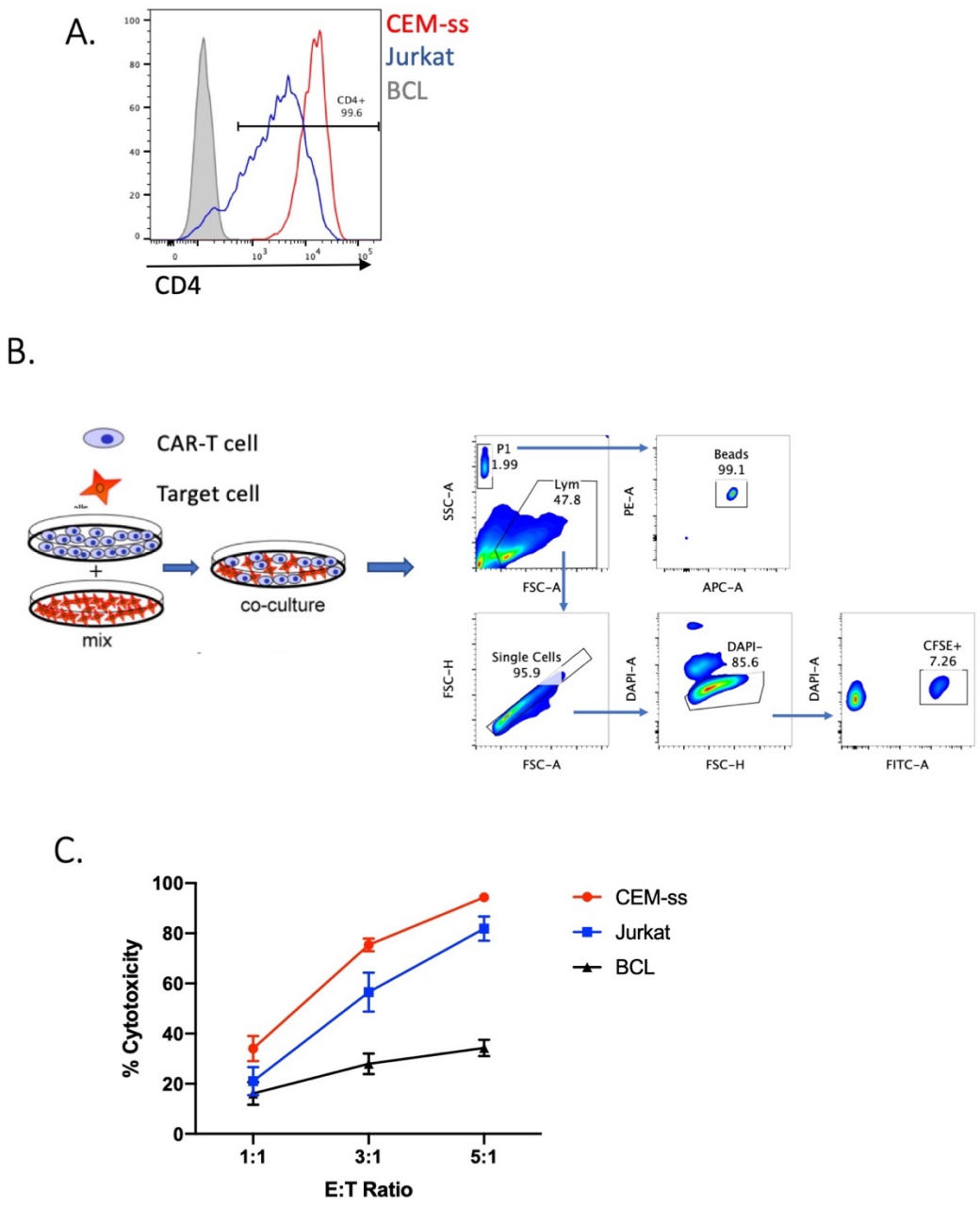

Figure 4-1 CART4 cells eliminate T-cell leukemic cell lines in co-culture assays.

A. Two T cell lines CEM-ss cell, Jurkat cell and one B cell line were stained by the anti-CD4 antibody. The CD4 expression level was assessed by flow cytometry analysis. **B**. CFSE-labelled target tumour cells were mixed with a different number of effector CAR-T cells. After 4-hour incubation, cells were collected and stained by DAPI for 5 minutes at room temperature. A fixed volume of 5 μl Countbright beads were added into each sample. The samples were loaded to flow cytometry for absolute quantification. **C**. Representative result of CART4 cells killing T tumour cells. Three replicates of each sample were performed. Data reflects typical results from three independent experiments.

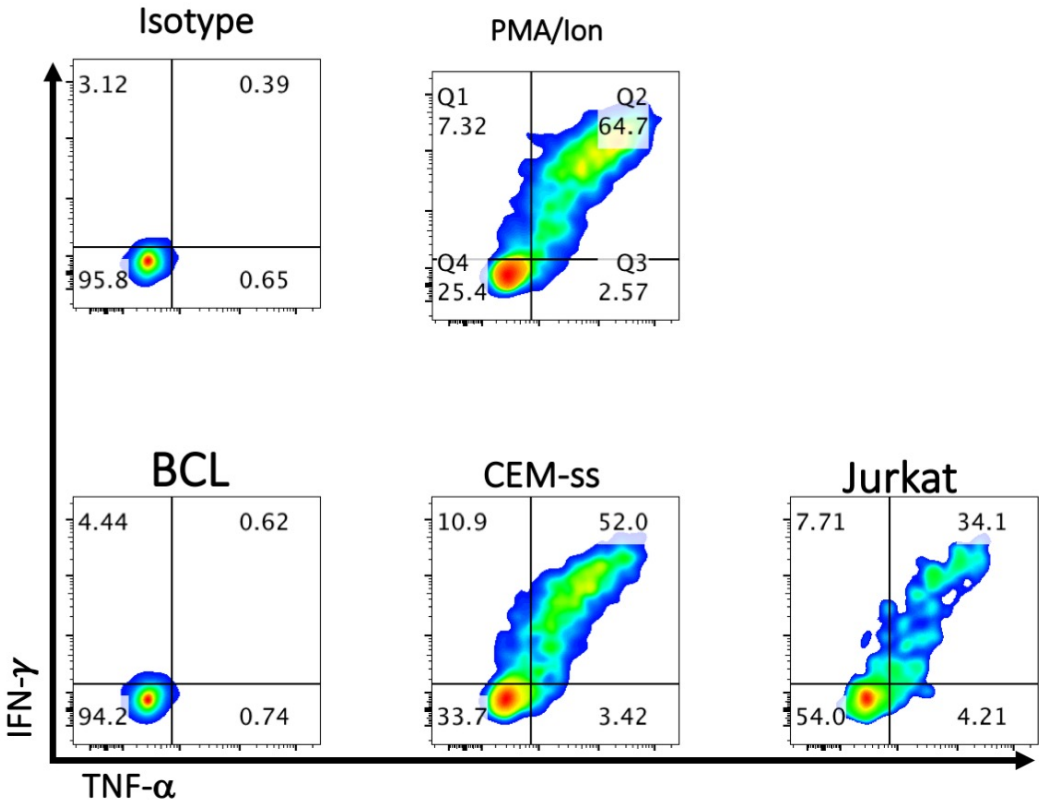

Figure 4-2 Cytokine production by CART4 cells co-cultured with target cell lines.

Effector CART4 cells were co-cultured with target cell line in 1:1 ratio. After one hour, brefeldin A was added to the co-culture system to inhibit protein transport. PMA/Ionomycin was used as a positive control. CART4 cells stained by isotype antibodies served to determine the background of fluorescent signal. Data reflects typical results from three independent experiments.

To further evaluate the function of CART4 cells, co-cultures were established against autologous primary healthy donor PBMCs. CFSE-labelled autologous PBMCs were co-cultured with either $CD8^+$ CART4 cells or CART20 cells. In both settings, CART4/20 cells mediated high-level cytotoxicity against respective target cells. 94% of $CD4^+$ cells in PBMCs were lysed by CART4 cells in the condition of E: T ratio 3:1 during 4-hour co-culture. However, there was no specific T-cell cytotoxicity of CART4 in response to $CD20^+$ cells, compared with NTD T cells (Figure 4-3).

Therefore, these data proved a strong dose-dependent response of CART4 against CD4 expression. When CART4 cells were incubated with CD4-negative cells, no killing effect was observed. These results show that CART4 cell ablation is specific to CD4.

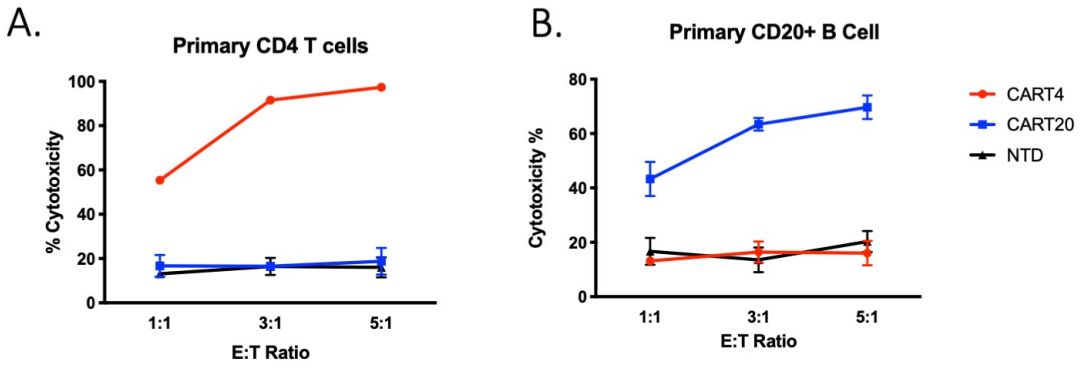

Figure 4-3 CART4 cells mediate potent and specific killing of primary CD4⁺ cells in vitro.

Primary CD4⁺ T cells (**A**) or CD20⁺ B cells (**B**) were co-cultured with either autologous CART4 cells, CART20 cells, or non-transduced CD8⁺ T cells. Co-culture system was harvested 4 hours after incubation and stained by DAPI. The absolute quantity of survived target cells was counted using Countbright beads by flow cytometry analysis. Three replicates of each condition were performed. Data are represented as mean ± SEM. Data reflects typical results from four independent experiments.

4.2. Targeting primary ATL and CTCL cells using CART4 T cells

To examine the function of CART4 to patient samples, PBMCs from ATLL patients were thawed and phenotyped. All the samples had a range of CD4 expression from 67.4% to 97.7%. Most of the CD4⁺ cells express one unique β chain of the T cell receptor (TCR Vβ) indicating the clonal development of T cell leukaemia[202-204] (Figure 4-4A). As quantified by flow cytometry analysis, co-culture of ATLL patient samples with CART4 cells for 4 hours resulted in rapid

and definitive ablation of $CD4^+$ malignancies. About 80% ablation was observed for all ATLL co-cultures, consistent with the ablation of blast T cell lines previously shown (Figure 4-4B).

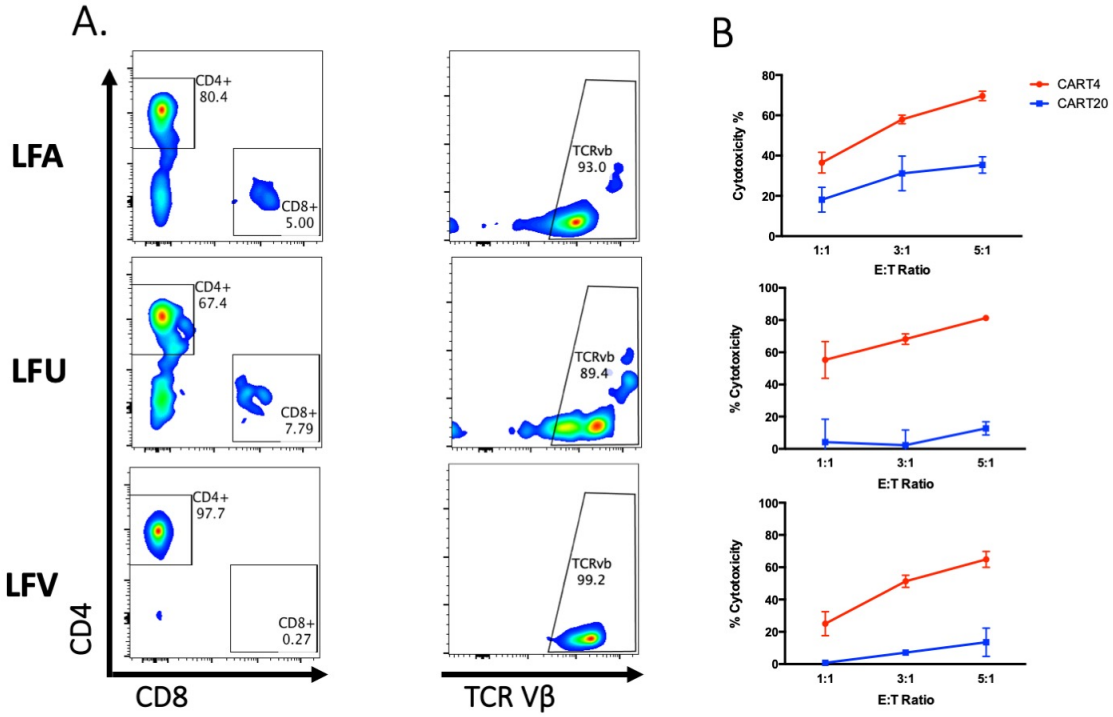

Figure 4-4 CART4 cell functionality against primary $CD4^+$ tumour cells from ATLL patients in vitro

PBMC vials from ATLL patients were revived from liquid nitrogen and rested in the incubator overnight before flow cytometry analysis and co-culture experiment. **A**. The PBMCs were stained by anti-CD4, CD8 and specific TCR Vβ. Flow cytometry was performed after two washes with PBS. **B**. Revived ATLL PBMCs were co-cultured with allogenic CART4 or CART20 cells for four hours before flow cytometry analysis. Three replicates of each condition were performed. Data are represented as mean ± SEM.

Studies were also conducted using samples from six CTCL patients. Similarly, observed robust cytotoxicity of CART4 cells against freshly thawed primary CTCL cells was observed, resulting in about 60%~80% reduction of malignant T cells after 4 hours of co-culture (Figure 4-5).

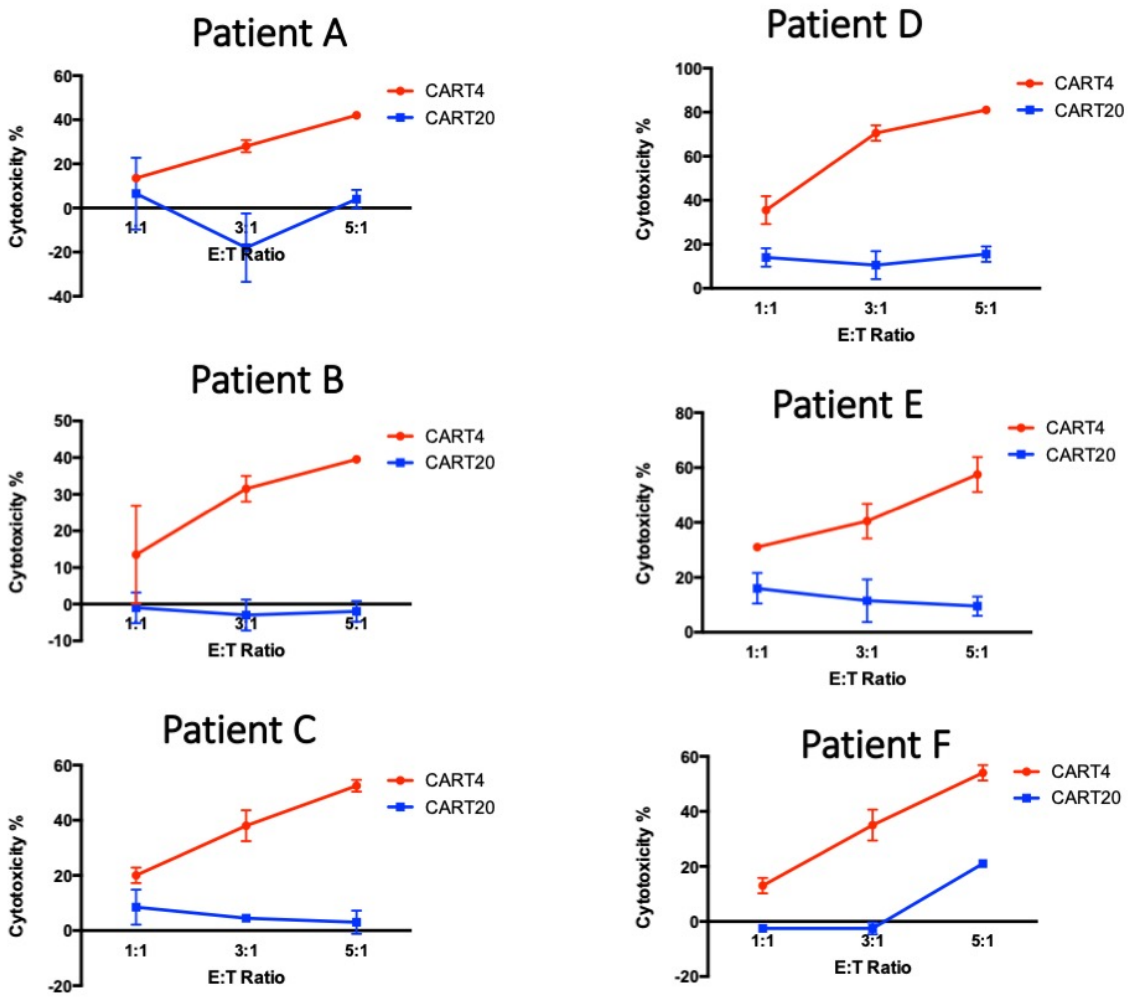

Figure 4-5 CART4 cells mediated potent killing of CD4⁺ tumour cells from CTCL patients in vitro.

Samples from six CTCL patients were revived from liquid nitrogen and co-cultured with allogenic CART4 or CART20 cells at different E:T ratios. Three replicates of each condition were performed. Data are represented as mean ± SEM.

Therefore, CART4 cells efficiently eliminated aggressive $CD4^+$ T-malignancies directly isolated from patients samples. These results indicate that CD4 is a promising therapeutic target for $CD4^+$ T-malignancy.

4.3. Development of an *in vivo* T-leukaemia xenograft model

In order to evaluate *in vivo* anti-tumour activities of CART4, a xenogeneic mouse model was developed using the CEM-ss cells which were transduced by a lentiviral vector containing Gaussia luciferase (Gluc) and enhanced GFP (eGFP) gene in order to quantitatively trace the tumour progress *in vivo*. Gluc is a 20kDa protein discovered from the marine copepod, *Gaussia princeps*. The bioluminescent enzyme is naturally secreted into the extracellular, allowing for live cell monitoring of reporter activity. The signal produced by Gluc shows active flash kinetics and is even higher than signals from firefly luciferase (ffluc). These properties make it an ideal reporter gene for *in vivo* tumour progress monitoring[205]. Here a lentiviral vector FG12 containing eGFP and Gluc genes (FG12-EG） was used to generate lentivirus particles (Figure 4-6A). The particles were used to establish the stable expression of Gluc/ eGFP in CEM-ss cell line to achieve >99% eGFP expression in the population (Figure 4-6B). The luciferase activity was measured from the cell lysate and culture supernatant using Gaussia Luciferase Flash Assay Kit. Active signalling was detected from the supernatant harvested from 24-hour cell culture. Note that although Gluc is a secreted reporter, there was sufficient measurable activity inside the cell (Figure 4-6C).

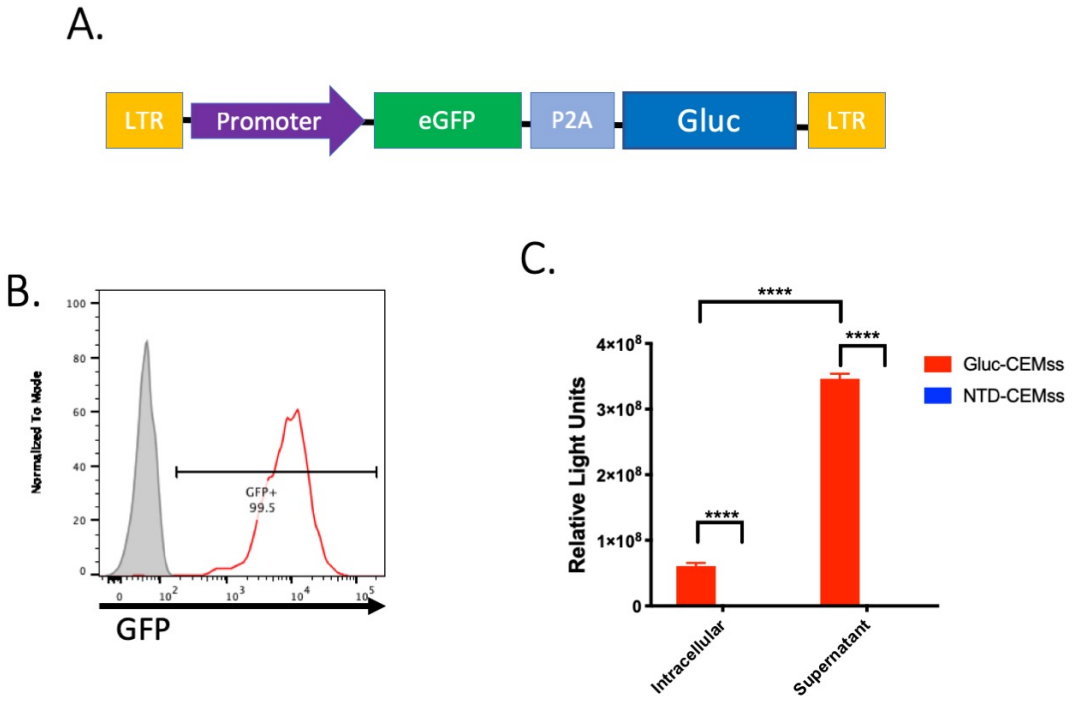

Figure 4-6 Preparation and Characterization of T cell line expressing Gaussia luciferase.

A. Schematic representation of eGFP-P2A-Gluc insertion of FG12-EG lentiviral vector. **B**. Transduced CEM-ss cells were assessed GFP expression by flow cytometry analysis. Grey histogram represents untransduced cells. **C**. Culture supernatant and cell lysis of CEM-ss transduced Gluc were tested for luciferase activity. Three replicates of each sample were performed. Data are represented as mean ± SEM. Data reflects typical results from three independent experiments. A two-tailed unpaired Student's t-test was used for significance analysis. **** = $p<0.0001$.

Then, xenograft formation by Gluc/eGFP-expressing leukaemia cell line was investigated in NRG (NOD/RAG1/2$^{-/-}$IL2Rγ$^{-/-}$) mice by inoculating 5x10^5 tumour cells via retro-orbital injections. Since tumour cells continuously secrete Gluc outside the cell, its activity in the serum would indicate the tumour engraftment. Indeed, Gluc activity was detected in mice that received tumour cells two days post-infusion (Figure 4-7A). However, all of the tumour-inoculated mice were died or euthanized due to the fast tumour progression within ten days

after the graft (Figure 4-7B). The fast disease progress indicated CEM-ss was a quite malignant tumour cell in the immunodeficient mice model. The fast development of tumour cell may require a higher dose of infused CAR-T cells and induce severe side effects. To better investigate the CAR-T efficacy, a reduced dose of administrated cancer cells $1x10^5$ for the subsequent studies was used.

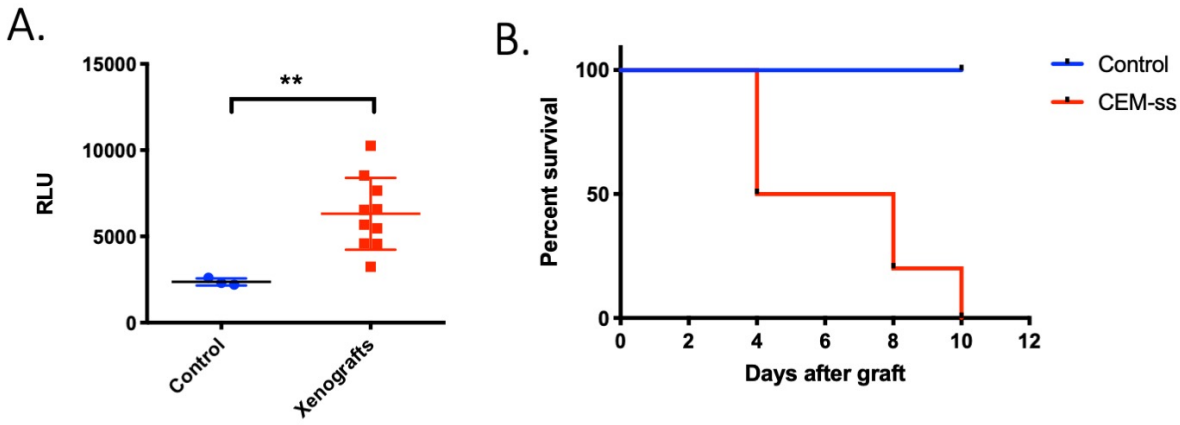

Figure 4-7 Luciferase activity and host death induced by transplantation of CEMss-Gluc

5 $x10^5$ CEMss-Gluc cells were transplanted to NRG mice (n=10) via retro-orbital route. **A**. Xenograft recipients were bled, and luciferase activity in peripheral blood was detected after two days. Control mice n=3. **B**. Kaplan-Meier survival analysis of survival curve. Data are represented as mean ± SEM. A two-tailed unpaired Student's t-test was used for significance analysis. ** = $p<0.01$.

4.4. Anti-tumour activity of CART4 cells in the T-leukaemia xenograft model

I tested the ability of the CART4 cells to control the T leukaemia in the NSG mice with a single dose ($4x10^6$) of CART4. Before the injection, about 50% of cells expressed the anti-CD4 CAR as demonstrated by flow cytometry analysis (data not shown). Mice received retro-orbital

injections of CEM-ss cells. Four days after tumour engraftment, a single dose of retro-orbital injection of CART4 cells or NTD $CD8^+$ T cells was administered to leukaemia-bearing mice (Figure 4-8A). Tumour burden was monitored by measuring luciferase activity in peripheral blood weekly. CART4 cells infused provided robust protection against leukaemia progression (Figure 4-8B) and significantly extended median survival of the mice (38 days in the control group vs 60 days in the CART4 group, P = 0.026 by Mantel-Cox log-rank test) (Figure 4-8C). Indeed, by the endpoint, $eGFP^+$ tumour progression was dramatically delayed in spleens and bone marrows by flow cytometry analysis (Figure 4-8D).

Although relapsed tumour cells retained expression of CD4, the expressing level dropped up to about 40% MFI compared to control group (Figure 4-9A). This downregulation, however, was insufficient to compromise the ability of CART4 cells to eliminate the relapsed tumour (Figure 4-9B). This result was indicating that a lack of CAR-T cell persistence rather than antigen escape was the primary reason for the tumour relapse.

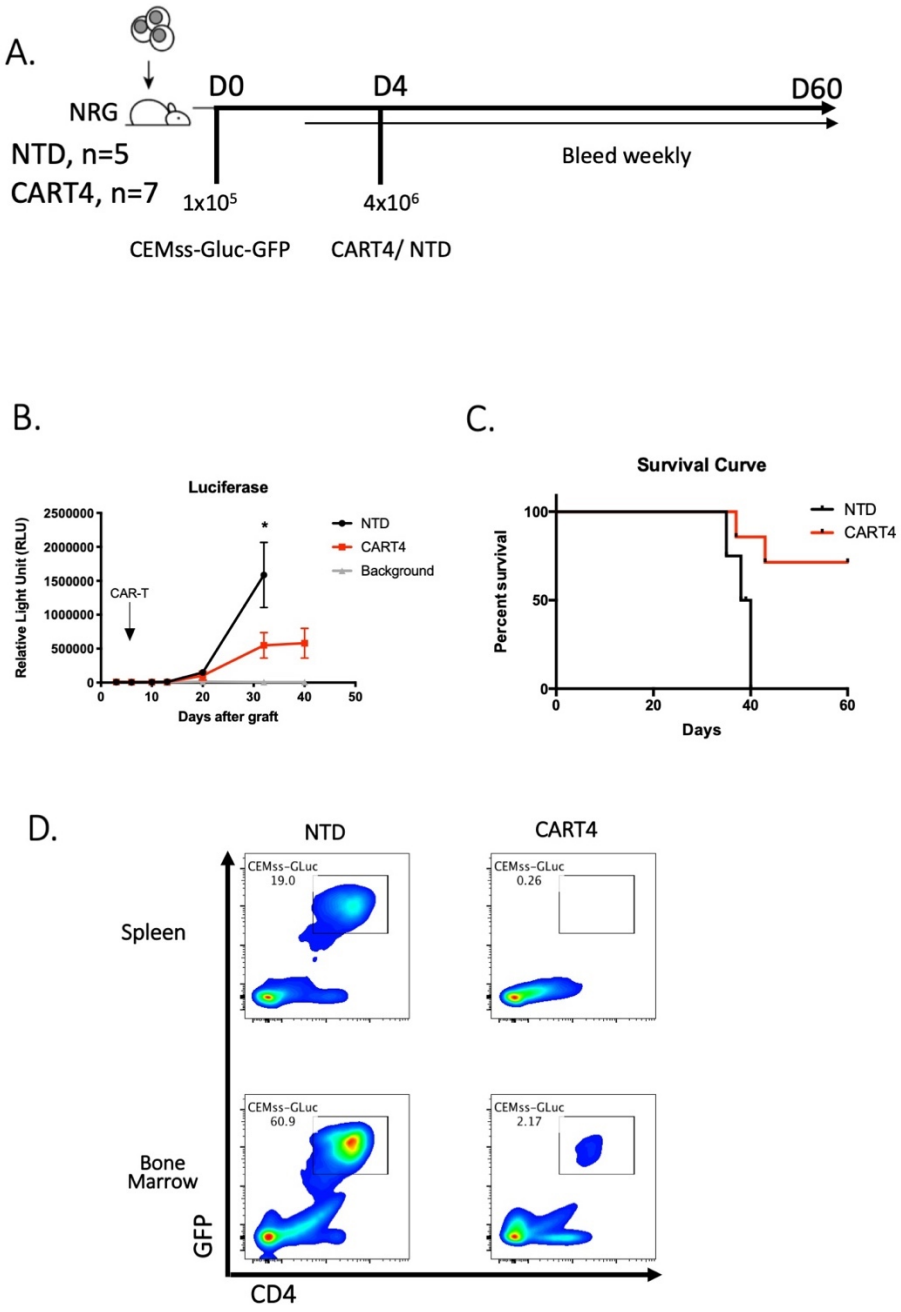

Figure 4-8 CART4 cells efficiently mediate antileukemic effects in vivo with the xenograft model

A. NRG immunodeficient mice were injected with 1x10^5 Gluc/ GFP-transduced CEM-ss cells, followed by another infusion of 4x10^6 T cells via the retro-orbital route. NTD n=5, CART4 n=7. **B**. 50 µl of peripheral blood of each mouse was bled and the plasma was used for the measurement of luciferase activity. Serial measurement of luciferase activity shown inhibition of CD4$^+$ leukaemia by CART4 T cells but not NTD CD8$^+$ T cells. **C**. Overall survival of mice treated with the indicated CART4 cells or the

control NTD T cells by Kaplan-Meier survival analysis. **D**. At the endpoint, the mice were dissected. The spleens and bone marrows were ground and stained by anti-CD4 mAb and DAPI for detection of residual tumour cells. Tumour cells were identified as $DAPI^{-}$ $CD4^{+}$ GFP^{+}. Data are represented as mean ± SEM. A two-tailed unpaired Student's t-test was used for significance analysis. * = $p<0.05$,

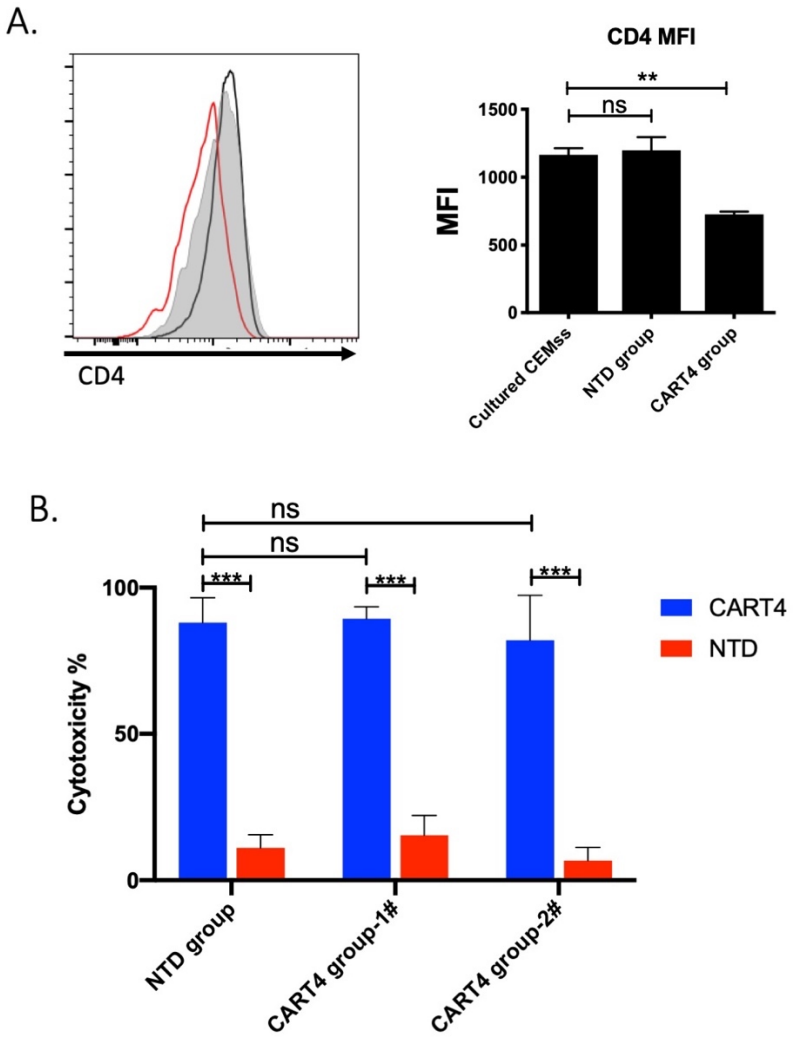

Figure 4-9 The relapsed tumour cells showed a reduced CD4 expression

The leukocytes of spleen were stained by anti-CD4 antibody and analysed by flow cytometry. Grey line-cultured CEMss cells, black line- CEMss cells from NTD control mice, red line-CEMss cells from CART4 treated mice (**A**). The splenic cells were co-cultured with CART4 cells or NTD T cells in 1:5 ratio for 4 hours, before being analysed by flow cytometry (**B**). Three replicates of each condition were performed. Data are represented as mean ± SEM. A two-tailed unpaired Student's t-test was used for significance analysis. ns= $p>0.05$, ** = $p<0.01$, *** = $p<0.001$.

4.5. Discussion

In this chapter, the therapeutic potential of CART4 for $CD4^+$ T-cell malignancies was investigated by *in vitro* assays as well as *in vivo* animal model.

The remarkable success of CD19-specific CAR-T therapy towards B-cell leukaemia/lymphoma inspired many researchers to discover new targets. CD4 was considered as a potential target for cellular therapy for its high expression in the majority of mature T-cell malignancies and absence from hematopoietic stem cells. Additionally, anti-CD4 monoclonal antibodies have been assessed in clinical trials for T-cell malignancies, such as CTCL[112 206], PTCL, nodal T-cell lymphoma[207]. Those studies indicated that a transient depletion of $CD4^+$ T cells in human was safe.

Several other targets also have been evaluated as potential targets for T-cell malignancies, such as CD3[85], CD5[87,208], CD7[88,102,103], CD30[89,105], etc. Most of them showed effective anti-tumour function in preclinical studies. However, most of those targets are also expressed on other normal T cells, both $CD4^+$ and $CD8^+$ T cells, causing profound T-cell aplasia. Additionally, the expression of target on CAR-T cells will induce a fratricide effect, which prevents generation and expansion of CAR-T cells. In order to prevent fratricide, the CAR-T cells were required to genetically edit or treat with specific antibodies for deleting or suppressing the expression of those T-cell targets on CAR-T cells[85,87,102,103,208,209]. Comparatively, CD4-targeting cellular therapy would keep the subset of CD8 CTL cells. The efficacy of CAR-T therapy is mainly attributed to the $CD8^+$ subset[210]. Infusion of *in vitro* expanded $CD8^+$ central memory T cells established persistent T cell memory in primates[39]. Additionally, CD19-specific CAR-T cells derived from $CD8^+$ central memory cells have been assessed in xenograft models[211] and applied in an FDA-authorized clinical trial[212].

The anti-tumour efficacy of CART4-transduced T cells was assessed by co-culture assay. After 4-hour incubation at E:T ratio of 5:1, 100% of CEM-ss cells and about 80% of Jurkat

cells were lysed (Figure 4-1). Also, a significant level of IFN-γ and TNF-α was detected in CART4 cells (Figure 4-2). Additionally, in the revived primary ATLL blasts from patients, clonal expansion of TCR Vβ in the $CD4^+$ population was observed, which indicated the malignant expansion of tumour cells. In an *ex vivo* experiment, CART4 cells effectively killed ATLL and PTCL cells from patients. The in vitro efficacy of CART4 is similar to that of CD19 CAR. Even though they are not comparable for different target and tumour types, the result indicated potent anti-tumour ability in the clinical setting.

A xenograft model was developed to evaluate the efficacy of CART4 further. CART4 cells were infused to xenografts bearing CEM-ss tumour cells. The tumour progression was monitored by luciferase activity in peripheral blood. Infused CART4 cells dramatically inhibited tumour progression, which was consistent with the observation in other organs, such as spleens and bone marrows (Figure 4-8). Though the CART4-infused mice suffered tumour relapse ultimately, the relapsed tumour cells were still sensitive to CART4 cells. It indicated that insufficient persistence of CAR-T cells was the main reason for the tumour relapse. Indeed, the immunodeficient mice model bearing tumour does not fully imitate the human microenvironment for CART4 cells, as there are no human cytokines and other cell types to support CAR-T cell function and persistence *in vivo*. Thus, the xenograft model may underestimate the actual anti-tumour potency of CART4 cell *in vivo*.

The long-term $CD4^+$ T-cell aplasia will result in severe immunodeficiencies such as an HIV/AIDS-like syndrome. However, the results from anti-CD4 monoclonal antibodies for patients with autoimmune disorders, T-cell malignancies and HIV infection suggested a transient CD4 depletion is likely acceptable. Besides, the incorporation of suicide gene iC9 and tEGFR in our CART4 construct could be used for elimination of CART4 cells if needed. As hematopoietic stem cells are prevented from the attack of CART4 cells, $CD4^+$ depletion could be reversible, consistent with the observation in non-human primate[126,211]. Alternatively, CART4 cells provide a bridging strategy by achieving complete remission before allogeneic HSPC transplantation.

Chapter 5. Determining the potential of CART4 T cells for HIV-1 cure

Though combination antiretroviral therapy (cART) has dramatically improved the life of HIV infected individuals, there are no effective treatments to eradicate the virus. cART, composed of a cocktail of anti-retrovirus drugs, can only affect cells with the active replicating virus. However, it is still a big challenge to eliminate or control the virus to achieve a 'sterilizing cure' or 'functional cure'. The infected cells which harbour transcriptionally silent HIV can persist in the patients for dozens of years. Virus rebounds rapidly following even brief cART interruption, despite prolonged suppression of plasma viremia[213-215].

CD4, which has a relatively high binding affinity to HIV viral envelope protein gp120, is the primary cellular receptor for HIV entry. Therefore, $CD4^+$ T cells, mainly resting CD4+ T cells, are considered to be a significant source of HIV reservoir[216]. After infection by HIV in an activated state, a small proportion of the CD4+ T cells differentiate into memory state, and function as a long-term HIV reservoir. Additionally, it is also well established that other $CD4^+$ cell subsets, including dendritic cells (DCs) and macrophages, can be infected by HIV and contribute to the HIV reservoir[217-220]. Therefore, CART4 cells were applied to eliminate the viral reservoir and examine if it is possible to achieve 'HIV cure' by depleting $CD4^+$ cells in a preclinical setting.

5.1. Targeting dendritic cells and macrophages using CART4 cells

The previous results have demonstrated the potent function of CART4 cells against $CD4^+$ T cells, which are recognized as the major obstacle to HIV-1 cure. Subsequently, the CART4 was investigated its function to other $CD4^+$ HIV infected cells, such as DCs and macrophages. To do this, DCs and macrophages were differentiated from monocytes *in vitro*. $CD14^+$ monocytes were positively isolated from the buffy coat by using CD14 magnetic beads and were cultured in DC medium (R10+ hGM-CSF+hrIL-4) or macrophage medium (R10+hGM-CSF) for nine days. The cells were collected for flow cytometry analysis. Cells harvested from DC medium exhibited CD1a-positive phenotype, while cells from macrophage medium expressed a high level of CD14 (Figure 5-1A). The surface markers demonstrated a successful differentiation outcome, consistent with the distinct phenotypes observed by microscopy (data not shown).

Both the monocyte-derived DCs and macrophages were CD4-positive, though the intensity of CD4 expression was lower than $CD4^+$ T cells (Figure 5-1B). The capacity of CART4 cells to kill the DCs and macrophages was assessed by co-culture assay. CART4 cells showed less effective cytotoxicity against DCs and macrophages during a 6-hour incubation period, which was due to lower antigen expression and probably cell-intrinsic resistance to cytotoxicity[148]. However, CART4 cells had robust cytotoxicity against CFSE-labelled DCs and macrophages, with >80% decrease in counts of viable target cells after 24 hours of co-culture even at a low E: T ratio (1:1) (Figure 5-2A and B). Co-culture with DCs or macrophages also induced significant intracellular TNF-α and IFN-γ production of CART4 cells (Figure 5-2C). Therefore, CART4 cells demonstrate potent killing activity against DCs and macrophages, which are considered to contribute to the HIV reservoir in infected patients.

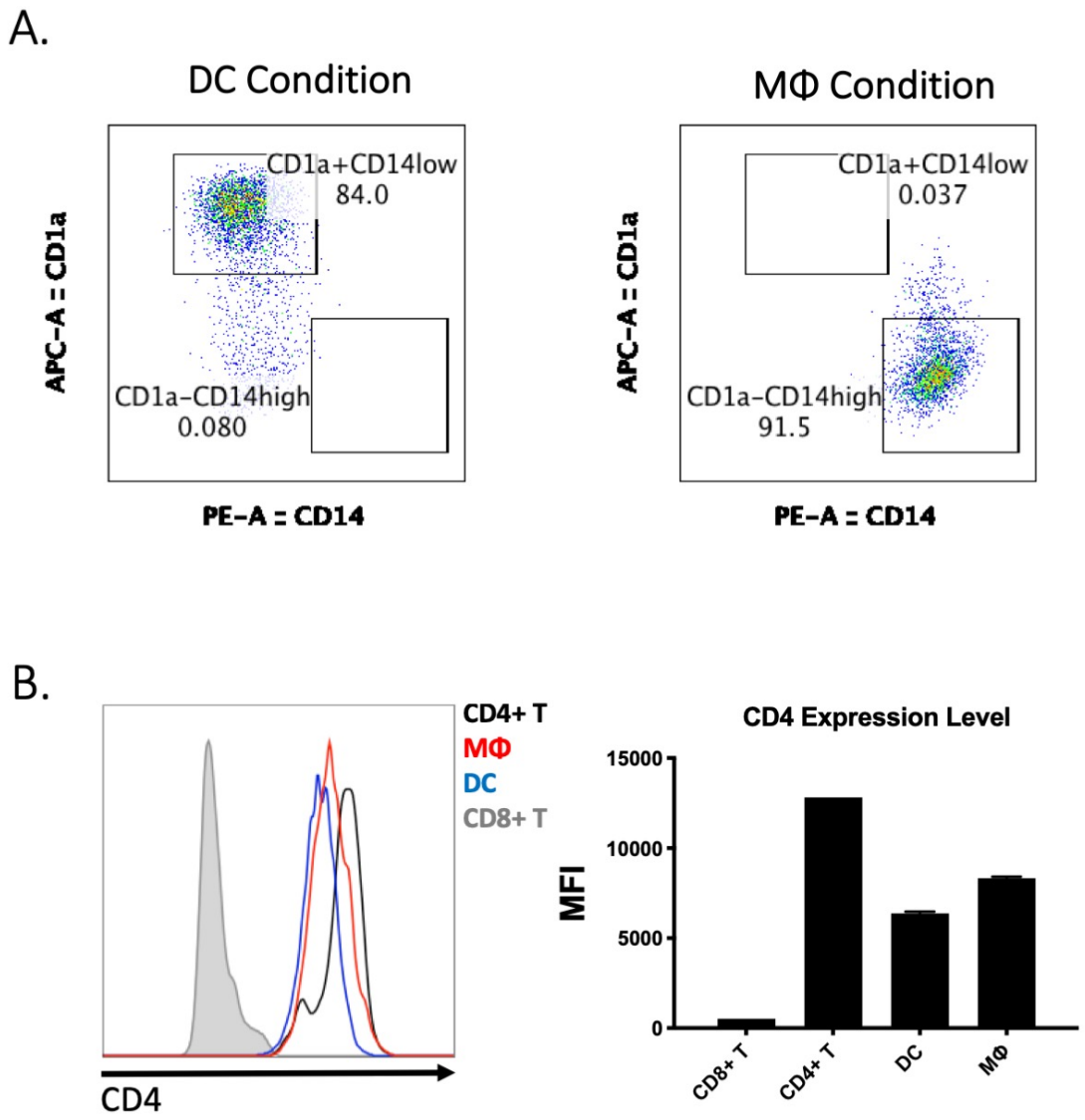

Figure 5-1 Monocyte-derived DCs and macrophages expressed CD4.

Cells cultured in conditional medium for DC or macrophage maturation were harvested on the ninth day. The expression patterns of CD14 and CD1a indicated successful differentiation of DCs and macrophages (**A**). Monocyte-derived DCs and macrophages expressed significant levels of CD4 (**B**). Three replicates of each sample were performed. Data are represented as mean ± SEM. Data reflects typical results from two independent experiments.

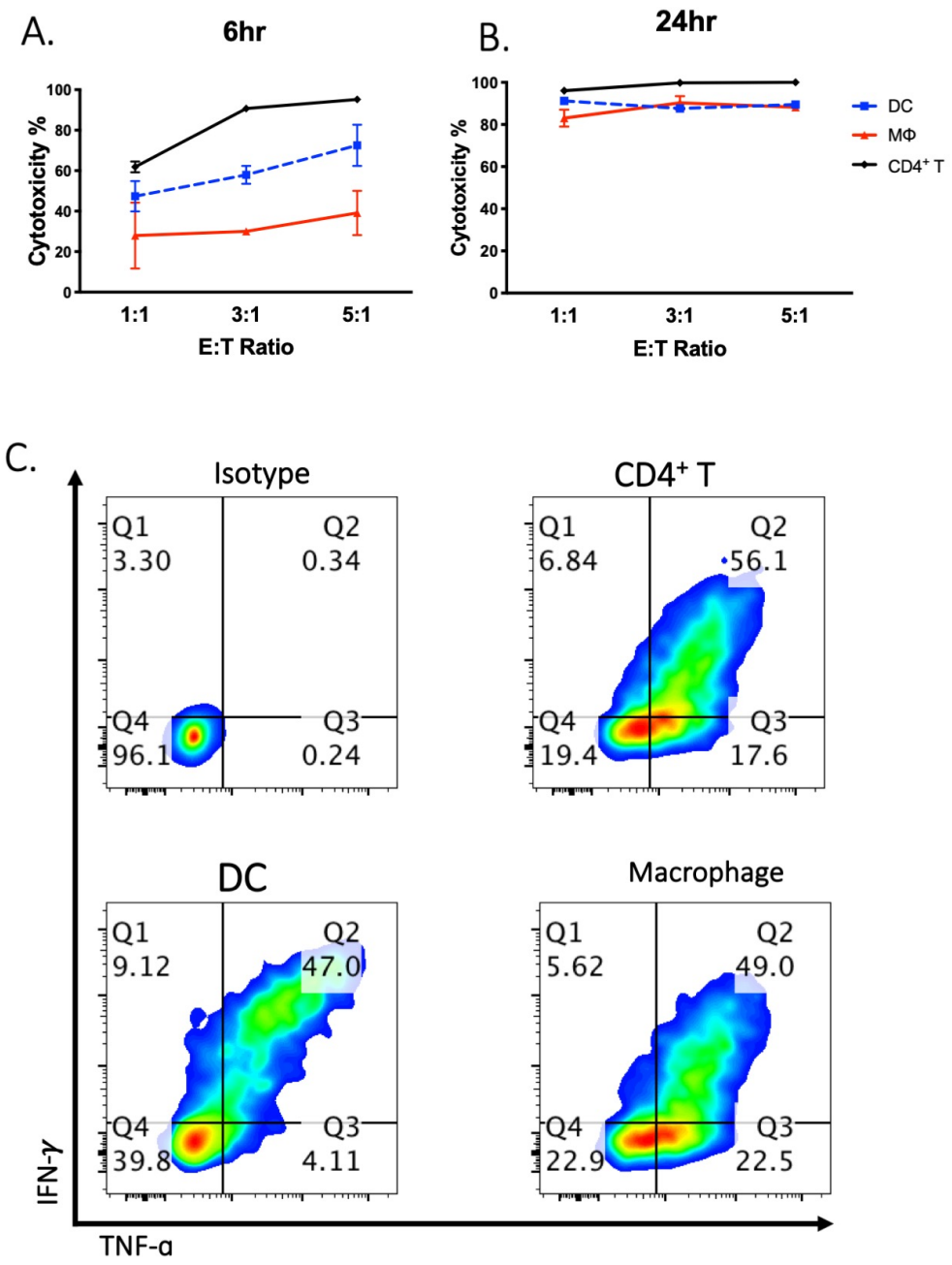

Figure 5-2 CART4 cell functionality against monocyte-derived DCs and macrophages.

CFSE-labelled CD4+ T cells, DCs or macrophages were co-cultured with autologous CART4 cells in different E: T ratio. Samples were collected and analysed by flow cytometry after 6- or 24-hour co-culture (**A and B**). CART4 cells were collected, fixed and stained for intracellular cytokine detection (**C**). Three replicates of each sample were performed. Data are represented as mean ± SEM. Data reflects typical results from two independent experiments.

5.2. Development of humanized mice

For proof-of-concept of anti-HIV efficacy of CART4 cells *in vivo*, a PBL-derived humanized mouse model with autologous material from humans was developed. 6-week old NRG (NOD/RAG1/2$^{-/-}$IL2Rγ$^{-/-}$) mice were injected via retro-orbit inoculation with 10x10^{6} human PBMCs in 100ul PBS. Peripheral blood was obtained by bleeding from the tail vein after three days, and then weekly after for up to four weeks. Reconstitution of human lymphocytes was detectable within three days and dominated in peripheral blood within ten days. Furthermore, 3.5 weeks after reconstitution, up to 98.6% of CD45^{+} human lymphocytes were T cells, about 54% of which are CD4^{+} cells (Figure 5-3A). Most of the CD4^{+} cells in peripheral blood expressed CD3 (>99.5%), indicating the CD4^{+} T cell subset (Figure 5-3B). CD4^{+} T cells were also detectable in organs such as the spleens and bone marrows at four weeks after reconstitution, though lower levels of engraftment occurred in the spleen(Figure 5-4). This model can survive about 3-4 months until becoming sick due to xenograft-mediated GVHD[221,222]. Therefore, a PBL hu-mice model was established, which can be utilized as a preclinical testing platform for assessing anti-HIV efficacy of CART4 cells.

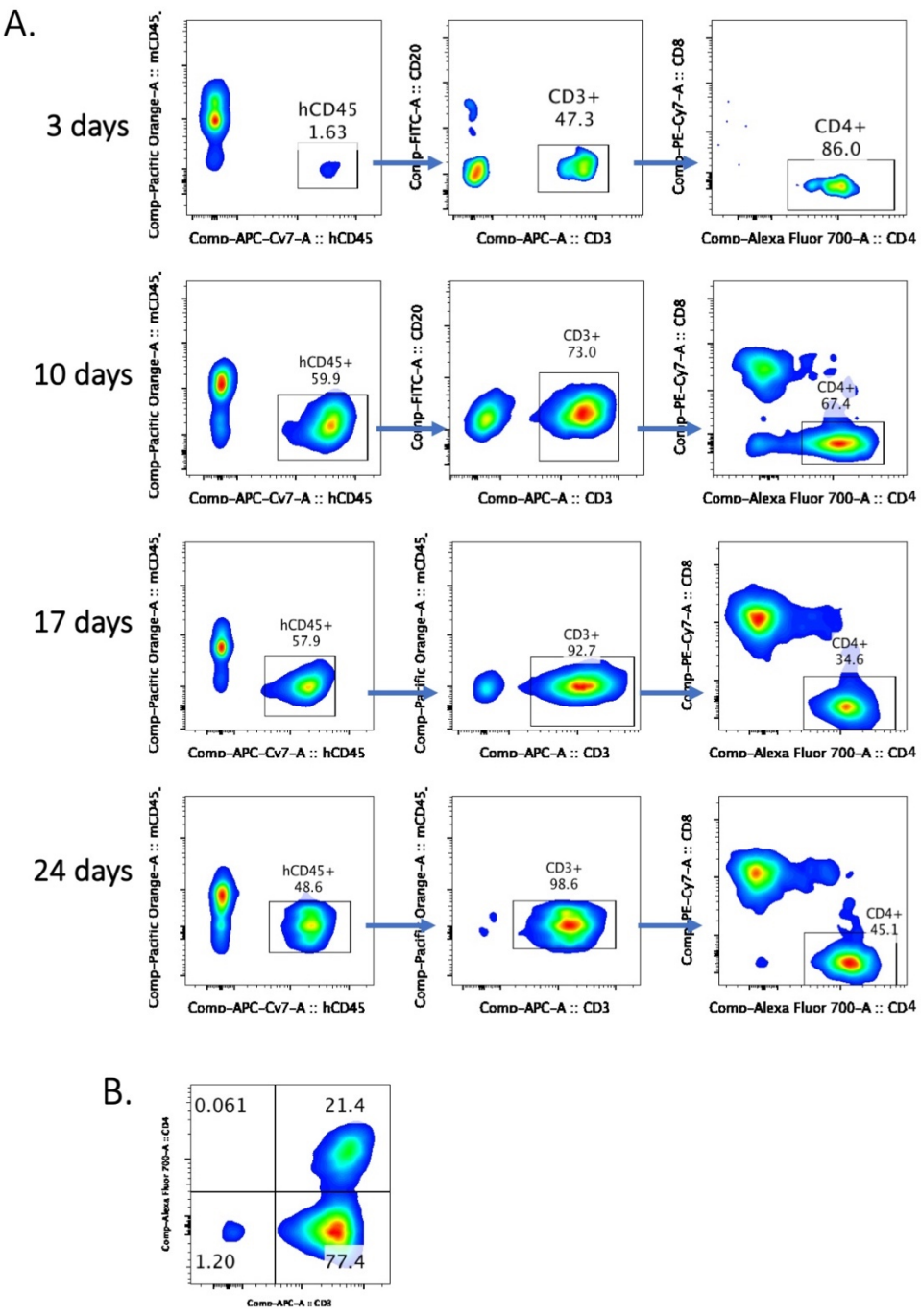

Figure 5-3 Reconstitution of PBL humanized mice

Peripheral blood was taken from the tail vein and assessed for human leukocytes engraftment. PBMCs were isolated after red blood cell lysis and stained by flow antibodies. **A**. The left plots are the lymphocytes. The middle plots are cells gated by $hCD45^+$ $mCD45^-$, while the right plots shows $CD3^+$ $CD20^-$ cells. **B**. More than 99.7% of $CD4^+$ cells are $CD3^+$ T cells in peripheral blood. Data reflects typical results from two independent experiment (n=8).

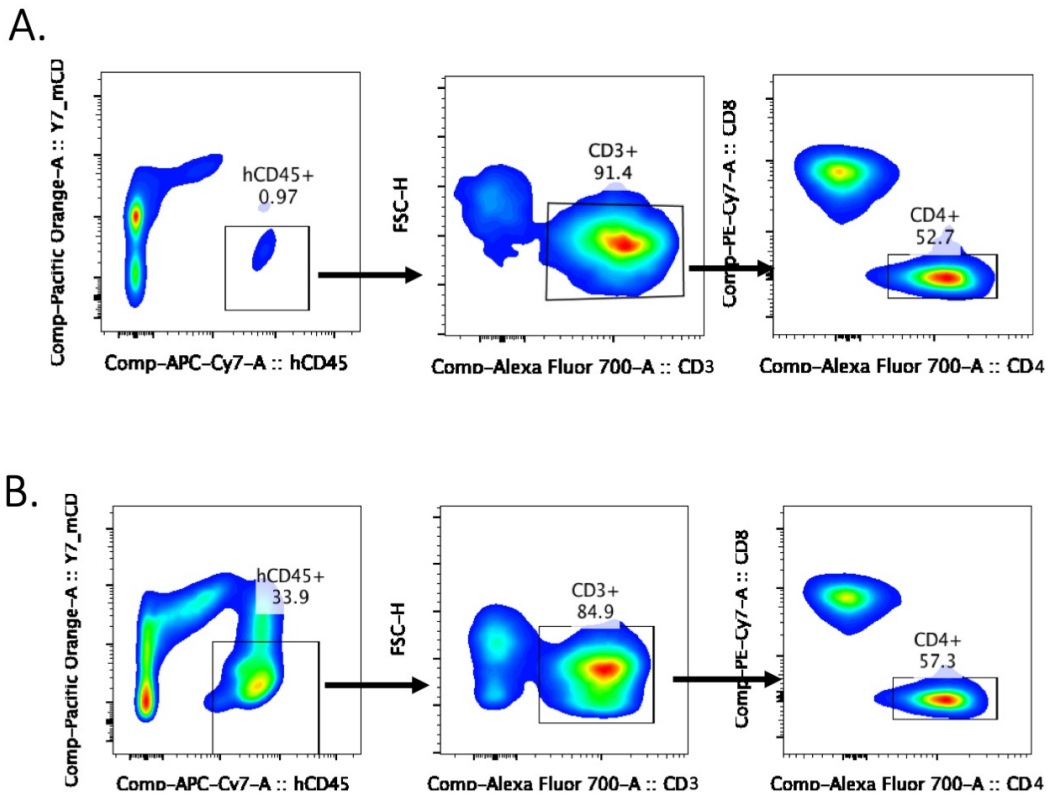

Figure 5-4 Humanization of PBL hu-mice in organs

Four weeks post reconstitution, humanized mice were euthanatized and dissected. Cells from the spleens (**A**) and bone marrows (**B**) were stained by flow antibodies (anti-mouse CD45, human CD45, CD3, CD4, CD8) and analysed by flow cytometry. Data reflects typical results from two independent experiment (n=8).

5.3. Targeting HIV-1 infection of CART4 cells in the humanized mouse model

To mimic how CART4 cells would be applied in a clinical setting, CART4 cells were injected into humanized NRG mice reconstituted by autologous PBMCs with a previously established

HIV infection in the presence of cART treatment, and measured virus rebound after cART was interrupted (Figure 5-5A).

Four days after cART treatment, the blood $CD4^+$ cell counts were similar in both groups. However, CD4 depletion was apparent in CART4 treated mice within three days after CAR-T infusion. In the non-transduced (NTD) cell treated group, $CD4^+$ cell counts continued to increase, which might be due to T cell activation and expansion induced by GVHD (Figure 5-5B and C). By the endpoint bleed, peripheral $CD4^+$ cell counts dropped to 253 ± 291 cells per millilitre blood from the CART4 treated group, while frequencies from the NTD control group increased to $3.8x10^7 \pm 4.6x10^7$ $CD4^+$ cells per millilitre blood, which suggested >99.999% elimination efficiency in peripheral blood (Figure 5-5D). Consistently, complete CD4+ depletion was observed in other organs, such as bone marrow and spleen （Figure 5.3C）, indicating CAR-T cells engraftment and function in these tissues.

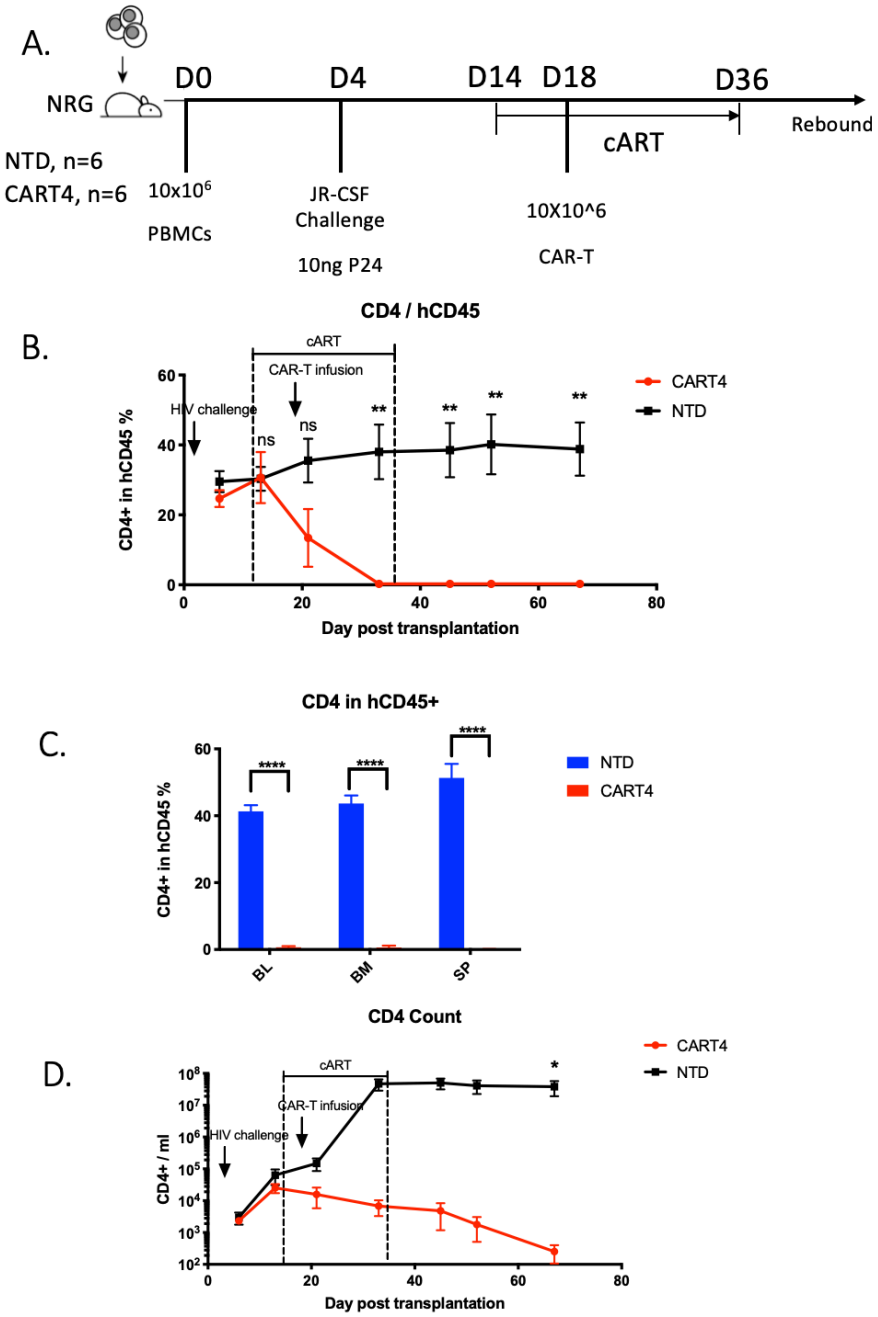

Figure 5-5 CART4 cells effectively eliminated CD4⁺ cells in PBL humanized mice model.

(**A**) Four days after transplantation of human PBMCs, 12 NRG mice were infected by JR-CSF strain HIV via retro-orbital route. The cART drug was administrated through food for three weeks to suppress viremia. 10x 10^6 autologous CART4 cells or NTD $CD8^+$ T cells were injected via retro-orbital route four days post cART administration. (**B**) Peripheral blood was taken from the tail vein and assessed for the quantity of residual $CD4^+$ cells. (**C**) $CD4^+$ population in blood (BL), bone marrow (BM) and spleen (SP)

was assessed at the end point. (**D**) The absolute number of $CD4^+$ cells was quantified in peripheral blood. Data are represented as mean ± SEM.

Indeed, CART4 cells were detectable within three days after infusion in peripheral blood and kept growing up to 30 days. At the peak, $tEGFR^+$ CART4 cells occupied 10.5% $\pm$ 5.1% $hCD45^+$ cells in peripheral blood. The fast expansion of CART4 cells may be due to a combination of CD4+ antigen stimulation and GVHD reaction. At the endpoint, CART4 cells decreased their population to about 3.8% in human $CD45^+$ cells due to the reduction of target $CD4^+$ cells (Figure 5-6A and B). As expected, CAR-T cells were detected in bone marrow and spleen (Figure 5-6C and D).

Next, the dynamics of plasma viral load during CART4 treatment was examined. Before $CD8^+$ CART4 injection, the animals had similar viremia. cART treatment dramatically decreased the viral load, although all of the animals still had a detectable level of plasma viremia. It might be due to the short-term treatment of cART treatment and the consistent activation of $CD4^+$ T cells induced by GVHD reaction. After the interruption of cART, all NTD mice had significant viral rebound as high as $1x10^8$ copy/ml within two weeks. Strikingly, all CART4 mice had very low or undetectable HIV, as quantified by plasma HIV RNA (Figure 5-7A). Thirty-four days after cART interruption, HIV was undetectable in most CART4 mice (4/6), and only two mice had relatively low levels of viral RNA. Meanwhile, all the NTD mice suffered from high-level viremia burden with an average of $3.7x10^6$ copy/ml in peripheral blood (Figure 5-7B).

In summary, these *in vivo* results demonstrated that the CART4 cells had a potent anti-HIV effect via eliminating $CD4^+$ cells and delay, or even prevent, a viral rebound in PBL hu-mice model.

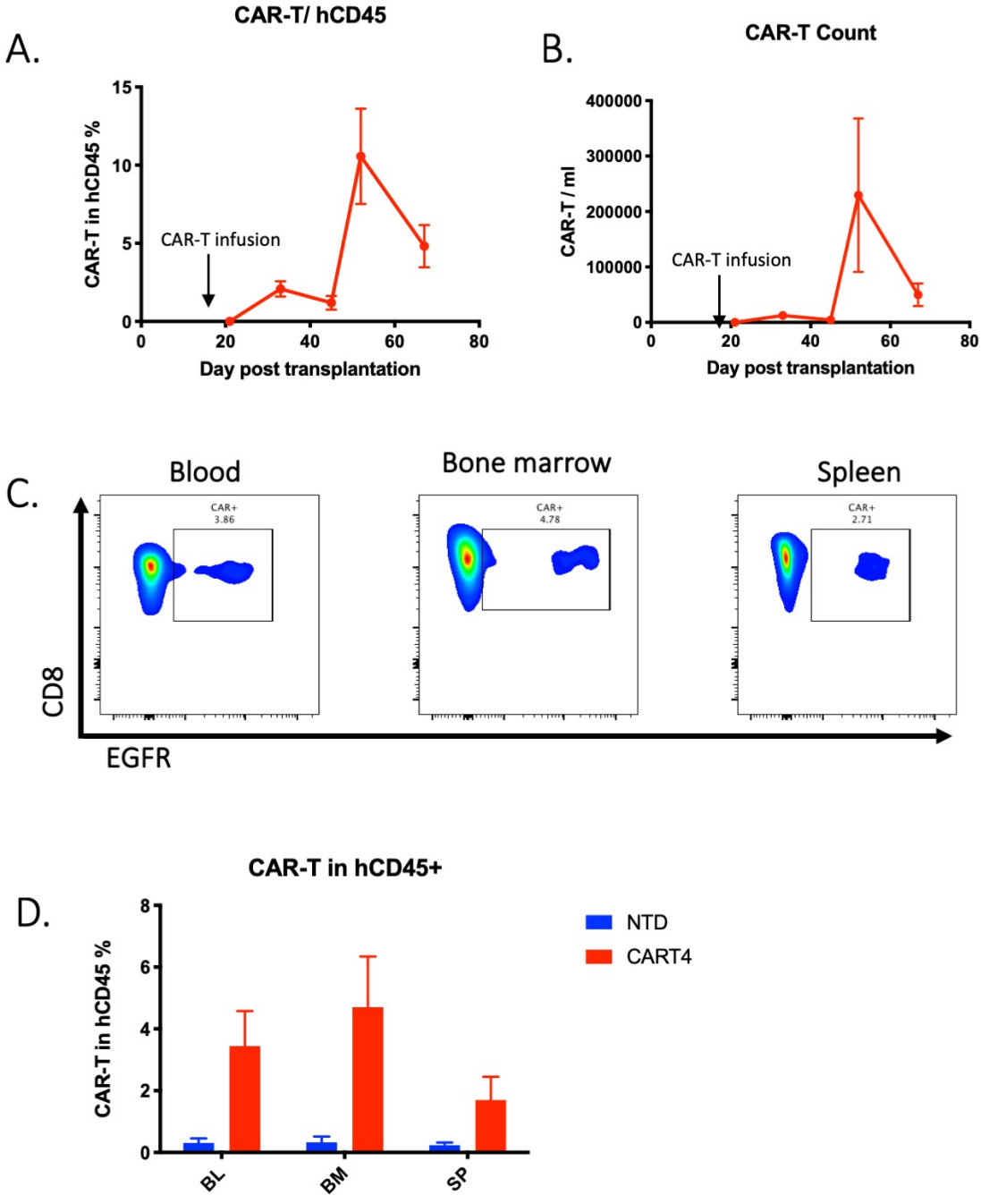

Figure 5-6 CART4 cells expanded in different organs in vivo.

Peripheral blood was weekly taken from the tail vein and assessed for the quantity of CART4 cells. CAR-T were detected from peripheral blood from the third-day post-injection and weekly to the endpoint (**A, B**). At the endpoint, the blood, spleen and bone marrow were stained by anti-CD8 and EGFR for detection of residual CAR-T cells (**C, D**). Data are represented as mean ± SEM. NTD, n=6; CART4, n=6.

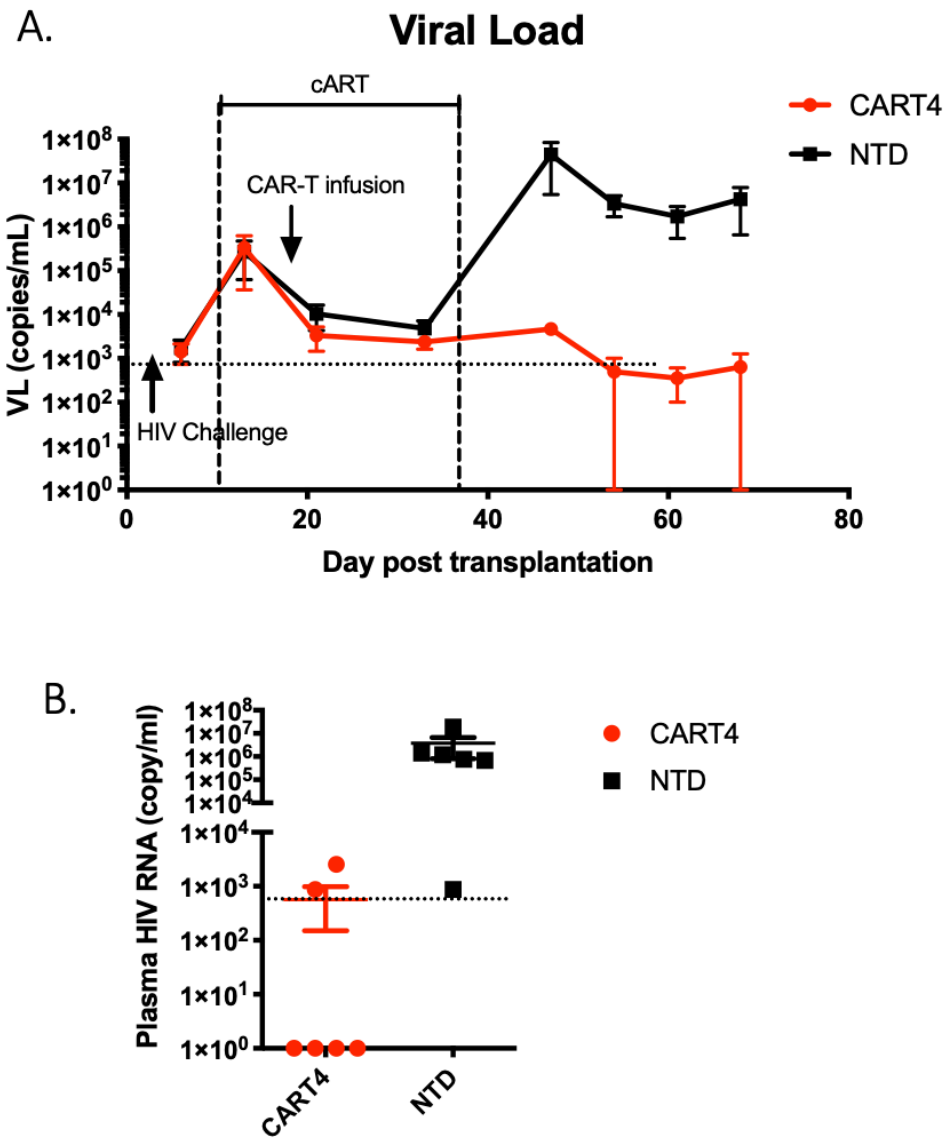

Figure 5-7 Depletion of CD4+ cells by CART4 suppressed viral rebound.

50 μl of plasma from peripheral blood was used for viral RNA measurement. Plasma viral RNA was quantified by One-Step RT-PCR weekly (**A**). By the endpoint of 34 days after cART interruption, two third of mice in CART4 group (n=6) did not display viral rebound, while the viral load from control group (n=6) increased to an average of $3.7x10^6$ copy/ml in peripheral blood (**B**). The detection limit is 800 copies/ml plasma. Data are represented as mean ± SEM.

5.4. Validation of HIV-1 cure of CART4 cells in CD34$^+$ HSC humanized mice: preliminary results

Although PBL humanized mice is a simple and easy preclinical model for HIV treatment studies, there are some drawbacks to this model. For example, GVHD-induced T cell activation and expansion is different from the physiological setting in which most of T cells are in resting status. Moreover, the short-term survival time limits the therapeutic efficacy of cART. More importantly, the lack of HSC does not truly reflect the natural renewal capacity[223]. The recent development of humanized mice reconstructed by human CD34$^+$ hematopoietic stem cells from the fetal liver has been proven as a more relevant and robust model for the research of HIV-1 infection, pathogenesis and therapies[223-225]. The procedure to construct the CD34$^+$ HSC humanized mice involves irradiating newborn immunodeficient NSG or NRG mice and injecting human CD34$^+$ HSCs. After several weeks, the transplanted mice develop a systemic population of human immune cells originating from the bone marrow, including T, B, natural killer, myeloid and dendritic cells[223,224,226-230]. This model has been widely used in pre-clinical studies to explore approaches to treat HIV infection[224,230-236].

Human CD34$^+$ HSC cells were isolated from fetal liver and injected into the livers of newborn NRG mice, which had been pre-irradiated. After ten weeks, CD45$^+$ human leukocytes were detected in the peripheral blood. Most of the CD4-expressing cells were CD3-positive, but there was a small proportion of CD3-negative cells expressing low levels of CD4, indicating the presence of DCs or macrophages in peripheral blood (Figure 5-8B). The mice were challenged by JR-CSF strain HIV and then treated with cART from the seventh week after infection. Initially, it was plan to infuse CART4 cells into the humanized mice when the plasma viremia dropped to an undetectable level (<1 copy/ μl) in the presence of cART. However, after being treated by cART for seven weeks, the viral loads remained above the limit of detection in those recipients, although a dramatic decrease was observed (Figure 5-9). Thus, the CART4 cells or non-transduced (NTD) CD8+ T cells were injected via retro-orbit

inoculation to those infected HSC hu-mice at the eighth week after cART treatment. Unfortunately, three-quarters of those recipients (8/12) died on the second day after T cell infusion, which was likely due to anaesthetic overdoses. The remaining two CART4 injected hu-mice exhibited remarkable declines of $CD4^+$ population during the first three weeks after CAR-T infusion, while the NTD control mice maintained the $CD4^+$ cell engraftment (Figure 5-8C). However, the $CD4^+$ population re-emerged in recipient No.3392 in the third week, and in No. 3386 within the sixth week. The recovery of CD4+ cells may be due to the short-term *in vivo* persistence of infused CART4 cells and renewal capacity of HSC cells in those hu-mice. Therefore, a second T cell injection was performed. As expected, the CART4 infusion induced $CD4^+$ population declined again. No $CD4^+$ cells were detected in peripheral blood in recipient No. 3392. Interestingly, CAR-T cell expansion was not observed in these mice after the second infusion (Figure 5-8D).

The results from plasma viral load implied an insufficient therapeutic effect of cART for this experiment. Usually, the plasma viremia would be controlled by three to four weeks treatment of cART[231,232]. This might be due to the over-activation of T cells induced by severe GVHD reaction. The virus rebounded in both of the CART4 hu-mice after the interruption of cART, though no $CD4^+$ cells were detected in the blood of No.3392 after stopping cART. This indicated an incomplete CD4 depletion in this recipient.

Due to the limitation of the number of recipients in this experiment and insufficient viral control of cART treatment, it was difficult to make any reliable conclusions for the anti-HIV function of CART4 cells tested. However, these data indicated that CART4 cells might well function in this preclinical animal model. Of course, more assessments need to be performed to confirm this speculation.

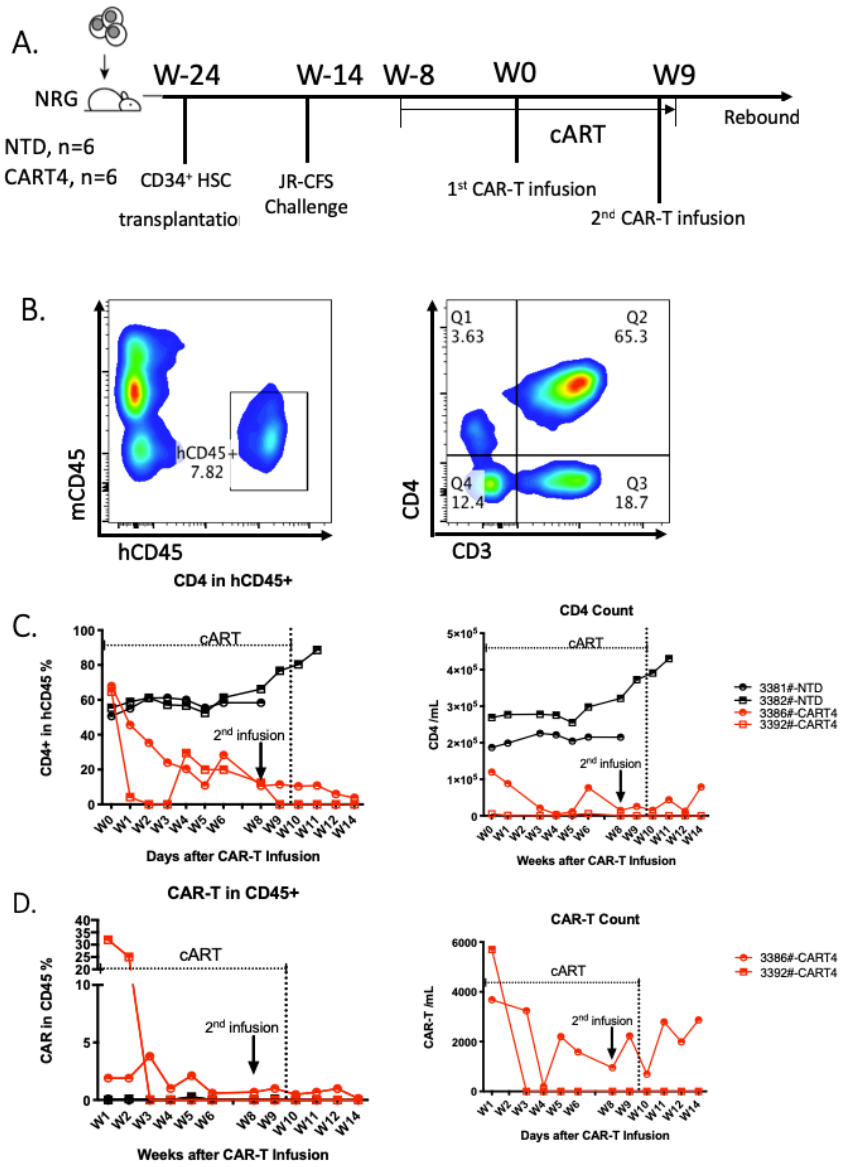

Figure 5-8 CART4 cells shown potent cytotoxic function against CD4+ cells in CD34⁺ HSC hu-mice

A. Experiment design: human CD34⁺ stem cells were isolated from the fetal liver by magnetic isolation kit before injection into livers of irradiated 2- to 6-day-old NRG mice. Humanized mice were infected by HIV JR-CSF before administration of cART treatment through food uptake for 17 weeks. CAR-T infusion was performed twice at eight and sixteen weeks, post cART treatment. **B**. Peripheral blood was taken via tail vein and lysed by ACK lysis buffer. Isolated PBMCs were stained by flow antibodies to identify human CD4⁺ cells. **C** and **D**. CD4⁺ cells and CAR-T cells in peripheral blood were quantified weekly by flow cytometry.

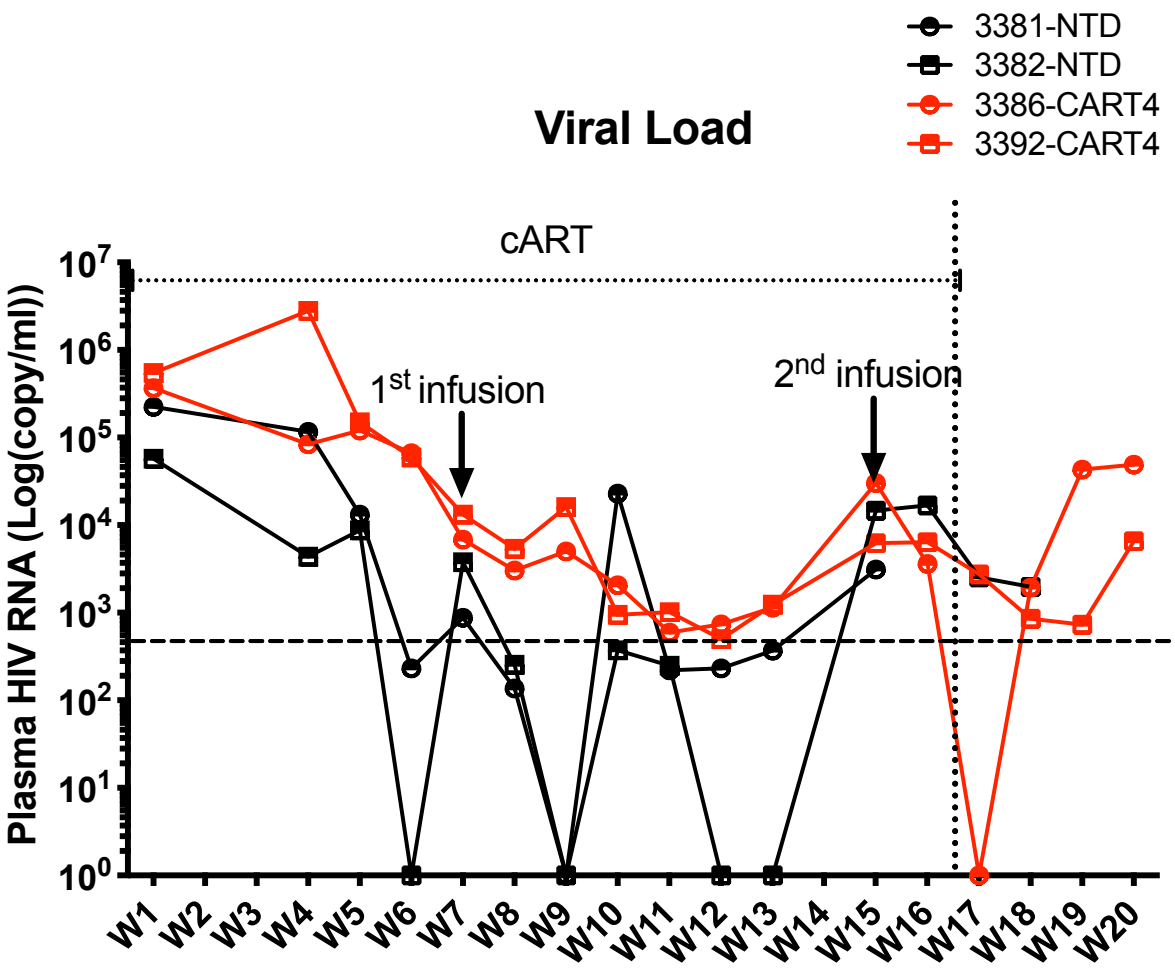

Figure 5-9 Dynamics of plasma viral loads in HIV infected HSC hu-mice infused CART4 cells

The plasma was obtained by centrifuging peripheral blood from HIV infected humanized mice. 50 μl of plasma from peripheral blood was used for viral RNA quantification. Plasma viral RNA was quantified by One-Step RT-PCR weekly. Sixteen weeks after CAR-T cell infusion, cART treatment was interrupted. The detection limit is 800 copies/mL plasma.

5.5. Discussion

Here in this chapter, the potential of CART4 for HIV cure was evaluated by *in vitro* assay and *in vivo* animal models.

Most of the identified HIV cellular reservoirs express CD4, such as helper T cells, DCs and macrophages. In co-culture cytotoxicity assay, CART4 T cells exhibited potent cytotoxic effect against $CD4^+$ DCs and macrophages. About 95% of DCs and macrophages were eradicated by 24-hour incubation with CART4 cells (Figure 5-2).

Based on the *in vitro* result, it was hypothesized that CART4 T cells would be able to eliminate the virus *in vivo*. An HIV treatment model using PBL humanized mice, which has been widely used for HIV study, was infused with CART4 T cells. A rapid expansion of CAR-T cells was observed, with 11.5% of $CD45^+$ human cells in peripheral blood. The CAR-T cells were detected in other organs, such as the spleen and bone marrow (Figure 5-6). Meanwhile, a dramatic drop of CD4 subpopulation occurred three days after CAR-T infusion (Figure 5-5). Twenty days post-CAR-T infusion, cART was terminated. Most of the control mice suffered a significant viral rebound as expected. Strikingly, viral load remained undetected in four mice infused with CAR-T one month post cART interruption (Figure 5-7).

Subsequently, the $CD34^+$ HSC humanized mice model was used to assess the efficacy of CART4 further. Similarly, the expansion of CAR-T and decline of $CD4^+$ cells was observed, though less rapid that that in PBL humanized mice. This was partially because $CD4^+$ T cells were renewed from the thymus. Another possibility was that the function and persistence of CART4 cells was inhibited by the immune-suppressive environment induced by chronic inflammation[231,233]. Indeed, viral rebound occurred in both CART4-infused mice. However, because of the lack of control mice and limitations of the number of mice, no reliable conclusions were made. Further animal experiments need to be performed.

Antigen escape from T cell recognition is a major obstacle for HIV cure. High rates of mutation during reverse transcription enables rapid emergence of viruses that can escape immune recognition[167]. Additionally, Nef protein downregulates the expression of MHC I, CD28 and CD1d protein to escape from T-cell surveillance[157,158 234 235].

One advantage of CAR-based therapy is that the engineered T cells lyse target cells by directly binding to surface proteins. Therefore CAR-T therapy overcomes the lack of MHC to target HIV-infected cells. Additionally, CAR-T cells have been proven to cross the blood-brain barrier, which is essential to HIV cure as CNS is a potential important reservoir [26].

To date, most CAR-studies for HIV mainly use bNAbs or CD4 as the binding domain for HIV infected cells. However, both of them have limitations. Indeed, CD4 extracellular domain- or bNAbs-based CARs showed robust cytotoxicity against latently infected cells reactivated by LRAs treatment [169,170,236,237]. However, there is still controversy surrounding the efficiency of those LRAs, especially in physiological settings[238,239]. None of the LRAs were effective enough to reactivate HIV-1 transcription in all $CD4^+$ T cell subsets *in vitro*[240,241]. Moreover, it has been noticed that LRAs have inhibitory effects on the cytotoxic function of $CD8^+$ T cells[240,241]. On the other hand, CD4- and bNAbs-CARs might work best in an environment full of antigen, that is, in patients without cART treatment. Although previous data suggest that interruption of cART treatment is safe, the ethical considerations would limit the validation of those concepts by the clinical trial. Besides, the envelope-binding domain (CD4 or bNAbs) on the CAR-T can potentially act as a virus receptor, causing infection of CAR-T cells. Indeed, increased HIV infection was noticed in CD4-based CAR-T cells[159].

In contrast, CART4 overcomes the drawbacks listed above by targeting a non-viral protein CD4. The adequate expression of CD4 protein warrants the efficacy of CAR-T cells. Additionally, the function of CART4 T cells requires the suppression of viral production by the administration of cART, as CD4 expression is downregulated by HIV virus[242]. Moreover,

previous studies using anti-CD4 monoclonal antibodies suggested that transient CD4 depletion is safe and reversible[112 206].

Finally, there are limitations to the artificial small animal models in HIV research. The outcomes from humanized mice model may not fully predict the clinical efficacy of CART4 in human. For example, in HIV-infected human individuals, most of the infected $CD4^+$ T cells localized outside the vascular system within secondary lymphoid organs [243]. Follicular helper cells (T_{FH} cells), named for their location in B follicular zone, are identified as major cell subset for HIV reservoir during cART treatment [244-248]. However, most of the $CD8^+$ T cells are absent in B follicular zone, due to lack of CXCR5 expression, which is the primary chemokine responsible for the accumulation of cells to follicular region [249,250]. Thus, the preclinical assessment using non-human primate model will be required.

Chapter 6. Discussion

6.1. Results summary

The overall aim of this project is to validate the function of anti-CD4 CAR against $CD4^+$ T-cell malignancies and HIV-1 infection, respectively. Here *in vitro* assay and *in vivo* animal models were utilized to systematically assess the potential use of CD4-directed CAR-T therapy in clinical settings.

In Chapter 3 of this thesis, a third-generation CAR derived from a CD4-specific humanized monoclonal antibody was designed with the corporation of a truncated human EGFR as a tracking marker and iC9 as a safety switch. By using a two-step retroviral method for gene delivery, human T cells were successfully engineered with this CAR. The flow cytometry analysis confirmed the successful co-expression of CAR and tEGFR marker. Also, the elimination of endogenous $CD4^+$ population indicated the correct specificity of CAR-equipped T cells. Additionally, iC9 was validated *in vitro* by the administration of CID drug. To further study on pre-clinical animal model or clinical trial, a GMP-compliant manufacturing method was developed for large scale production of CAR-T cells.

In Chapter 4 of this thesis, the anti-tumour activity of CART4 cells was assessed *in vitro* and *in vivo*. By using co-culture cytotoxicity assay with $CD4^+$ tumour cell lines and primary tumour cells from ATL and CTCL patients, CART4 cells were demonstrated to upregulate cytotoxic cytokines, including TNF-α and IFN-γ significantly. 60%-100% of tumour cells were lysed within 4-hour co-culture with CART4 cells at E: T ratio of 5:1. In vivo study using a xenograft model of T cell leukaemia further demonstrated that CART4 cells were functional *in vivo*. The infusion of CART4 cells inhibited tumour progression and expanded the overall survival of xenografts.

Chapter 5 of this thesis showed that CART4 cells effectively eliminated other cell subsets DCs and macrophages *in vitro*, which may serve as HIV reservoir in patients, besides of $CD4^+$ T cells. In order to examine whether CART4 cells achieve *in vivo* control, an HIV-treatment model was used. Injection of CART4 cells into humanized NSG mice with HIV infection rendered rapid depletion of $CD4^+$ cell population and functional cure in 4 of 6 mice. Though limited to the number of recipients, the experiment with $CD34^+$ HSC humanized mice showed robust CD4-target cytotoxicity in the more physiological environment.

6.2. General discussion

6.2.1. Clinical assessment of CD4-specific CAR

Most of TCL and ATL are CD4-positive. CD4 molecule is considered as a promising target for CAR-T therapy for its broad coverage in T-cell malignancies and restriction in the hematopoietic compartment. Indeed, infusion of CART4 cells would eliminate $CD4^+$ cell populations including normal $CD4^+$ T cells, causing AIDS-like condition. Evidences from pre-clinical studies and clinical trials demonstrated the safety of short-term CD4 T-cell aplasia. Targeting CD4 with monoclonal antibodies has been widely validated in clinical trials for a variety of immune-related diseases [251-253]. Transient elimination of $CD4^+$ cells in small animal models, nonhuman primate models and humans has demonstrated its safety but increased susceptibility to viral infection[254]. Also, CD4 depletion was reversible in nonhuman primates with SIV infection, as CD4 expression is absent on hematopoietic stem cells[126].

By being equipped with safety switch iC9 and tEGFR, CART4 cells can be eliminated effectively by the administration of CID drug or EGFR-specific mAb after depletion of tumour or infected cells. Healthy $CD4^+$ cells would gradually recover from hematopoietic stem cells.

Alternatively, transient $CD4^+$ eradication mediated by CART4 cells would allow patients with $CD4^+$ T-cell malignancies to be eligible for bone marrow transplantation.

Unlike life-threatening T-cell malignancies, HIV infection has been considered as a 'chronic disease' with the ART treatment. Although the life-long administration of cART drugs renders several side effects, a 20-year-old infected individual could live to 67 years with treatment[255]. The success of cART treatment limits the possibility to perform CAR-T trial for HIV treatment. However, it can be initially achieved to recruit T-cell malignancy patients with HIV infection[256-258]. Although T-cell malignancy remains rare among HIV infected individuals, the risk of T-cell lymphoma increases up to 15 fold among HIV infected patients compared with the incidence in the whole population[259].

6.2.2. Challenges of designing CAR-T for T-cell malignancies

One hurdle in the development of CAR-T therapy for the treatment of T-cell malignancies is to identify a tumour-specific antigen, which is difficult in the case of these diseases. Most of the current target candidates, including CD1a, CD3, CD4, CD7, CCR4, are also widely expressed in normal T cells and other cell types. This will cause two considerable problems, fratricide and T-cell aplasia. The mutual cytotoxicity of CAR-engineered cells would prevent the proliferation and persistence of CAR-T cells. Although B-cell aplasia is acceptable in anti-CD19 CAR-T therapy, long-term T-cell aplasia is life-threatening.

Fratricide may be prevented by disrupting the target gene by gene-editing tools (such as TALEN and CRISPR/Cas9) in the CAR-T cells. This strategy has been assessed with CD3 CAR-T cells and CD7 CAR-T cells. The expression of CD3 or CD7 was effectively depleted from CAR-T cells and reduced T-cell fratricide. Importantly, ablation of CD3 and CD7 did not affect the function of CAR-T cells *in vitro* and *in vivo* [85,103]. However, it is not clear if CD3- or CD7-deficiency would reduce the long-term function and persistence of CAR-T cells *in vivo*.

Alternatively, using other cell subtypes that lack this target expression is a promising approach to evade fratricide. NK cells are important members of the innate immune system and CAR engineered NK cells have been evaluated in multiple studies [260]. NK cells do not express TCR, CD3, CD4 or CD5. They do not induce GVHD and can be used for allogeneic transfer. Moreover, their short lifespan may prevent long-term T-cell aplasia [261]. However, it is challenging to manufacture CAR-NK cells from peripheral blood [262]. Therefore, a human NK lymphoma cell line, NK-92, has been utilized to be engineered with CARs against CD3 [263], CD4 [264], and CD5 [265]. No fratricide effect was observed. However, the anti-tumour potency of CAR-NK cells was moderate in xenograft models. NK-92 cells are irradiated before infusion since the potential tumorigenicity of NK-92 cells is concerned. Irradiation would limit the proliferation and persistence of CAR-engineered cells, which may compromise therapeutic efficacy.

In order to limit T-cell aplasia, one obvious strategy is to select a target with restricted expression on normal T cells, such as TRBC1/2, CCR4. Another approach is to incorporate a suicide gene to T cells with CAR. Several available suicide genes, such as tEGFR[63], iC9, CD20[62], have been evaluated in animal models, and showed robust effect of safety switch. However, this strategy needs to be assessed in CAR-T clinical trials.

Another risk for CAR-T cell therapy for hematologic malignancies is contamination of circulating tumour cells in the cell product, which may lead to the generation of 'CAR tumour-cell'. One such case was reported recently in a patient with B-cell leukaemia [266]. One single leukaemic B cell was unintentionally transduced with anti-CD19 CAR, which led to the escape from CAR recognition and eventual relapse after therapy. Although it is extremely rare in CAR-T therapy for B-cell malignancies, it may be a critical risk as T-cell cancer cells are more likely to survive and expand in culture condition for CAR-T manufacturing. One way to avoid the risk of tumour contamination is to use allogeneic T cells or NK cells. Depletion of the surface expression of TCR by disrupting the gene of one TCR component is a common strategy to produce a universal CAR-T product[267-269]. Cooper *et al*. developed universal anti-CD7 CAR-T

(UCART7) cells, by disrupting both CD7 and TCR α chain using CRISPR/Cas9. UCART7 effectively killed T-ALL in a patient-derived xenograft (PDX), without inducing GvHD reaction[88,103]. However, the loss of endogenous TCR signalling may compromise T cell function. These allogeneic CAR-T cells would have a short life because they will be eliminated by the host-versus-graft effect. This short lifespan would help the prevention of T-cell aplasia but may be detrimental to prevent cancer recurrence.

6.2.3. Perspective for anti-HIV CAR

The remarkable success of CAR-T therapy for B-cell malignancies is due to the unique and restricted biomarker CD19, which is highly expressed in most B-cell leukaemia and lymphomas. However, it is not easy to find such a suitable target for HIV treatment. Most of the CAR constructs developed to date utilized the high binding affinity of CD4 extracellular domain or bNAbs to viral proteins presented on the surface of infected cells. An environment with high-antigen burden might be favourable for the activation and function of HIV-specific CAR-T cells. However, the ART treatment dramatically suppresses the production of the virus to undetectable level. Although recent data from several clinical trials suggest that interruption of ART treatment in HIV infected individuals is safe[270], the potential risks associated with active plasma viremia, will limit CAR-T trials for HIV treatment. Moreover, latency-reversing agents (LRAs) might need to activate rapid virus production. However, several studies showed that only a remarkably small number (less than 5%) of latent reservoir are reactivated by LRAs[271,272]. While some data indicated the low frequent, ongoing viral transcription in ART-treated individuals, it may require the life-long persistence of CAR-T cells in the absence of antigen.

One obstacle to studying CAR-T therapy for HIV treatment is the lack of suitable *in vivo* models. Ideally, the CAR-T cells should be studied in an *in vivo* model with ART-induced latency, in a similar physiological condition to infected human. This is important because the biodistribution

of HIV reservoir, immune-suppressive environment induced by $CD4^+$ T cell depression and chronic inflammation is expected to affect the efficacy of CAR-T cells. However, the establishment of ART-treated animal models, such as humanized mice or nonhuman primates, can be costly and time-consuming. The humanized mice model is an artificial system with short-term preserving duration. The primate model is more physiological; however, the human proteins of the CAR construct are potentially immunogenic to primates.

6.2.4. The pros and cons of CART4 therapy

To date, there is no standard CAR-T therapy for T-cell malignancies or HIV treatment. Though several targets have been widely studies, such as CD3, CD5, CD7, CD30, CCR4, it is difficult to identify targets uniquely expressed on malignant but not on normal tissues. All of those target molecules are also expressed by a subpopulation of T cells. Several groups used gene editing approaches to disrupt the genome locus of targets, such as CD3[85] and CD7[88,102,103]. However, the further clinical assessment would be limited by the manufacturing complexity of gene editing. Also, It requires special cautions to perform gene editing using donor human T cells, because it may disrupt the surface expression of target on tumour cells mixed in the culture, causing tumour antigen escape from CAR-T therapy. Other targets, such as CD5[87], CD30[89], are not expressed by many malignant T cell clones and can be easily regulated, potentially leading to antigen escape. CD4 is highly and uniformly expressed by T cell lymphomas. The restriction of regular expression in helper T cells and some myeloid cells makes it another potential therapeutic candidate for T-cell malignancies[111]. CD4 monoclonal antibodies have been used clinically for over 25 years[112-114]. These mAb studies have demonstrated that CD4 cell depletion is well-tolerated and reversible. The addition of suicide genes would also reduce the potential side effects of CART4 therapy.

On the other hand, while other studies[86] and our results showed that $CD8^+$ CAR-T cells were cytotoxic against tumour cells, the most effective ratio of $CD4^+$ to $CD8^+$ T cells for adoptive transfer remains the subject of ongoing investigation.

6.2.5. Future works

Here, this project demonstrated the feasibility of using CD4 CAR-T cells for the targeting therapy of T-cell malignancies and HIV cure. To further study and optimize CD4-directed CAR-T therapy, further work is required:

- To continue to validate CART4 cells in $CD34^+$ HSC humanized mice model with ART-induced latency. To date, HSC humanized mice is one of the most physiological small animal models for HIV research.

- To assess safety switch based on iC9 and tEGFR *in vivo*.

- To preclinically examine safety and efficacy of CART4 cells in nonhuman primate models.

- To improve the potency, safety and availability of CD4-directed CAR with new generation of CARs, such as fourth-generation CAR incorporated with immune stimulatory cytokines[30-32] improve CAR-T persistence and expansion, or universal CAR-T cell platform based on the interaction between soluble target ligands and immune receptors on cell surface to precisely mediate CAR-T function *in vivo*[237].

References

1. Janeway, C. A., Jr, Travers, P., Science, M. W. N. Y. G.2012. *Immunobiology. 8th Editio*.
2. Dushek, O., Goyette, J. & van der Merwe, P. A. Non-catalytic tyrosine-phosphorylated receptors. *Immunol. Rev.* **250,** 258–276 (2012).
3. Call, M. E., Pyrdol, J., Wiedmann, M. & Wucherpfennig, K. W. The Organizing Principle in the Formation of the T Cell Receptor-CD3 Complex. *Cell* **111,** 967–979 (2002).
4. Gross, G., Waks, T. & Eshhar, Z. Expression of immunoglobulin-T-cell receptor chimeric molecules as functional receptors with antibody-type specificity. *PNAS* **86,** 10024–10028 (1989).
5. Eshhar, Z., Waks, T., Gross, G. & Schindler, D. G. Specific activation and targeting of cytotoxic lymphocytes through chimeric single chains consisting of antibody-binding domains and the gamma or zeta subunits of the immunoglobulin and T-cell receptors. *PNAS* **90,** 720–724 (1993).
6. van der Merwe, P. A. & Davis, S. J. Molecular Interactions Mediating T Cell Antigen Recognition. *https://doi.org/10.1146/annurev.immunol.21.120601.141036* **21,** 659–684 (2003).
7. Cole, D. K. *et al.* Human TCR-Binding Affinity is Governed by MHC Class Restriction. *J Immunol* **178,** 5727–5734 (2007).
8. Gong, M. C. *et al.* Cancer Patient T Cells Genetically Targeted to Prostate-Specific Membrane Antigen Specifically Lyse Prostate Cancer Cells and Release Cytokines in Response to Prostate-Specific Membrane Antigen. *Neoplasia (New York, N.Y.)* **1,** 123–127 (1999).
9. Hombach, A. *et al.* Chimeric anti-TAG72 receptors with immunoglobulin constant Fc domains and gamma or zeta signalling chains. *International Journal of Molecular Medicine* **2,** 99–202 (1998).
10. Irving, B. A. & Weiss, A. The cytoplasmic domain of the T cell receptor ζ chain is sufficient to couple to receptor-associated signal transduction pathways. *Cell* **64,** 891–901 (1991).
11. Till, B. G. *et al.* Adoptive immunotherapy for indolent non-Hodgkin lymphoma and mantle cell lymphoma using genetically modified autologous CD20-specific T cells. *Blood* **112,** 2261–2271 (2008).

12. Park, J. R. *et al.* Adoptive Transfer of Chimeric Antigen Receptor Re-directed Cytolytic T Lymphocyte Clones in Patients with Neuroblastoma. *Molecular Therapy* **15,** 825–833 (2007).
13. Kershaw, M. H. *et al.* A Phase I Study on Adoptive Immunotherapy Using Gene-Modified T Cells for Ovarian Cancer. *Clin. Cancer Res.* **12,** 6106–6115 (2006).
14. Finney, H. M., Akbar, A. N. & Lawson, A. D. G. Activation of Resting Human Primary T Cells with Chimeric Receptors: Costimulation from CD28, Inducible Costimulator, CD134, and CD137 in Series with Signals from the TCRζ Chain. *J Immunol* **172,** 104–113 (2004).
15. Imai, C. *et al.* Chimeric receptors with 4-1BB signaling capacity provoke potent cytotoxicity against acute lymphoblastic leukemia. *Leukemia* **18,** 676–684 (2004).
16. Finney, H. M., Lawson, A. D. G., Bebbington, C. R. & Weir, A. N. C. Chimeric Receptors Providing Both Primary and Costimulatory Signaling in T Cells from a Single Gene Product. *J Immunol* **161,** 2791–2797 (1998).
17. Maher, J., Brentjens, R. J., Gunset, G., Riviere, I. & Sadelain, M. Human T-lymphocyte cytotoxicity and proliferation directed by a single chimeric TCRζ /CD28 receptor. *Nature Biotechnology* **20,** 70–75 (2002).
18. Pule, M. A. *et al.* A chimeric T cell antigen receptor that augments cytokine release and supports clonal expansion of primary human T cells. *Molecular Therapy* **12,** 933–941 (2005).
19. Guedan, S. *et al.* ICOS-based chimeric antigen receptors program bipolar TH17/TH1 cells. *Blood* **124,** 1070–1080 (2014).
20. Song, D.-G. *et al.* CD27 costimulation augments the survival and antitumor activity of redirected human T cells in vivo. *Blood* **119,** 696–706 (2012).
21. Friedmann-Morvinski, D., Bendavid, A., Waks, T., Schindler, D. & Eshhar, Z. Redirected primary T cells harboring a chimeric receptor require costimulation for their antigen-specific activation. *Blood* **105,** 3087–3093 (2005).
22. Haynes, N. M. *et al.* Redirecting Mouse CTL Against Colon Carcinoma: Superior Signaling Efficacy of Single-Chain Variable Domain Chimeras Containing TCR-ζ vs FcεRI-γ. *J Immunol* **166,** 182–187 (2001).
23. Hombach, A. *et al.* Tumor-Specific T Cell Activation by Recombinant Immunoreceptors: CD3ζ Signaling and CD28 Costimulation Are Simultaneously Required for Efficient IL-2 Secretion and Can Be Integrated into One Combined CD28/CD3ζ Signaling Receptor Molecule. *J Immunol* **173,** 695–695 (2004).
24. Eshhar, Z., Waks, T., Bendavid, A. & Schindler, D. G. Functional expression of chimeric receptor genes in human T cells. *Journal of Immunological Methods* **248,** 67–76 (2001).

25. Carpenito, C. *et al.* Control of large, established tumor xenografts with genetically retargeted human T cells containing CD28 and CD137 domains. *PNAS* **106,** 3360–3365 (2009).
26. Grupp, S. A. *et al.* Chimeric Antigen Receptor–Modified T Cells for Acute Lymphoid Leukemia. *http://dx.doi.org/10.1056/NEJMoa1215134* **368,** 1509–1518 (2013).
27. Porter, D. L., Levine, B. L., Kalos, M., Bagg, A. & June, C. H. Chimeric Antigen Receptor–Modified T Cells in Chronic Lymphoid Leukemia. *http://dx.doi.org/10.1056/NEJMoa1103849* **365,** 725–733 (2011).
28. Wang, J. *et al.* Optimizing adoptive polyclonal T cell immunotherapy of lymphomas, using a chimeric T cell receptor possessing CD28 and CD137 costimulatory domains. *Hum. Gene Ther.* **18,** 712–725 (2007).
29. Till, B. G. *et al.* CD20-specific adoptive immunotherapy for lymphoma using a chimeric antigen receptor with both CD28 and 4-1BB domains: pilot clinical trial results. *Blood* **119,** 3940–3950 (2012).
30. Avanzi, M. P. *et al.* Engineered Tumor-Targeted T Cells Mediate Enhanced Anti-Tumor Efficacy Both Directly and through Activation of the Endogenous Immune System. *Cell Reports* **23,** 2130–2141 (2018).
31. Koneru, M., Purdon, T. J., Spriggs, D., Koneru, S. & Brentjens, R. J. IL-12 secreting tumor-targeted chimeric antigen receptor T cells eradicate ovarian tumors in vivo. *Oncoimmunology* **4,** e994446 (2015).
32. Pegram, H. J. *et al.* Tumor-targeted T cells modified to secrete IL-12 eradicate systemic tumors without need for prior conditioning. *Blood* **119,** 4133–4141 (2012).
33. Krenciute, G. *et al.* Transgenic Expression of IL15 Improves Antiglioma Activity of IL13Rα2-CAR T Cells but Results in Antigen Loss Variants. *Cancer immunology research* **5,** 571–581 (2017).
34. Hu, B. *et al.* Augmentation of Antitumor Immunity by Human and Mouse CAR T Cells Secreting IL-18. *Cell Reports* **20,** 3025–3033 (2017).
35. Zhang, C., Liu, J., Zhong, J. F. & Zhang, X. Engineering CAR-T cells. *Biomark Res* **5,** 1–6 (2017).
36. Johnson, L. A. & June, C. H. Driving gene-engineered T cell immunotherapy of cancer. *Cell Research* **27,** 38–58 (2017).
37. Garfall, A. L. *et al.* Chimeric Antigen Receptor T Cells against CD19 for Multiple Myeloma. *http://dx.doi.org/10.1056/NEJMoa1504542* **373,** 1040–1047 (2015).
38. Zhang, W.-Y. *et al.* Treatment of CD20-directed Chimeric Antigen Receptor-modified T cells in patients with relapsed or refractory B-cell non-Hodgkin lymphoma: an early phase IIa trial report. *Sig Transduct Target Ther* **1,** 1–9 (2016).

39. Berdeja, J. G., Lin, Y., Raje, N., Munshi, N. & Siegel, D. Durable clinical responses in heavily pretreated patients with relapsed/refractory multiple myeloma: updated results from a multicenter study of bb2121 anti-Bcma …. (2017).
40. O'Rourke, D. M. *et al.* A single dose of peripherally infused EGFRvIII-directed CAR T cells mediates antigen loss and induces adaptive resistance in patients with recurrent glioblastoma. *Science Translational Medicine* **9,** eaaa0984 (2017).
41. Bugelski, P. J., Achuthanandam, R., Capocasale, R. J., Treacy, G. & Bouman-Thio, E. Monoclonal antibody-induced cytokine-release syndrome. *Expert Review of Clinical Immunology* **5,** 499–521 (2014).
42. Suntharalingam, G. *et al.* Cytokine Storm in a Phase 1 Trial of the Anti-CD28 Monoclonal Antibody TGN1412. *https://doi.org/10.1056/NEJMoa063842* **355,** 1018–1028 (2009).
43. Panelli, M. C. *et al.* Forecasting the cytokine storm following systemic interleukin (IL)-2 administration. *J Transl Med* **2,** 1–14 (2004).
44. Porter, D. L. *et al.* Chimeric antigen receptor T cells persist and induce sustained remissions in relapsed refractory chronic lymphocytic leukemia. *Science Translational Medicine* **7,** 303ra139–303ra139 (2015).
45. Turtle, C. J. *et al.* CD19 CAR–T cells of defined CD4+:CD8+ composition in adult B cell ALL patients. *J Clin Invest* **126,** 2123–2138 (2016).
46. Kochenderfer, J. N. *et al.* Chemotherapy-Refractory Diffuse Large B-Cell Lymphoma and Indolent B-Cell Malignancies Can Be Effectively Treated With Autologous T Cells Expressing an Anti-CD19 Chimeric Antigen Receptor. *JCO* **33,** 540–549 (2015).
47. Kochenderfer, J. N. *et al.* B-cell depletion and remissions of malignancy along with cytokine-associated toxicity in a clinical trial of anti-CD19 chimeric-antigen-receptor–transduced T cells. *Blood* **119,** 2709–2720 (2012).
48. Sadelain, M. *et al.* Abstract CT102: Efficacy and toxicity management of 19-28z CAR T cell therapy in B cell acute lymphoblastic leukemia. *Cancer Research* **74,** CT102–CT102 (2014).
49. Lee, D. W. *et al.* T cells expressing CD19 chimeric antigen receptors for acute lymphoblastic leukaemia in children and young adults: a phase 1 dose-escalation trial. *The Lancet* **385,** 517–528 (2015).
50. Maude, S. L. *et al.* Chimeric antigen receptor T cells for sustained remissions in leukemia. *N Engl J Med* **371,** 1507–1517 (2014).
51. Lee, D. W. *et al.* Current concepts in the diagnosis and management of cytokine release syndrome. *Blood* **124,** 188–195 (2014).

52. Neelapu, S. S. *et al.* Axicabtagene Ciloleucel CAR T-Cell Therapy in Refractory Large B-Cell Lymphoma. *http://dx.doi.org/10.1056/NEJMoa1707447* **377,** 2531–2544 (2017).
53. Turtle, C. J. *et al.* Immunotherapy of non-Hodgkin's lymphoma with a defined ratio of CD8+ and CD4+ CD19-specific chimeric antigen receptor–modified T cells. *Science Translational Medicine* **8,** 355ra116–355ra116 (2016).
54. Santomasso, B. D. *et al.* Clinical and Biological Correlates of Neurotoxicity Associated with CAR T-cell Therapy in Patients with B-cell Acute Lymphoblastic Leukemia. *Cancer Discov* **8,** 958–971 (2018).
55. Maude, S. L. *et al.* Tisagenlecleucel in Children and Young Adults with B-Cell Lymphoblastic Leukemia. *N Engl J Med* **378,** 439–448 (2018).
56. Morgan, R. A. *et al.* Case Report of a Serious Adverse Event Following the Administration of T Cells Transduced With a Chimeric Antigen Receptor Recognizing ERBB2. *Molecular Therapy* **18,** 843–851 (2010).
57. Park, J. H. *et al.* Long-Term Follow-up of CD19 CAR Therapy in Acute Lymphoblastic Leukemia. *N Engl J Med* **378,** 449–459 (2018).
58. Davila, M. L., Kloss, C. C., Gunset, G. & Sadelain, M. CD19 CAR-Targeted T Cells Induce Long-Term Remission and B Cell Aplasia in an Immunocompetent Mouse Model of B Cell Acute Lymphoblastic Leukemia. *PLOS ONE* **8,** e61338 (2013).
59. Davila, M. L. *et al.* Efficacy and toxicity management of 19-28z CAR T cell therapy in B cell acute lymphoblastic leukemia. *Sci Transl Med* **6,** 224ra25–224ra25 (2014).
60. Introna, M. *et al.* Genetic Modification of Human T Cells with CD20: A Strategy to Purify and Lyse Transduced Cells with Anti-CD20 Antibodies. *https://home.liebertpub.com/hum* **11,** 611–620 (2004).
61. Griffioen, M. *et al.* Retroviral transfer of human CD20 as a suicide gene for adoptive T-cell therapy. *Haematologica* **94,** 1316–1320 (2009).
62. Serafini, M. *et al.* Characterization of CD20-transduced T lymphocytes as an alternative suicide gene therapy approach for the treatment of graft-versus-host disease. *Hum. Gene Ther.* **15,** 63–76 (2004).
63. Wang, X. *et al.* A transgene-encoded cell surface polypeptide for selection, in vivo tracking, and ablation of engineered cells. *Blood* **118,** 1255–1263 (2011).
64. Paszkiewicz, P. J. *et al.* Targeted antibody-mediated depletion of murine CD19 CAR T cells permanently reverses B cell aplasia. *J Clin Invest* **126,** 4262–4272 (2016).
65. Rufener, G. A. *et al.* Preserved Activity of CD20-Specific Chimeric Antigen Receptor–Expressing T Cells in the Presence of Rituximab. *Cancer immunology research* **4,** 509–519 (2016).

66. Druškovič, M., Šuput, D. & Milisav, I. Overexpression of Caspase-9 Triggers Its Activation and Apoptosis in Vitro. *Croatian medical journal* **47,** 832–0 (2006).
67. Clackson, T. *et al.* Redesigning an FKBP-ligand interface to generate chemical dimerizers with novel specificity. *PNAS* **95,** 10437–10442 (1998).
68. Straathof, K. C. *et al.* An inducible caspase 9 safety switch for T-cell therapy. *Blood* **105,** 4247–4254 (2005).
69. Iuliucci, J. D. *et al.* Intravenous Safety and Pharmacokinetics of a Novel Dimerizer Drug, AP1903, in Healthy Volunteers. *The Journal of Clinical Pharmacology* **41,** 870–879 (2001).
70. Ciceri, F. *et al.* Infusion of suicide-gene-engineered donor lymphocytes after family haploidentical haemopoietic stem-cell transplantation for leukaemia (the TK007 trial): a non-randomised phase I–II study. *Lancet Oncology* **10,** 489–500 (2009).
71. Diaconu, I. *et al.* Inducible Caspase-9 Selectively Modulates the Toxicities of CD19-Specific Chimeric Antigen Receptor-Modified T Cells. *Mol. Ther.* **25,** 580–592 (2017).
72. Marin, V. *et al.* Comparison of Different Suicide-Gene Strategies for the Safety Improvement of Genetically Manipulated T Cells. *http:www.liebertpub.com/hgtb* **23,** 376–386 (2012).
73. The Non-Hodgkin's Lymphoma Classification Project. A Clinical Evaluation of the International Lymphoma Study Group Classification of Non-Hodgkin's Lymphoma. *Blood* **89,** 3909–3918 (1997).
74. International T-Cell Lymphoma Project. International Peripheral T-Cell and Natural Killer/T-Cell Lymphoma Study: Pathology Findings and Clinical Outcomes. *JCO* **26,** 4124–4130 (2008).
75. Guenova, E. *et al.* Expression of CD164 on Malignant T Cells in Sézary Syndrome. *Acta Derm Venerol* **96,** 464–467 (2016).
76. Mak, V. *et al.* Survival of patients with peripheral T-cell lymphoma after first relapse or progression: spectrum of disease and rare long-term survivors. *J. Clin. Oncol.* **31,** 1970–1976 (2013).
77. Ishitsuka, K. & Tamura, K. Human T-cell leukaemia virus type I and adult T-cell leukaemia-lymphoma. *Lancet Oncology* **15,** e517–e526 (2014).
78. Winter, S. S. *et al.* Improved Survival for Children and Young Adults With T-Lineage Acute Lymphoblastic Leukemia: Results From the Children's Oncology Group AALL0434 Methotrexate Randomization. *JCO* **36,** 2926–2934 (2018).
79. Asselin, B. L. *et al.* Effectiveness of high-dose methotrexate in T-cell lymphoblastic leukemia and advanced-stage lymphoblastic lymphoma: a randomized study by the Children's Oncology Group (POG 9404). *Blood* **118,** 874–883 (2011).

80. Johnstone, R. W., Ruefli, A. A. & Lowe, S. W. Apoptosis: A Link between Cancer Genetics and Chemotherapy. *Cell* **108,** 153–164 (2002).
81. Sitzia, J., North, C., Stanley, J. & Winterberg, N. Side effects of CHOP in the treatment of non-Hodgkin's lymphoma. *Cancer Nursing* **20,** 430 (1997).
82. Mehta-Shah, N., Teja, S., Tao, Y., Cashen, A. F. & Beaven, A. Successful treatment of mature T-cell lymphoma with allogeneic stem cell transplantation: the largest multicenter retrospective analysis. (2017).
83. Li, C. *et al.* Outcome of allogeneic stem cell transplantation in T cell lymphoblastic lymphoma. (2017).
84. Cudillo, L. *et al.* Allogeneic hematopoietic stem cell transplantation in Primary Cutaneous T Cell Lymphoma. *Ann Hematol* **97,** 1041–1048 (2018).
85. Rasaiyaah, J., Georgiadis, C., Preece, R., Mock, U. & Qasim, W. TCRαβ/CD3 disruption enables CD3-specific antileukemic T cell immunotherapy. *JCI Insight* **3,** 56219 (2018).
86. Pinz, K. *et al.* Preclinical targeting of human T-cell malignancies using CD4-specific chimeric antigen receptor (CAR)-engineered T cells. *Leukemia* **30,** 701–707 (2016).
87. Mamonkin, M., Rouce, R. H., Tashiro, H. & Brenner, M. K. A T-cell-directed chimeric antigen receptor for the selective treatment of T-cell malignancies. *Blood* **126,** 983–992 (2015).
88. Cooper, M. L. *et al.* An 'off-the-shelf' fratricide-resistant CAR-T for the treatment of T cell hematologic malignancies. *Leukemia* **32,** 1970–1983 (2018).
89. Ramos, C. A. *et al.* Clinical and immunological responses after CD30-specific chimeric antigen receptor–redirected lymphocytes. *J Clin Invest* **127,** 3462–3471 (2017).
90. Perera, L. P. *et al.* Chimeric antigen receptor modified T cells that target chemokine receptor CCR4 as a therapeutic modality for T-cell malignancies. *Am. J. Hematol.* **92,** 892–901 (2017).
91. Maciocia, P. M. *et al.* Targeting the T cell receptor β-chain constant region for immunotherapy of T cell malignancies. *Nat Med* **23,** 1416–1423 (2017).
92. Onuoha, S., Ferrari, M., Bulek, A., Bughda, R. & Manzoor, S. Structure Guided Engineering of Highly Specific Chimeric Antigen Receptors for the Treatment of T Cell Lymphomas. (2018).
93. Sabattini, E., Bacci, F., Sagramoso, C. & Pileri, S. A. WHO classification of tumours of haematopoietic and lymphoid tissues in 2008: an overview. *Pathologica* **102,** 83–87 (2010).
94. Frankel, A. E. *et al.* Anti-CD3 recombinant diphtheria immunotoxin therapy of cutaneous T cell lymphoma. *Curr Drug Targets* **10,** 104–109 (2009).

95. Pui, C.-H., Behm, F. G. & Crist, W. M. Clinical and biologic relevance of immunologic marker studies in childhood acute lymphoblastic leukemia. *Blood* **82,** 343–362 (1993).
96. Campana, D. *et al.* Stages of T-cell receptor protein expression in T-cell acute lymphoblastic leukemia. *Blood* **77,** 1546–1554 (1991).
97. Kernan, N. A. *et al.* Specific inhibition of in vitro lymphocyte transformation by an anti-pan T cell (gp67) ricin A chain immunotoxin. *J Immunol* **133,** 137–146 (1984).
98. LeMaistre, C. F. *et al.* Phase I trial of H65-RTA immunoconjugate in patients with cutaneous T- cell lymphoma. *Blood* **78,** 1173–1182 (1991).
99. Bertram, J. H. *et al.* Monoclonal antibody T101 in T cell malignancies: a clinical, pharmacokinetic, and immunologic correlation. *Blood* **68,** 752–761 (1986).
100. Arber, D. A. Atlas of Differential Diagnosis in Neoplastic Hematopathology. *The American Journal of Surgical Pathology* **29,** 1121 (2005).
101. Frankel, A. E. *et al.* Therapy of Patients with T-cell Lymphomas and Leukemias Using an Anti-CD7 Monoclonal Antibody-Rich a Chain Immunotoxin. *Leukemia & Lymphoma* **26,** 287–298 (2009).
102. Png, Y. T. *et al.* Blockade of CD7 expression in T cells for effective chimeric antigen receptor targeting of T-cell malignancies. *Blood Adv* **1,** 2348–2360 (2017).
103. Gomes-Silva, D. *et al.* CD7-edited T cells expressing a CD7-specific CAR for the therapy of T-cell malignancies. *Blood* **130,** 285–296 (2017).
104. Zheng, W. *et al.* CD30 expression in acute lymphoblastic leukemia as assessed by flow cytometry analysis. *Leukemia & Lymphoma* **55,** 624–627 (2013).
105. Wang, C.-M. *et al.* Autologous T cells expressing CD30 chimeric antigen receptors for relapsed or refractory Hodgkin's lymphoma: an open-label phase 1 trial. *The Lancet* **386,** S12 (2015).
106. Acosta-Rodriguez, E. V. *et al.* Surface phenotype and antigenic specificity of human interleukin 17–producing T helper memory cells. *Nature Immunology* **8,** 639–646 (2007).
107. Sinigaglia, F. & D'Ambrosio, D. Selective Upregulation of Chemokine Receptors CCR4 and CCR8 upon Activation of Polarized Human Type 2 T Helper Cells. *Immunology - Supplement* **95,** (1998).
108. Hirahara, K. *et al.* The Majority of Human Peripheral Blood CD4+CD25highFoxp3+ Regulatory T Cells Bear Functional Skin-Homing Receptors. *J Immunol* **177,** 4488–4494 (2006).
109. Zinzani, P. L. *et al.* European phase II study of mogamulizumab, an anti-CCR4 monoclonal antibody, in relapsed/refractory peripheral T-cell lymphoma. *Haematologica* **101,** e407–e410 (2016).

110. Sims, J. E., Tunnacliffe, A., Smith, W. J. & Rabbitts, T. H. Complexity of human T-cell antigen receptor β -chain constant- and variable-region genes. *Nature* **312,** 541–545 (1984).
111. Asnafi, V. *et al.* Analysis of TCR, pTα, and RAG-1 in T-acute lymphoblastic leukemias improves understanding of early human T-lymphoid lineage commitment. *Blood* **101,** 2693–2703 (2003).
112. Kim, Y. H. *et al.* Clinical efficacy of zanolimumab (HuMax-CD4): two phase 2 studies in refractory cutaneous T-cell lymphoma. *Blood* **109,** 4655–4662 (2007).
113. Hagberg, H., Pettersson, M., Bjerner, T. & Enblad, G. Treatment of a patient with a nodal peripheral T-cell lymphoma (angioimmunoblastic T-Cell lymphoma) with a human monoclonal antibody against the CD4 antigen (HuMax-CD4). *Med. Oncol.* **22,** 191–194 (2005).
114. d'Amore, F. *et al.* Phase II trial of zanolimumab (HuMax-CD4) in relapsed or refractory non-cutaneous peripheral T cell lymphoma. *British Journal of Haematology* **150,** 565–573 (2010).
115. Hymes, K. *et al.* KAPOSI'S SARCOMA IN HOMOSEXUAL MEN—A REPORT OF EIGHT CASES. *The Lancet* **318,** 598–600 (1981).
116. Chermann, J. C. *et al. Isolation of a New Retrovirus in a Patient at Risk for Acquired Immunodeficiency Syndrome*. *Epidemic of Acquired Immune Deficiency Syndrome (AIDS) and Kaposi's Sarcoma* **32,** 48–53 (Karger Publishers, 1984).
117. WHO. WHO | HIV/AIDS. *WHO*
118. Smith, J. A. & Daniel, R. Following the Path of the Virus: The Exploitation of Host DNA Repair Mechanisms by Retroviruses. *ACS Chem. Biol.* **1,** 217–226 (2006).
119. Gilbert, P. B. *et al.* Comparison of HIV-1 and HIV-2 infectivity from a prospective cohort study in Senegal. *Stat Med* **22,** 573–593 (2003).
120. Gao, F. *et al.* Origin of HIV-1 in the chimpanzee Pan troglodytes troglodytes. *Nature* **397,** 436–441 (1999).
121. Reeves, J. D. & Doms, R. W. Human immunodeficiency virus type 2. *Journal of General Virology* **83,** 1253–1265 (2002).
122. Wyatt, R. & Sodroski, J. The HIV-1 Envelope Glycoproteins: Fusogens, Antigens, and Immunogens. *Science* **280,** 1884–1888 (1998).
123. Pierson, T. C. & Doms, R. W. in *Cellular Factors Involved in Early Steps of Retroviral Replication* **281,** 1–27 (Springer, Berlin, Heidelberg, 2003).
124. Jacobson, J. M. *et al.* Safety, pharmacokinetics, and antiretroviral activity of multiple doses of ibalizumab (formerly TNX-355), an anti-CD4 monoclonal antibody, in human immunodeficiency virus type 1-infected adults. *Antimicrob. Agents Chemother.* **53,** 450–457 (2009).

125. Kuritzkes, D. R. *et al.* Antiretroviral activity of the anti-CD4 monoclonal antibody TNX-355 in patients infected with HIV type 1. *J. Infect. Dis.* **189,** 286–291 (2004).
126. Micci, L. *et al.* CD4 depletion in SIV-infected macaques results in macrophage and microglia infection with rapid turnover of infected cells. *PLOS Pathog* **10,** e1004467 (2014).
127. Berson, J. F. & Doms, R. W. Structure–function studies of the HIV-1 coreceptors. *Seminars in Immunology* **10,** 237–248 (1998).
128. Eugen-Olsen, J. *et al.* Heterozygosity for a deletion in the CKR-5 gene leads to prolonged AIDS-free survival and slower CD4 T-cell decline in a cohort of HIV-seropositive individuals. *Aids* **11,** 305 (1997).
129. Gupta, R. K. *et al.* HIV-1 remission following CCR5Δ32/Δ32 haematopoietic stem-cell transplantation. *Nature* **568,** 244–248 (2019).
130. Daar, E. S., Moudgil, T. & Meyer, R. D. Transient high levels of viremia in patients with primary human immunodeficiency virus type 1 infection. *New England Journal of …* (1991).
131. Koup, R. A. *et al.* Temporal association of cellular immune responses with the initial control of viremia in primary human immunodeficiency virus type 1 syndrome. *Journal of virology* **68,** 4650–4655 (1994).
132. Zhang, Z. Sexual Transmission and Propagation of SIV and HIV in Resting and Activated CD4+ T Cells. *Science* **286,** 1353–1357 (1999).
133. Schacker, T. *et al.* Productive infection of T cells in lymphoid tissues during primary and early human immunodeficiency virus infection. *J. Infect. Dis.* **183,** 555–562 (2001).
134. Pope, M. & Haase, A. T. Transmission, acute HIV-1 infection and the quest for strategies to prevent infection. *Nat Med* **9,** 847–852 (2003).
135. World Health Organization. *Antiretroviral therapy for HIV infection in adults and adolescents: recommendations for a public health approach - 2010 revision*. (Geneva : World Health Organization, 2010).
136. AIDSinfo, A. Guidelines for the Use of Antiretroviral Agents in HIV-1-Infected Adults and Adolescents. (2013).
137. Molina, J.-M. *et al.* Efficacy and safety of once daily elvitegravir versus twice daily raltegravir in treatment-experienced patients with HIV-1 receiving a ritonavir-boosted protease inhibitor: randomised, double-blind, phase 3, non-inferiority study. *The Lancet Infectious Diseases* **12,** 27–35 (2012).
138. Montessori, V., Press, N., Harris, M., Akagi, L. & Montaner, J. S. G. Adverse effects of antiretroviral therapy for HIV infection. *CMAJ* **170,** 229–238 (2004).
139. Barton, K., Winckelmann, A. & Palmer, S. HIV-1 Reservoirs During Suppressive Therapy. *Trends Microbiol* **24,** 345–355 (2016).

140. Kulpa, D. A. & Chomont, N. HIV persistence in the setting of antiretroviral therapy: when, where and how does HIV hide? *J Virus Erad* **1,** 59–66 (2015).
141. Chomont, N. *et al.* HIV reservoir size and persistence are driven by T cell survival and homeostatic proliferation. *Nat Med* **15,** 893–900 (2009).
142. Descours, B. *et al.* CD32a is a marker of a CD4 T-cell HIV reservoir harbouring replication-competent proviruses. *Nature* **543,** 564–567 (2017).
143. Osuna, C. E. *et al.* Evidence that CD32a does not mark the HIV-1 latent reservoir. *Nature* **561,** E20–E28 (2018).
144. Bertagnolli, L. N. *et al.* The role of CD32 during HIV-1 infection. *Nature* **561,** E17–E19 (2018).
145. Pérez, L. *et al.* Conflicting evidence for HIV enrichment in CD32 + CD4 T cells. *Nature* **561,** E9–E16 (2018).
146. Badia, R. *et al.* CD32 expression is associated to T-cell activation and is not a marker of the HIV-1 reservoir. *Nat Comms* **9,** 2739 (2018).
147. Stevenson, M. Role of myeloid cells in HIV-1-host interplay. *J. Neurovirol.* **21,** 242–248 (2014).
148. Clayton, K. L. *et al.* Resistance of HIV-infected macrophages to CD8 + T lymphocyte–mediated killing drives activation of the immune system. *Nature Immunology* **19,** 475–486 (2018).
149. McDonald, D. *et al.* Recruitment of HIV and Its Receptors to Dendritic Cell-T Cell Junctions. *Science* **300,** 1295–1297 (2003).
150. Eisele, E. & Siliciano, R. F. Redefining the Viral Reservoirs that Prevent HIV-1 Eradication. *Immunity* **37,** 377–388 (2012).
151. Saksena, N. K., Wu, J. Q., Potter, S. J., Wilkinson, J. & Wang, B. Human Immunodeficiency Virus Interactions with CD8+ T Lymphocytes. *CHR* **6,** 1–9 (2008).
152. Sáez-Cirión, A. *et al.* HIV controllers exhibit potent CD8 T cell capacity to suppress HIV infection ex vivo and peculiar cytotoxic T lymphocyte activation phenotype. *PNAS* **104,** 6776–6781 (2007).
153. Kinter, A. *et al.* Suppression of HIV-specific T cell activity by lymph node CD25+ regulatory T cells from HIV-infected individuals. *PNAS* **104,** 3390–3395 (2007).
154. Goonetilleke, N. *et al.* The first T cell response to transmitted/founder virus contributes to the control of acute viremia in HIV-1 infection. *J Exp Med* **206,** 1253–1272 (2009).
155. Miura, T. *et al.* HLA-B57/B*5801 human immunodeficiency virus type 1 elite controllers select for rare gag variants associated with reduced viral replication capacity and strong cytotoxic T-lymphocyte [corrected] recognition. *Journal of virology* **83,** 2743–2755 (2009).

156. Varela-Rohena, A. *et al.* Control of HIV-1 immune escape by CD8 T cells expressing enhanced T-cell receptor. *Nature Medicine* **14,** 1390–1395 (2008).
157. Xu, X.-N. *et al.* Evasion of Cytotoxic T Lymphocyte (CTL) Responses by Nef-dependent Induction of Fas Ligand (CD95L) Expression on Simian Immunodeficiency Virus–infected Cells. *Journal of Experimental Medicine* **186,** 7–16 (1997).
158. Landi, A., Iannucci, V., Van Nuffel, A., Meuwissen, P. & Verhasselt, B. One Protein to Rule them All: Modulation of Cell Surface Receptors and Molecules by HIV Nef. *CHR* **9,** 496–504 (2011).
159. Romeo, C. & Seed, B. Cellular immunity to HIV activated by CD4 fused to T cell or Fc receptor polypeptides. *Cell* **64,** 1037–1046 (1991).
160. Deeks, S. G. *et al.* A Phase II Randomized Study of HIV-Specific T-Cell Gene Therapy in Subjects with Undetectable Plasma Viremia on Combination Antiretroviral Therapy. *Molecular Therapy* **5,** 788–797 (2002).
161. Scholler, J. *et al.* Decade-long safety and function of retroviral-modified chimeric antigen receptor T cells. *Sci Transl Med* **4,** 132ra53 (2012).
162. Brentjens, R. J. *et al.* CD19-targeted T cells rapidly induce molecular remissions in adults with chemotherapy-refractory acute lymphoblastic leukemia. *Sci Transl Med* **5,** 177ra38–177ra38 (2013).
163. Kochenderfer, J. N. *et al.* Eradication of B-lineage cells and regression of lymphoma in a patient treated with autologous T cells genetically engineered to recognize CD19. *Blood* **116,** 4099–4102 (2010).
164. Leibman, R. S. & Riley, J. L. Engineering T Cells to Functionally Cure HIV-1 Infection. *Molecular Therapy* **23,** 1149–1159 (2015).
165. Liu, L. *et al.* Novel CD4-Based Bispecific Chimeric Antigen Receptor Designed for Enhanced Anti-HIV Potency and Absence of HIV Entry Receptor Activity. *Journal of virology* **89,** 6685–6694 (2015).
166. MacLean, A. G. *et al.* A novel real-time CTL assay to measure designer T-cell function against HIV Env+ cells. *Journal of Medical Primatology* **43,** 341–348 (2014).
167. Hale, M. *et al.* Engineering HIV-Resistant, Anti-HIV Chimeric Antigen Receptor T Cells. *Molecular Therapy* **25,** 570–579 (2017).
168. Sahu, G. K. *et al.* Anti-HIV designer T cells progressively eradicate a latently infected cell line by sequentially inducing HIV reactivation then killing the newly gp120-positive cells. *Virology* **446,** 268–275 (2013).
169. Ali, A. *et al.* HIV-1-Specific Chimeric Antigen Receptors Based on Broadly Neutralizing Antibodies. *Journal of virology* **90,** 6999–7006 (2016).

170. Leibman, R. S. *et al.* Supraphysiologic control over HIV-1 replication mediated by CD8 T cells expressing a re-engineered CD4-based chimeric antigen receptor. *PLOS Pathog* **13,** e1006613 (2017).
171. Zhen, A. *et al.* HIV-specific Immunity Derived From Chimeric Antigen Receptor-engineered Stem Cells. *Mol. Ther.* **23,** 1358–1367 (2015).
172. Rowan, A. G. *et al.* Cytotoxic T lymphocyte lysis of HTLV-1 infected cells is limited by weak HBZ protein expression, but non-specifically enhanced on induction of Tax expression. *Retrovirology 2016 13:1* **11,** 116–12 (2014).
173. Halper-Stromberg, A. *et al.* Broadly neutralizing antibodies and viral inducers decrease rebound from HIV-1 latent reservoirs in humanized mice. *Cell* **158,** 989–999 (2014).
174. Wang, Y. *et al.* Effective response and delayed toxicities of refractory advanced diffuse large B-cell lymphoma treated by CD20-directed chimeric antigen receptor-modified T cells. *Clinical Immunology* **155,** 160–175 (2014).
175. Sadelain, M., Brentjens, R. & Rivière, I. The basic principles of chimeric antigen receptor design. *Cancer Discov* **3,** 388–398 (2013).
176. June, C. H. & Levine, B. L. T cell engineering as therapy for cancer and HIV: our synthetic future. *Philos Trans R Soc Lond B Biol Sci* **370,** (2015).
177. Kim, J. H. *et al.* High Cleavage Efficiency of a 2A Peptide Derived from Porcine Teschovirus-1 in Human Cell Lines, Zebrafish and Mice. *PLOS ONE* **6,** e18556 (2011).
178. Liu, Z. *et al.* Systematic comparison of 2A peptides for cloning multi-genes in a polycistronic vector. *Scientific Reports* **7,** 663–9 (2017).
179. Kalos, M. *et al.* T Cells with Chimeric Antigen Receptors Have Potent Antitumor Effects and Can Establish Memory in Patients with Advanced Leukemia. *Science Translational Medicine* **3,** 95ra73–95ra73 (2011).
180. Wagner, T. A. Quarter Century of Anti-HIV CAR T Cells. 1–8 (2018). doi:10.1007/s11904-018-0388-x
181. Beaudoin, E. L., Bais, A. J. & Junghans, R. P. Sorting vector producer cells for high transgene expression increases retroviral titer. *J. Virol. Methods* **148,** 253–259 (2008).
182. Lamers, C. H. J. *et al.* Retronectin-assisted retroviral transduction of primary human T lymphocytes under good manufacturing practice conditions: tissue culture bag critically determines cell yield. *Cytotherapy* **10,** 406–416 (2008).
183. Lamers, C. H. J., Willemsen, R. A., Luider, B. A., Debets, R. & Bolhuis, R. L. H. Protocol for gene transduction and expansion of human T lymphocytes for clinical immunogene therapy of cancer. *Cancer Gene Therapy* **9,** 613–623 (2002).

184. Lamers, C. H. J. *et al.* Phoenix-ampho outperforms PG13 as retroviral packaging cells to transduce human T cells with tumor-specific receptors: implications for clinical immunogene therapy of cancer. *Cancer Gene Therapy* **13,** 503–509 (2006).
185. Yee, J.-K., Friedmann, T. & Burns, J. C. Chapter 5 Generation of High-Titer Pseudotyped Retroviral Vectors with Very Broad Host Range. *Methods in Cell Biology* **43,** 99–112 (1994).
186. Xu, Y. *et al.* Closely related T-memory stem cells correlate with in vivo expansion of CAR.CD19-T cells and are preserved by IL-7 and IL-15. *Blood* **123,** 3750–3759 (2014).
187. Avgoustiniatos, E. S. *et al.* Commercially Available Gas-Permeable Cell Culture Bags May Not Prevent Anoxia in Cultured or Shipped Islets. *Transplantation Proceedings* **40,** 395–400 (2008).
188. Klebanoff, C. A., Rosenberg, S. A. & Restifo, N. P. Prospects for gene-engineered T cell immunotherapy for solid cancers. *Nat Med* **22,** 26–36 (2016).
189. Berger, C. *et al.* Adoptive transfer of effector CD8+ T cells derived from central memory cells establishes persistent T cell memory in primates. *J Clin Invest* **118,** 294–305 (2008).
190. Singh, H., Huls, H., Kebriaei, P. & Cooper, L. J. N. A new approach to gene therapy using Sleeping Beauty to genetically modify clinical-grade T cells to target CD19. *Immunol. Rev.* **257,** 181–190 (2014).
191. Kebriaei, P. *et al.* Adoptive Therapy Using Sleeping Beauty Gene Transfer System and Artificial Antigen Presenting Cells to Manufacture T Cells Expressing CD19-Specific Chimeric Antigen Receptor. *Blood* **124,** 311–311 (2014).
192. Huls, M. H. *et al.* Clinical Application of Sleeping Beauty and Artificial Antigen Presenting Cells to Genetically Modify T Cells from Peripheral and Umbilical Cord Blood. *J Vis Exp* e50070 (2013). doi:10.3791/50070
193. Monjezi, R. *et al.* Enhanced CAR T-cell engineering using non-viral Sleeping Beauty transposition from minicircle vectors. *Leukemia* **31,** 186–194 (2017).
194. Kebriaei, P. *et al.* First Clinical Trials Employing Sleeping Beauty Gene Transfer System and Artificial Antigen Presenting Cells To Generate and Infuse T Cells Expressing CD19-Specific Chimeric Antigen Receptor. *Blood* **122,** 166–166 (2013).
195. Wiesinger, M. *et al.* Clinical-Scale Production of CAR-T Cells for the Treatment of Melanoma Patients by mRNA Transfection of a CSPG4-Specific CAR under Full GMP Compliance. *Cancers 2019, Vol. 11, Page 1198* **11,** 1198 (2019).
196. Foster, J. B., Barrett, D. M. & Karikó, K. The Emerging Role of In Vitro-Transcribed mRNA in Adoptive T Cell Immunotherapy. *Molecular Therapy* **27,** 747–756 (2019).

197. Marcucci, K. T. *et al.* Retroviral and Lentiviral Safety Analysis of Gene-Modified T Cell Products and Infused HIV and Oncology Patients. *Molecular Therapy* **26,** 269–279 (2018).
198. Peréz-Soler, R. & Saltz, L. Cutaneous Adverse Effects With HER1/EGFR-Targeted Agents: Is There a Silver Lining? *JCO* **23,** 5235–5246 (2005).
199. Zhang, P. *et al.* Phase I Trial of Inducible Caspase 9 T Cells in Adult Stem Cell Transplant Demonstrates Massive Clonotypic Proliferative Potential and Long-term Persistence of Transgenic T Cells. *Clin. Cancer Res.* **25,** 1749–1755 (2019).
200. Schneider, U., Schwenk, H. U. & Bornkamm, G. Characterization of EBV-genome negative "null" and "T" cell lines derived from children with acute lymphoblastic leukemia and leukemic transformed non-Hodgkin lymphoma. *International Journal of Cancer* **19,** 621–626 (1977).
201. Foley, G. E. *et al.* Continuous culture of human lymphoblasts from peripheral blood of a child with acute leukemia. *Cancer* **18,** 522–529 (1965).
202. Salameire, D. *et al.* Efficient characterization of the TCR repertoire in lymph nodes by flow cytometry. *Cytometry A* **75,** 743–751 (2009).
203. Kanagawa, O. In vivo T cell tumor therapy with monoclonal antibody directed to the V beta chain of T cell antigen receptor. *Journal of Experimental Medicine* **170,** 1513–1519 (1989).
204. Vonderheid, E. C. *et al.* Evidence for restricted Vbeta usage in the leukemic phase of cutaneous T cell lymphoma. *J. Invest. Dermatol.* **124,** 651–661 (2005).
205. Tannous, B. A. Gaussia luciferase reporter assay for monitoring biological processes in culture and in vivo. *Nat Protoc* **4,** 582–591 (2009).
206. Knox, S. J. *et al.* Observations on the effect of chimeric anti-CD4 monoclonal antibody in patients with mycosis fungoides. *Blood* **77,** 20–30 (1991).
207. dAmore, F., Relander, T., Hagberg, H. & Osterborg, A. *HuMax-CD4 (Zanolimumab), a Fully Human Monoclonal Antibody: Early Results of an Ongoing Clinical Trial in CD4+ Peripheral T-Cell Lymphoma of Non …*. (Blood, 2005). doi:10.1182/blood.V106.11.3354
208. Mamonkin, M. *et al.* Reversible Transgene Expression Reduces Fratricide and Permits 4-1BB Costimulation of CAR T Cells Directed to T-cell Malignancies. *Cancer immunology research* **6,** 47–58 (2018).
209. Sánchez-Martínez, D. *et al.* Fratricide-resistant CD1a-specific CAR T cells for the treatment of cortical T-cell acute lymphoblastic leukemia. *Blood* **133,** 2291–2304 (2019).
210. Maus, M. V. *et al.* Adoptive Immunotherapy for Cancer or Viruses. *http://dx.doi.org/10.1146/annurev-immunol-032713-120136* **32,** 189–225 (2014).

211. Wang, X. *et al.* Comparison of naïve and central memory derived CD8+ effector cell engraftment fitness and function following adoptive transfer. *Oncoimmunology* **5,** e1072671 (2016).
212. Wang, X. *et al.* Phenotypic and functional attributes of lentivirus-modified CD19-specific human CD8+ central memory T cells manufactured at clinical scale. *J. Immunother.* **35,** 689–701 (2012).
213. Chun, T.-W. *et al.* Presence of an inducible HIV-1 latent reservoir during highly active antiretroviral therapy. *PNAS* **94,** 13193–13197 (1997).
214. Finzi, D. *et al.* Identification of a Reservoir for HIV-1 in Patients on Highly Active Antiretroviral Therapy. *Science* **278,** 1295–1300 (1997).
215. Wong, J. K. *et al.* Recovery of Replication-Competent HIV Despite Prolonged Suppression of Plasma Viremia. *Science* **278,** 1291–1295 (1997).
216. Chun, T.-W. *et al.* Early establishment of a pool of latently infected, resting CD4+ T cells during primary HIV-1 infection. *PNAS* **95,** 8869–8873 (1998).
217. Gartner, S. *et al.* The role of mononuclear phagocytes in HTLV-III/LAV infection. *Science* **233,** 215–219 (1986).
218. Igarashi, T. *et al.* Macrophage are the principal reservoir and sustain high virus loads in rhesus macaques after the depletion of CD4+ T cells by a highly pathogenic simian immunodeficiency virus/HIV type 1 chimera (SHIV): Implications for HIV-1 infections of humans. *PNAS* **98,** 658–663 (2001).
219. Smed-Sörensen, A. *et al.* Differential susceptibility to human immunodeficiency virus type 1 infection of myeloid and plasmacytoid dendritic cells. *Journal of virology* **79,** 8861–8869 (2005).
220. Patterson, S., Rae, A., Hockey, N., Gilmour, J. & Gotch, F. Plasmacytoid Dendritic Cells Are Highly Susceptible to Human Immunodeficiency Virus Type 1 Infection and Release Infectious Virus. *Journal of virology* **75,** 6710–6713 (2001).
221. Perez, E. E. *et al.* Establishment of HIV-1 resistance in CD4+ T cells by genome editing using zinc-finger nucleases. *Nature Biotechnology* **26,** 808–816 (2008).
222. Mukherjee, R. *et al.* HIV Sequence Variation Associated With env Antisense Adoptive T-cell Therapy in the hNSG Mouse Model. *Molecular Therapy* **18,** 803–811 (2010).
223. Denton, P. W. & Garcia, J. V. Novel humanized murine models for HIV research. *Curr HIV/AIDS Rep* **6,** 13–19 (2009).
224. Garcia, J. V. In vivo platforms for analysis of HIV persistence and eradication. *J Clin Invest* **126,** 424–431 (2016).
225. Cheng, L., Ma, J., Li, G. & Su, L. Humanized Mice Engrafted With Human HSC Only or HSC and Thymus Support Comparable HIV-1 Replication, Immunopathology, and Responses to ART and Immune Therapy. *Frontiers in Immunology* **9,** 293 (2018).

226. Denton, P. W. & Garcia, J. V. Humanized Mouse Models of HIV Infection. *AIDS reviews* **13,** 135–148 (2011).
227. Zhang, L. & Su, L. HIV-1 immunopathogenesis in humanized mouse models. *Cell. Mol. Immunol.* **9,** 237–244 (2012).
228. Borkow, G. Mouse models for HIV-1 infection. *IUBMB Life* **57,** 819–823 (2005).
229. Hatziioannou, T. & Evans, D. T. Animal models for HIV/AIDS research. *Nature Reviews Microbiology* **10,** 852–867 (2012).
230. Zhang, L. & Su, L. HIV-1 immunopathogenesis in humanized mouse models. *Cell. Mol. Immunol.* **9,** 237–244 (2012).
231. Cheng, L. *et al.* Blocking type I interferon signaling enhances T cell recovery and reduces HIV-1 reservoirs. *J Clin Invest* **127,** 269–279 (2017).
232. Li, G. *et al.* Plasmacytoid dendritic cells suppress HIV-1 replication but contribute to HIV-1 induced immunopathogenesis in humanized mice. *PLOS Pathog* **10,** e1004291 (2014).
233. Choudhary, S. K. *et al.* Suppression of Human Immunodeficiency Virus Type 1 (HIV-1) Viremia with Reverse Transcriptase and Integrase Inhibitors, CD4+ T-Cell Recovery, and Viral Rebound upon Interruption of Therapy in a New Model for HIV Treatment in the Humanized Rag2−/−γc−/− Mouse. *Journal of virology* **83,** 8254–8258 (2009).
234. Schwartz, O., Maréchal, V., Le Gall, S., Lemonnier, F. & Heard, J.-M. Endocytosis of major histocompatibility complex class I molecules is induced by the HIV–1 Nef protein. *Nat Med* **2,** 338–342 (1996).
235. Chen, N. *et al.* HIV-1 down-regulates the expression of CD1d via Nef. *European Journal of Immunology* **36,** 278–286 (2006).
236. Liu, B. *et al.* Chimeric Antigen Receptor T Cells Guided by the Single-Chain Fv of a Broadly Neutralizing Antibody Specifically and Effectively Eradicate Virus Reactivated from Latency in CD4+ T Lymphocytes Isolated from HIV-1-Infected Individuals Receiving Suppressive Combined Antiretroviral Therapy. *Journal of virology* **90,** 9712–9724 (2016).
237. Herzig, E. *et al.* Attacking Latent HIV with convertibleCAR-T Cells, a Highly Adaptable Killing Platform. *Cell* **179,** 880–894.e10 (2019).
238. Pardons, M., Fromentin, R., Pagliuzza, A., Routy, J.-P. & Chomont, N. Latency-Reversing Agents Induce Differential Responses in Distinct Memory CD4 T Cell Subsets in Individuals on Antiretroviral Therapy. *Cell Reports* **29,** 2783–2795.e5 (2019).

239. Ruiz, A. *et al.* Antigen Production After Latency Reversal and Expression of Inhibitory Receptors in CD8+ T Cells Limit the Killing of HIV-1 Reactivated Cells. *Frontiers in Immunology* **9,** 1525 (2019).
240. Clutton, G. T. & Jones, R. B. Diverse Impacts of HIV Latency-Reversing Agents on CD8+ T-Cell Function: Implications for HIV Cure. *Frontiers in Immunology* **9,** 1452 (2018).
241. Walker-Sperling, V. E., Pohlmeyer, C. W., Tarwater, P. M. & Blankson, J. N. The Effect of Latency Reversal Agents on Primary CD8+ T Cells: Implications for Shock and Kill Strategies for Human Immunodeficiency Virus Eradication. *EBioMedicine* **8,** 217–229 (2016).
242. Dalgleish, A. G. *et al.* The CD4 (T4) antigen is an essential component of the receptor for the AIDS retrovirus. *Nature* **312,** 763–767 (1984).
243. Estes, J. D. *et al.* Defining total-body AIDS-virus burden with implications for curative strategies. *Nat Med* **23,** 1271–1276 (2017).
244. Miles, B. & Connick, E. TFH in HIV Latency and as Sources of Replication-Competent Virus. *Trends Microbiol* **24,** 338–344 (2016).
245. Perreau, M. *et al.* Follicular helper T cells serve as the major CD4 T cell compartment for HIV-1 infection, replication, and production. *J Exp Med* **210,** 143–156 (2013).
246. Leong, Y. A., Atnerkar, A. & Di Yu. Human Immunodeficiency Virus Playing Hide-and-Seek: Understanding the TFH Cell Reservoir and Proposing Strategies to Overcome the Follicle Sanctuary. *Frontiers in Immunology* **8,** 182 (2017).
247. Banga, R. *et al.* PD-1(+) and follicular helper T cells are responsible for persistent HIV-1 transcription in treated aviremic individuals. *Nat Med* **22,** 754–761 (2016).
248. Zaunders, J., Xu, Y., Kent, S. J., Koelsch, K. K. & Kelleher, A. D. Divergent Expression of CXCR5 and CCR5 on CD4+ T Cells and the Paradoxical Accumulation of T Follicular Helper Cells during HIV Infection. *Frontiers in Immunology* **8,** 1 (2017).
249. Fukazawa, Y. *et al.* B cell follicle sanctuary permits persistent productive simian immunodeficiency virus infection in elite controllers. *Nat Med* **21,** 132–139 (2015).
250. Förster, R. *et al.* A putative chemokine receptor, BLR1, directs B cell migration to defined lymphoid organs and specific anatomic compartments of the spleen. *Cell* **87,** 1037–1047 (1996).
251. Pitzalis, C., Kingsley, G., Murphy, J. & Panayi, G. Abnormal distribution of the helper-inducer and suppressor-inducer T-lymphocyte subsets in the rheumatoid joint. *Clinical Immunology and Immunopathology* **45,** 252–258 (1987).
252. Herzog, C. *et al.* Anti-CD4 antibody treatment of patients with rheumatoid arthritis: I. Effect on clinical course and circulating T cells. *J. Autoimmun.* **2,** 627–642 (1989).

253. Racadot, E. *et al.* Treatment of Multiple Sclerosis with Anti-CD4 Monoclonal Antibody: A Preliminary Report on B-F5 in 21 Patients. *J. Autoimmun.* **6,** 771–786 (1993).
254. Knox, S. *et al.* Treatment of cutaneous T-cell lymphoma with chimeric anti-CD4 monoclonal antibody. *Blood* **87,** 893–899 (1996).
255. Trickey, A. *et al.* Survival of HIV-positive patients starting antiretroviral therapy between 1996 and 2013: a collaborative analysis of cohort studies. *The Lancet HIV* **4,** e349–e356 (2017).
256. Nasr, S. A., Brynes, R. K., Garrison, C. P. & Chan, W. C. Peripheral T-cell lymphoma in a patient with acquired immune deficiency syndrome. *Cancer* **61,** 947–951 (1988).
257. Gonzalez-Clemente, J. M. *et al.* Ki-1+ anaplastic large-cell lymphoma of T-cell origin in an HIV-infected patient. *Aids* **5,** 751–755 (1991).
258. Arber, D. A., Chang, K. L. & Weiss, L. M. Peripheral T-cell Lymphoma With Toutonlike Tumor Giant Cells Associated With HIV Infection: Report of Two Cases. *The American Journal of Surgical Pathology* **23,** 519 (1999).
259. Biggar, R. J., Engels, E. A., Frisch, M. & Goedert, J. J. Risk of T-cell lymphomas in persons with AIDS. *JAIDS Journal of Acquired Immune Deficiency Syndromes* **26,** 371–376 (2001).
260. Natural killer cells for cancer immunotherapy: a new CAR is catching up. *EBioMedicine* **39,** 1–2 (2019).
261. Daher, M. & Rezvani, K. Next generation natural killer cells for cancer immunotherapy: the promise of genetic engineering. *Current Opinion in Immunology* **51,** 146–153 (2018).
262. Klingemann, H., Boissel, L. & Toneguzzo, F. Natural Killer Cells for Immunotherapy - Advantages of the NK-92 Cell Line over Blood NK Cells. *Frontiers in Immunology* **7,** 91 (2016).
263. Chen, K. H. *et al.* Novel anti-CD3 chimeric antigen receptor targeting of aggressive T cell malignancies. *Oncotarget* **7,** 56219–56232 (2016).
264. Pinz, K. G. *et al.* Targeting T-cell malignancies using anti-CD4 CAR NK-92 cells. *Oncotarget* **8,** 112783–112796 (2017).
265. Chen, K. H. *et al.* Preclinical targeting of aggressive T-cell malignancies using anti-CD5 chimeric antigen receptor. *Leukemia* **31,** 2151–2160 (2017).
266. Ruella, M. *et al.* Induction of resistance to chimeric antigen receptor T cell therapy by transduction of a single leukemic B cell. *Nat Med* **24,** 1499–1503 (2018).
267. Kamiya, T., Wong, D., Png, Y. T. & Campana, D. A novel method to generate T-cell receptor–deficient chimeric antigen receptor T cells. *Blood Adv* **2,** 517–528 (2018).

268. Torikai, H. *et al.* A foundation for universal T-cell based immunotherapy: T cells engineered to express a CD19-specific chimeric-antigen-receptor and eliminate expression of endogenous TCR. *Blood* **119,** 5697–5705 (2012).
269. Qasim, W., Zhan, H., Samarasinghe, S. & of, S. A. T. F. R. O. T. U. *Molecular remission of infant B-ALL after infusion of universal TALEN gene-edited CAR T cells. Sci Transl Med. 2017; 9 (374)*.
270. Clarridge, K. E. *et al.* Effect of analytical treatment interruption and reinitiation of antiretroviral therapy on HIV reservoirs and immunologic parameters in infected individuals. *PLOS Pathog* **14,** e1006792 (2018).
271. Archin, N. M. *et al.* Administration of vorinostat disrupts HIV-1 latency in patients on antiretroviral therapy. *Nature* **487,** 482–485 (2012).
272. Kim, Y., Anderson, J. L. & Lewin, S. R. Getting the “Kill” into “Shock and Kill”: Strategies to Eliminate Latent HIV. *Cell Host & Microbe* **23,** 14–26 (2018).